

POLITECNICO DI TORINO

Collegio di Ingegneria Elettrica

**Corso di Laurea Magistrale
in Ingegneria Elettrica**

Tesi di Laurea Magistrale

PM-assisted Synchronous Reluctance motor: MTPA trajectory accuracy studies.



Relatori

prof. Aldo Boglietti
ing. Giulio Secondo
ing. Alessandro Castagnini

Candidato

Andrea Di Vinci

Luglio 2018

Table of Contents

<i>Introduction</i>	7
Part I	11
<i>Chapter 1</i>	13
PMASynRel Construction & Control Theory	13
1.1 Electro-magnetic model of SynRel machine on dq axes.....	13
1.1.1 <i>Background</i>	13
1.1.2 <i>Mathematical model</i>	14
1.2 Constructional aspects of the Synchronous Reluctance Machine's rotor	15
1.2.1 <i>Performance Analysis of Salient Pole Rotor</i>	15
1.2.2 <i>High anisotropy structures</i>	17
1.2.3 <i>Metal sheet lamination techniques</i>	18
1.3 From SynRel to PMAssistedSynRel	21
1.3.1 <i>Used Convention</i>	21
1.3.2 <i>Machine performance and efficiency considerations</i>	22
1.3.3 <i>Vector diagram in dq axes and electrical equivalent circuits</i>	23
1.4 Control Trajectories	25
1.5 Performance comparison between AC motors	26
<i>Chapter 2</i>	29
ABB Industrial contest and programs used	29
2.1 R&D team	29
2.2 Used program	29
2.2.1 <i>Adept for FEM simulation</i>	29
2.2.2 <i>FCSmek input</i>	31
2.2.3 <i>FCSmek output</i>	34
2.2.4 <i>Adept optimization tool</i>	37
2.2.5 <i>Limitations</i>	37
<i>Chapter 3</i>	39
SynRM2 Objective, design and optimization phase	39
3.2 SynRM2 ABB	41
3.2.1 <i>Preliminary mechanical evaluation</i>	41
3.2.2 <i>Optimization phase</i>	42
3.2.3 <i>Final design</i>	49
Part II	53
<i>Chapter 4</i> Thesis proposal	55
4.1 ABB	55

4.2 Thesis proposal	56
4.3 Grade of access to the motor drive	56
<i>Chapter 5</i> MTPA trajectory Time-step simulations	57
5.1 FEM - theory overview	57
5.2 MTPA trajectory research.....	58
5.2.1 <i>MTPA research</i>	59
5.2.2 <i>MTPA mediated from all preliminary characteristics</i>	61
5.2.3 <i>Mediated MTPA supply voltage characteristics</i>	63
<i>Chapter 6</i> MTPA trajectory Magneto-static simulations.....	65
6.1 Flux tables.....	65
6.2 Search MTPA trajectory by manipulating the flow chart	67
<i>Chapter 7</i> Compensation of ripple derived by stator effects	71
7.1 Method	71
7.1.1 <i>Stator effects</i>	71
7.1.2 <i>Problem solving</i>	72
7.2 Application.....	72
7.2.1 <i>Idea</i>	72
7.2.2 <i>Realization and results</i>	73
7.3 MTPA final	75
7.3.1 <i>Characteristic construction from new flux table</i>	75
7.3.2 <i>Comparison between the two magnetostatic simulations</i>	76
<i>Chapter 8</i> Dependence on temperature of MTPA and maximum efficiency characteristics.....	79
8.1 MTPA at different temperature	79
8.1.1 <i>Case A vs case B</i>	80
8.2 LM characteristics.....	81
<i>Chapter 9</i> Cross verify on time step characteristic Comparison between different MTPA derived by FEM studies	83
9.1 Cross-check – MTPA from time-step correction	83
9.1.1 <i>Problem individuation</i>	83
9.1.2 <i>Problem solution</i>	84
9.1.3 <i>MTPA adjustment</i>	85
9.2 MTPA from FEM simulations compare.....	87
Part III	89
<i>Chapter 10</i> Test bench and prove description	91
10.1 Test bench overview.....	91
10.2 Experiment description	94
<i>Chapter 11</i> Experiment results.....	97

11.1 Case A: stator temperature of 35°C	97
11.2 Case B: stator temperature of 65°C.....	101
11.3 Case A and case B compare.....	102
<i>Conclusions</i>	103
<i>Bibliographical references and sitography</i>	105
Appendix.....	107
A1.....	108
<i>Plot characteristic MTPA</i>	108
A2.....	109
<i>MTPA average</i>	109
A3.....	111
a- <i>3D flux rapresentation</i>	111
b- <i>Flux matrix interpolation</i>	112
c- <i>MTPA trajectory from flux matrix manipulation</i>	114
A4.....	122
a- <i>60 degree elt excursion of rotor – simulations and mediated output</i>	122
b- <i>launchFCSmek.m matlab function</i>	123
c- <i>IniConfig.m</i>	125
d- <i>launchFCSmek.bat</i>	125
Thanks – Ringraziamenti.....	127

Introduction

One of the issues currently more sensitive in the world of electrical engineering is to create more and more efficient motors. In fact, the new European targets related to the efficiency are on the agenda (eg Directive 2005_32_EC_Ecodesign Requirements for Electric Motors_22 July 2009, or the EU 327-2011 - Fan Ecodesign).

This period is therefore distinct from IE4 and IE5 standards as efficiency classes, hence it sees the groups of R & D develop new prototypes of motors to be within the strict rules that these efficiency classes recomand.

In addition, as we know, the motors must also be competitive in terms of performance regarding the application and economic environment.

There are three design targets for R&D teams:

- Performance
- Efficiency
- Cost

In this environment particular interest was addressed by companies to the reluctance motors, particularly those with assisted reluctance (PMASR - *permanent magnet assisted synchronous reluctance*), as it does not involve high costs like PMSM motors despite the presence of magnets. In fact they don't need to use these rare earth as the only source of magnetic flux, but the magnets are used here to "assist" the motor in the field weakening, making them competitive in these terms to induction motors while remaining physically synchronous. They also remain strongly overloadable, the driver must not be oversized, contrarily to what happens for PMSM motors (*surface mounted permanent magnet*), mechanically they are very easy to build and their efficiency is very high, making them suitable for a type IE4 / IE5 mission.

The thesis presented here was conducted entirely in the industrial complex of 'ABB Vittuone (MI), in the R & D division for application to low-voltage motors (LV - low voltage).

The elaborate is therefore in line with the questions that a real company poses to herself and it's useful to ensure consistency between its various divisions, which is often a critical passage as the entire motor driving system is only adapted, not revolutionized when a company faces technological changes of this type, while physically the motor is completely revolutionized.

This thesis tries to get into the action of the R & D group that meets the objectives set by the European community.

At this document will also be attached most of the Matlab script in the appendix(useful for the understanding of the analysis step of the control trajectories) and the description of the calculation sheets made.

The topics discussed in the thesis are organized in three parts, each divided into several chapters.

Part I is purely introductory, both in terms of the theories that surround the thesis and inherently the industrial context where it is made, marking the instruments used to carry out the activities set forth in this paper.

It is divided into three chapters:

Chapter 1 It is introductory about the basic theory, which is necessary for the understanding of the thesis, of the motors described: PMASR and, in general, reluctance motors (SynRel) that includes the first ones.

Chapter 2 starring the ABB business environment, in particular the programs and calculation tools available in the office, highlighting the potential and limitations.

In Chapter 3 will be described the objectives to which IE4 and IE5 classes set. Then, it will be described the range of prototypes developed by R & D group ABB, seeing in particular the delicate phase of optimization, which is fundamental for the company to reduce production costs, but annoying from the point of view of maintaining the characteristics in terms of efficiency, performance and mechanical safety coefficient. It will also make a short note on the Pareto method with regard to the used optimization methods.

Part II finally enters into the heart of this elaborate. Here are described in chapters the steps for characterizing the Max Torque per Ampère control characteristic (MTPA) by finite element analysis (FEM) with high precision. After considerations on the distance of LM characteristics (*loss minimization*) from MTPA at different speeds, and the influence that the temperature has on the MTPA trajectory, the last goal of the second part is to highlight any difference between the trajectories derived from FEM time dependent analysis, whose trajectory must be searched "manually", and the trajectory resulting from an analytical study on the magnetic flux table by magnetostatic simulations, mediated and not with respect to an excursion angle of 60 electrical degrees of the rotor to evaluate the effects of stator on the useful magnetic flux in the gap.

This is divided into six chapters:

Introductory to this second part, Chapter 4 tries to clarify what the company wants and why, thus introducing and justifying the work that was proposed to carry out during this thesis activity.

Chapter 5 describes the method used to search the MTPA trajectory from time step simulations, doing as a brief overview regard to the FEM techniques.

Chapter 6 performs the method of manipulation of the information enclosed by the outputs of a magnetostatic simulation, to extrapolate information useful to the description of the minimum current trajectory even for high levels of overload.

Chapter 7 will use the same method of manipulation of the magnetic flux table in direct and quadrature axes, but this time the table will be made from about 260000 simulations which mediates the effect that the teeth and the stator slots have on the magnetic flux, as well as the effects saturation of axis and cross effects, to get more and more physical considerations and make the machine less ideal. The effects that the ripple of the rotor flux has on the MTPA characteristic comparing the two minimum current trajectories resulting from magnetostatic simulations will be highlighted here.

Chapter 8 will take the scruple to see how the characteristic of a minimum current control that maximizes the torque is influenced by the temperature; it also highlights, through time step simulations, the distance that exists between this trajectory and those with maximum efficiency at different speeds.

In Chapter 9 will be compared the trajectories from the two types of FEM simulation and it highlights the correction of MTPA trajectory previously found in step time, due to an error on identifying the direct axis committed by the simulation program.

In **Part III**, it will remain to be checked if the simulations correspond at which pilots the ABB drive with its CDT (*Direct Torque Control*) control technique.

The true control characteristic will then be compared to those derived from FEM simulations assuming the reasons for the deviations, trying to enter into the control logic implemented by the ABB drive.

It is divided in two chapters:

In Chapter 10, we will describe the test bench and measuring instruments, accompanied by photos. It also describes the *modus operandi* used to trace the searched control feature.

The last chapter of the elaborate, Chapter 11, will compare the three trajectories found highlighting the distances and the points instead of closeness, assuming how the ABB drive acts in order to command the PMASR motor to the MTPA logic, even in overload.

Part I

Chapter 1

PMASynRel

Construction & Control Theory

This chapter, as mentioned above, will give the basics of theory useful for understanding the entire elaborate, assuming consolidate, even superficial, the functional knowledge of an asynchronous or synchronous permanent magnet machine.

It will start by describing the electrical and magnetic formulations of the reluctance machine and then its constructive aspects, after that it will continue with the modification of these for the permanent magnet assisted machine. After finishing this part, you will see models in the dq axis of the machine until the output of the equivalent circuits in the two axes, direct and quadrature, with particular attention to the vector diagrams.

It will then be described the vector control by describing the control technique following the MTPA and MTPV deflection trajectories,

The final part of this chapter will make a direct comparison between the various types of motors and the one considered here, highlighting their conveniences and disadvantages.

For further information, refer to the bibliographic notes.

1.1 Electro-magnetic model of SynRel machine on dq axes

1.1.1 Background

The peculiarity of this motor is the rotor; we don't have, in fact, neither permanent magnets nor coils, but its geometry gives it a strong anisotropy. We will refer to the simplest anisotropic structure, the classical "bone structure", which will prove completely unsuitable for applications in reality, but which is useful for understanding the basic concepts of physics related to the operation of this particular machine.

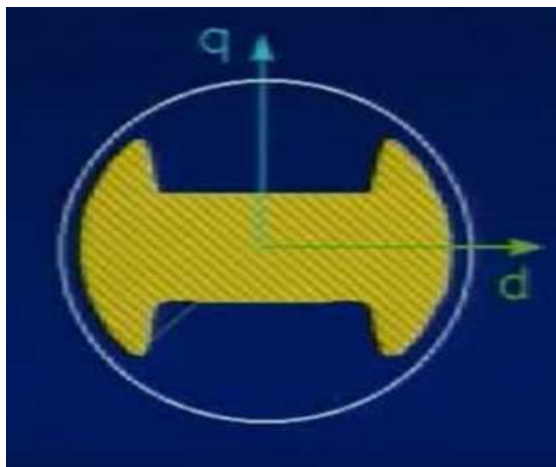


Fig 1.1: salient pole structure

1.1.2 *Mathematical model*

Let us first remember the equations valid for quadrature axes for an induction motor:

Assuming,

T – torque

P – pole pair

λ_s – stator flux

i_s – stator current vector

γ – angle between rotor flux vector and its vector on dq axes

δ – angle between rotor and staror's flux vector

L_s – stator inductance

i_{sd}/i_{sq} – the axes components of i_s vector

$$T = \frac{3}{2} * p * (\lambda_s \wedge i_s) = \frac{3}{2} * p * |\lambda_s| * |i_s| * \sin(\gamma - \delta) \quad (1.1)$$

$$\lambda_{sd} = L_s * i_{sd} = L_d * i_{sd} \quad (1.2)$$

$$\lambda_{sq} = \sigma * L_s * i_{sq} = L_q * i_{sq} \quad (1.3)$$

From these equations it is important to observe how the motor is asynchronous, however constructively totally isotropic, modeled in quadrature axes enjoy a certain " equivalent anisotropy " due to the presence of rotor currents (generated due to the non-synchronism between the two windings), where $L_d \gg L_q$ because σ is about 0.05, that represent the ratio $\left(\frac{L_q}{L_d}\right)$;

This equivalent but non-physical anisotropy guarantees to the asynchronous motor to provide high performance.

The question that comes is: if rotor currents did not circulate, but I still managed to guarantee σ quite similar to the induction motors ones only constructively, for example privileging or preventing rotor flow in an axis rather than in the other by lowering thus, or raising its inductance?

The figure that appears in our minds, the classic bone structure mentioned before, will let us understand the *mathematical model* of the machine.

On direct axes the inductance matrix is decoupled, in fact there are no mixed diagonal terms, the axes are not mutually coupled and the matrix simply becomes:

$$\begin{vmatrix} L_d & 0 \\ 0 & L_q \end{vmatrix} \quad (1.4)$$

From here, the equations:

$$\lambda_d = L_d * i_d \quad (1.5)$$

$$\lambda_q = L_q * i_q \quad (1.6)$$

As can be seen, the equations in quadrature axes are the same as for the SMPM motors, in fact the machine that we analyze *is still synchronous* and the mathematical model can follow

the classic formulation of these machines, but with the absence of the direct-axis flow component of the magnets, here not present for the main component on axis d (which we remember being the axis with minimum reluctance).

By analogy to the brushless, the electric equations and the expression of the torque in dq axes will be as follows, where it is simply located the portion of magnetic flux equal to zero ($\lambda_m = 0$) because in the motor we study there aren't the permanent magnets and the relative contribution:

$$V_{dq} = R_{dq} i_{dq} + \frac{d\lambda_{dq}}{dt} + j\omega\lambda_{dq} \quad (1.7)$$

$$\lambda_{dq} = L_{dq} * i_{dq} \quad (1.8)$$

$$T = \frac{3}{2} * p * (\lambda_{dq} \wedge i_{dq}) \quad (1.9)$$

where the multiplier factor $j\omega$; indicates the term motion because it is modeled on speed-rotating axes, at speed ω ;

1.2 Constructional aspects of the Synchronous Reluctance Machine's rotor

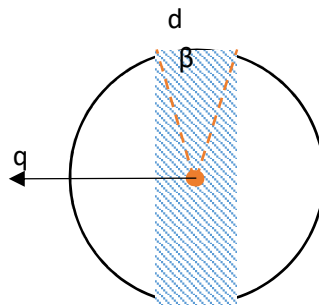
1.2.1 Performance Analysis of Salient Pole Rotor

After modeling, briefly, the particular electric machine, we extrapolate some more information from the relationship that indicates the torque:

$$T = \frac{3}{2} * p * (\lambda_{dq} \wedge i_{dq}) = \frac{3}{2} * p * (\lambda_d * i_q - \lambda_q * i_d) = \frac{3}{2} * p * (L_d * i_d * i_q - L_q * i_q * i_d)$$

$$T = \frac{3}{2} * p * (L_d - L_q) * i_d * i_q; \quad (1.10)$$

The need to maximize the difference $(L_d - L_q)$ is evident as well as having low ratio $\left(\frac{L_q}{L_d}\right)$ as mentioned in the previous chapter when comparing the performance with the induction machine. The classic two-pole structure we have referred to the start is inadequate for such a mission. Let's see why:



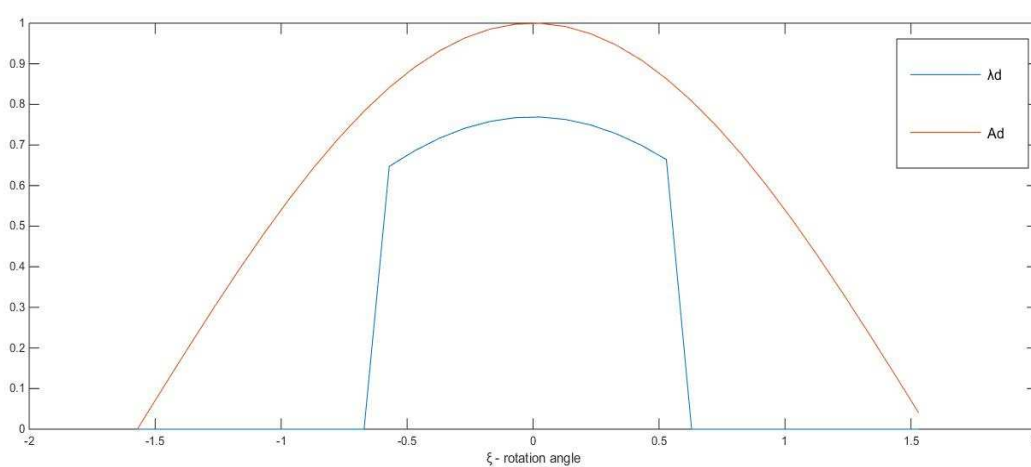
Indicated with ξ , the anti-clockwise rotation angle from d axis.

β is the pole step and doing the assumption that the magnetic flux is just below the pole step, we will have that:

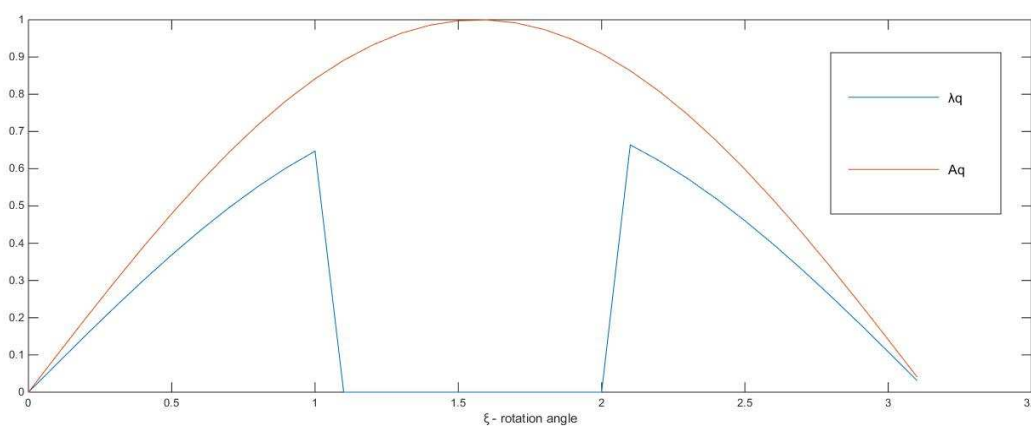
1. A_d will be proportional to $\cos(\xi)$
2. A_q will be proportional to $\sin(\xi)$

Where A_{dq} is the magnetic potential vector.

Let us see the functions of the magnetic fluxes in the dq axes under the pole, given a magnetic potential distribution as described above:



(a) Distribution on d axis



(b) Distribution on q axis

Figure 1.2: magnetic flux distribution under the pole step.

The inductances of the two axes will then be proportional to the square of the potential magnetic function of the respective axis integrated along the respective path where there is a magnetic flux; we have to refer to the image above:

$$Ld \sim \int_{-\frac{\beta}{2}}^{\frac{\beta}{2}} \cos^2(\xi) d\xi = \int_{-\frac{\beta}{2}}^{\frac{\beta}{2}} \frac{1 + \cos(2\xi)}{2} d\xi = \frac{\beta}{2} + \frac{\text{sen}(\beta) + \text{sen}(\beta)}{4} = \frac{\beta}{2} + \frac{\text{sen}(\beta)}{2}$$

$$Lq \sim 2 \int_0^{\frac{\beta}{2}} \sin^2(\xi) d\xi = \int_{-\frac{\beta}{2}}^{\frac{\beta}{2}} \frac{1 - \cos(2\xi)}{2} d\xi = \frac{\beta}{2} - \frac{\text{sen}(\beta) + \text{sen}(\beta)}{4} = \frac{\beta}{2} - \frac{\text{sen}(\beta)}{2}$$

The goal is to maximize the difference ($Ld - Lq$); then we can find the maximum of the function:

$$\frac{d(Ld - Lq)}{d\beta} = 0$$

$$\frac{d(\text{sen}(\beta))}{d\beta} = \cos(\beta) = 0$$

$$\beta = \frac{\pi}{2}$$

hence, the polar step that maximizes reluctance between the two axes is $\frac{\pi}{2}$ radians.

Having established and maximized the difference between Ld and Lq , it remains to be seen whether their relationship is competitive with respect to that of the asynchronous machine:

$$\sigma^{-1} = \frac{Ld}{Lq} = \frac{\beta + \text{sen}(\beta)}{\beta - \text{sen}(\beta)} = \frac{\frac{\pi}{2} + 1}{\frac{\pi}{2} - 1} \cong 4.5 \ll 20 \text{ of the asynchronous machine}$$

It is therefore inappropriate the use of high-salient geometry for the construction of a reluctance motor.

1.2.2 High anisotropy structures

The principle of these particular structures is to isolate magnetically different segments dividing the rotor into several parts. The purpose is to drive the direct axis inductance $Ld \rightarrow M$, mutual inductance of the asynchronous motor, and $Lq \rightarrow 0$;

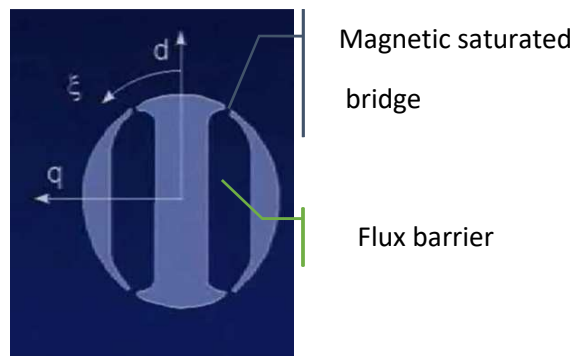


Fig 1.3: High anisotropy structures

Direct-axis induction depends exclusively on the induction on the gap, as it did for induction machines and $Ld \rightarrow M$ as wanted; in addition, the quadrature axis sees only the circulation flow due to the air barriers present in the structure and "counts" the amount of air that encounters: the distribution of magnetomotive force in axis q polarizes the rotor; increasing the number of flow barriers we decrease more and more the rotational flow rate in q-axis.

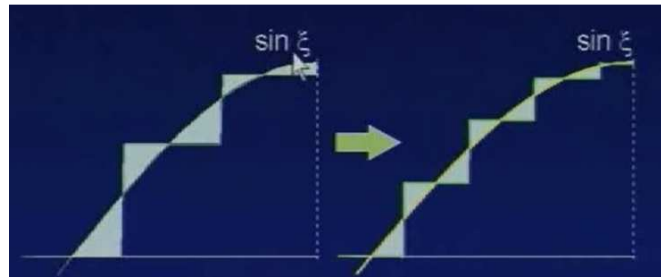


Fig 1.4: distribution of MMF and its flow in q axis as the number of flow barriers increases

Ideally, if the flow barriers tended to an infinite number, the circulation flow would be reduced to zero and $Ld \rightarrow 0$.

Obviously, there is a mechanical limitation in order to do this, also they would lead to high ripple of anisotropic torque to be compensated due to the interaction with the statoric slots.

1.2.3 *Metal sheet lamination techniques*

Axial lamination

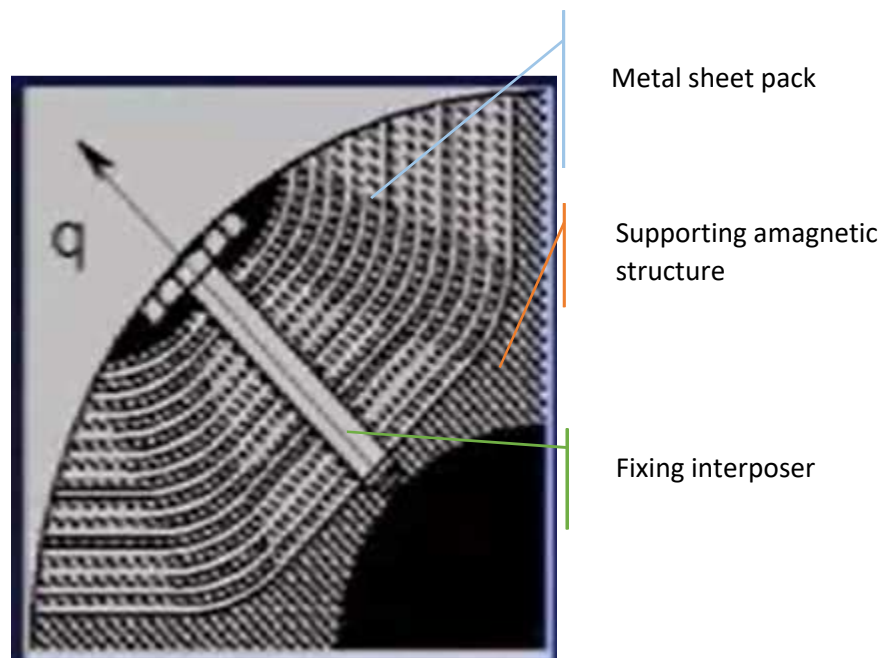


Fig 1.5: Diagram of a rotor pole with axial lamination

The most obvious advantages of this structure are essentially two:

1. very high number of segments, which guarantees high anisotropy;
2. Thickness of the magnetic material sufficiently high, which guarantees high ratios $\left(\frac{Ld}{Lq}\right)$ and consequently high anisotropy.

However, there are numerous disadvantages, in fact, in addition to a non-conventional lamination method, this type of structure does not allow skewing practice and, last but certainly not least, doesn't cut pathways of parasitic currents.

Another disadvantage of this technique is the enormous losses in the iron which it would go encounter during its use.

In fact, the magnetic potential jumps would be high when the considered magnetic sheet goes from being under a stator tooth (high induction level) to a slot (very low magnetic flow). The high frequency at which this magnetic potential jump occurs would lead to very high losses in the iron, losing efficiency.

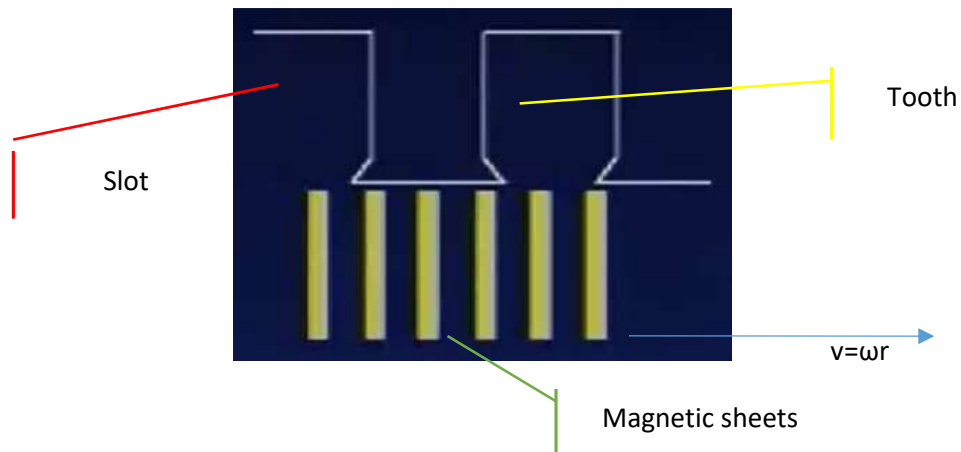


Fig 1.6: high frequency magnetic potential jumps

Cross laminating

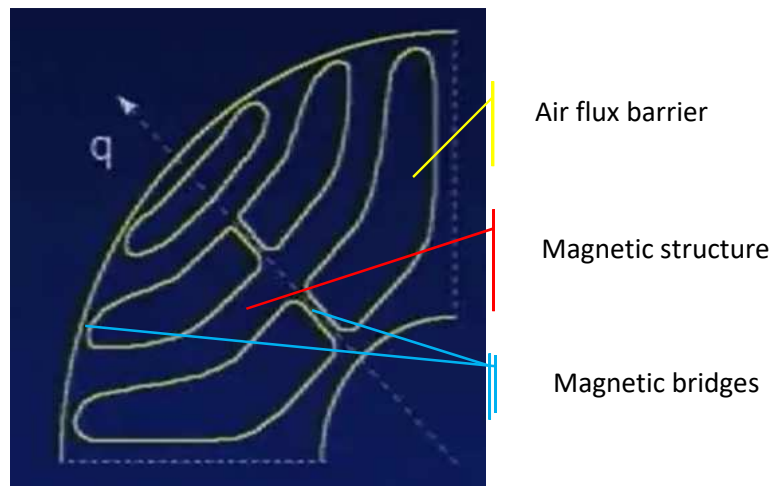


Fig 1.7: transverse lamination structure

The most obvious advantage is the using of cross-lamination method as it is conventional, cuts the paths to parasitic currents and optimizes each magnetic sheet of magnetic flow so as to improve its permeance; for the latter reason, $B_q(\xi)$ is very close to the trend of an ideal sinusoid, as a direct consequence of having very low torque ripple despite the anisotropy is not altogether distributed.

Ultimately, with both structures are reached values of $\sigma^{-1} = \frac{Ld}{Lq} \cong 10$, however lower of the asynchronous machine, but constructively we won't do anything anymore.

I advance here the key factor that allows the motors of this type, including assisted PM, to compete in performances with asynchronous motors: without rotor windings, these don't have rotor resistance ($R_r = 0$) and consequently there are no period of electrical transients, as well as the losses for Joule effect in the rotor; that is, despite the fact that these motors always need magnetizing current in quadrature axis like asynchronous machines, the control may vary to pleasure both d and q, because they don't generate delays in control because the rotor flux that derives from it does not follow transient and it can, therefore, vary differently from what happens with asynchronous motors, where the control sets a certain value of λ_r and therefore of the i_d (field oriented control).

In these machines, the cross - saturation effects can't be neglected: the current in an axis always has demagnetizing effect for the other axis.

This means that the axis magnetic flux will not only affected by its own current axis, but will also vary depending on the presence or absence of current in the other axis; this phenomenon follows the physical principle of equality of coenergy, namely $\frac{d(\lambda d)}{d(iq)} = \frac{d(\lambda q)}{d(id)}$ (1.10.1) ;

Below the images taken directly from the prototype motor that the thesis has as main object that makes it well-known as what just affirmed.

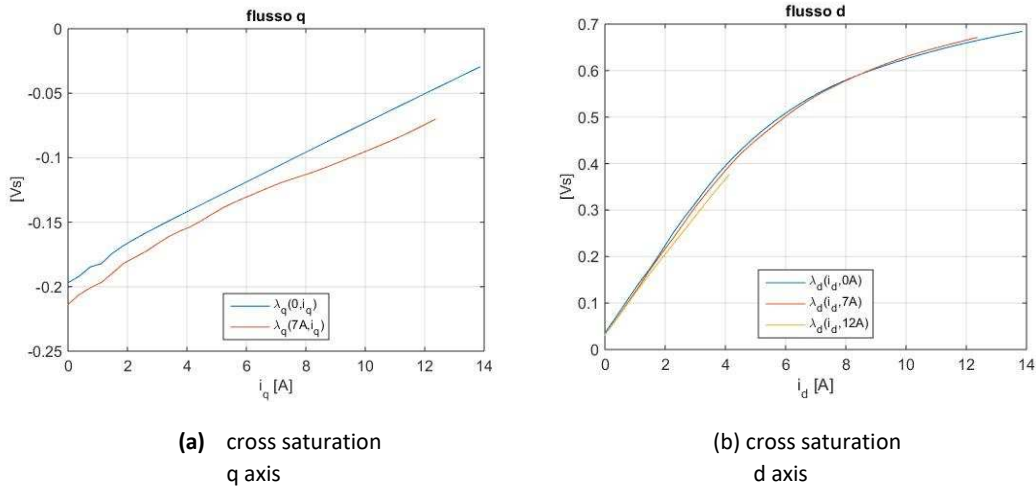


Fig. 1.8

The two areas that are identified between the characteristics 0A and 7A in the two plots must be the same for the principle of coenergy before defined.

1.3 From SynRel to PMAssistedSynRel

Switching from reluctance to reluctance rotors assist by magnets is constructively simple and consists in inserting into the axis with most reluctance value some permanent magnets. Let's see how the expression of the torque in this case changes and the various pros and cons of this choice in terms of performance, flux weakening and efficiency.

1.3.1 Used Convention

Before starting to analyze what the presence of magnets involves, we need to have the understand about the different conventions that can be used for this type of machine. There are, in fact, two different ways of thinking about which is the quadrature axis and which is the direct.

Indeed, the presence of magnets would suggest that, as was in the case of SMPMs, these are oriented as the direct axis; if instead we considered the definitions of the two axes more strictly, that is the one with a minimum reluctance and the one in quadrature with maximum reluctance, the magnets would be considered in the quadrature axis.

The convention used in this paper is the one that sees the magnets oriented as the direct axis, this due to the fact that in ABB it is the most used. Any switch to other convention during the elaborate will be announced time to time.

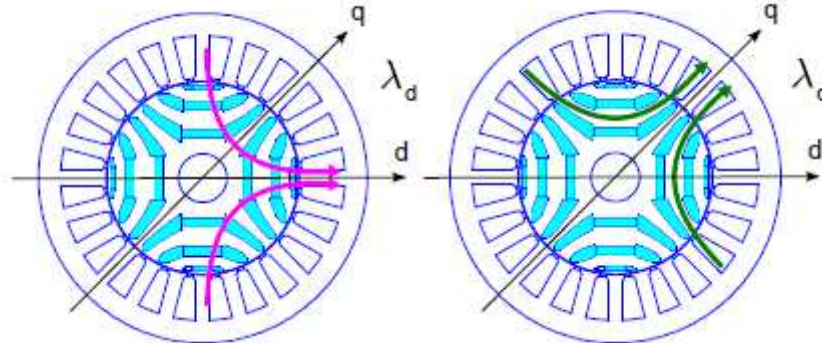


Fig. 1.9: Used Convention

1.3.2 Machine performance and efficiency considerations

Let's see how the torque equation changes for an assisted reluctance motor:

$$T_{rel} = \frac{3}{2} * p * [(L_d - L_q) * i_d] * i_q \quad (1.11)$$

$$T_{PMASR} = \frac{3}{2} * p * [\lambda_m + (L_d - L_q) * i_d] * i_q \quad (1.12)$$

As evident from the expression of torque, which usually comes from the *energy balance* on machine, the presence of magnets adds torque due to the isotropy given by the presence of them.

Differently from SMPM machines, the portion of magnetic flux from the added magnets can't be high (like rare earth magnets) due to the fact that the axis to which they are oriented (the direct one, for our convention) has a high magnetic reluctance due to geometry and it could be saturated under the action of the magnets.

To reinforce this last statement, let's think about the machine flux weakening.

In fact, the key reason for adding permanent magnets is to add direct axis flux, in order to increase machine constant power range. In order to weak the flux in the gap of the machine, we have to add demagnetizing current: if the flow deriving from magnets λ_m was too big, the demagnetizing currents would be as high as the flux of the magnet is high; the consequence would be a drastic drop in efficiency, depending on its quadratic function.

The most used magnets are ferrite, the choice is justified by the last observations.

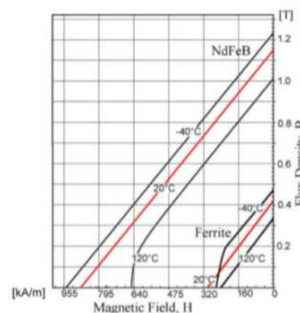


fig 1.10: magnetic material hysteresis cycle

Wanting to summarize the advantages of adding permanent magnets to the direct axis, these are essentially 3:

1. Increased $\cos\phi$ and therefore the available torque
2. Increased constant power range (flux weakening characteristic)
3. Direct consequence of the first, the ratio $\frac{kW}{kVA}$ for assisted reluctance motors is very similar to the induction motors ones, with consequent advantage for the inverter that doesn't need to be oversized.

On the other hand, the controversies resulting from this change can be summarized in four points:

1. Increased Joule loss for high speed as it increases quadrature axis current
2. The control is very complex, such as the inversion of the torque
3. UGO problems (uncontrolled generator operation), although not to the same dimension of SMPM because $(\lambda m_{PMASR} \ll \lambda m_{SMPM})$
4. Ferrite thermal drift, which will limit the field weakening once certain temperatures have been reached

1.3.3 Vector diagram in dq axes and electrical equivalent circuits

The diagrams refer to the other convention, the one for which the magnets are oriented along the axis in quadrature; the transition from one convention to the other is trivial and it involves the following passage for obvious geometric issues:

$$d \rightarrow q \qquad q \rightarrow (-d)$$

Vector diagrams derive directly from the mathematical model of the motor already seen, except for the change of convention.

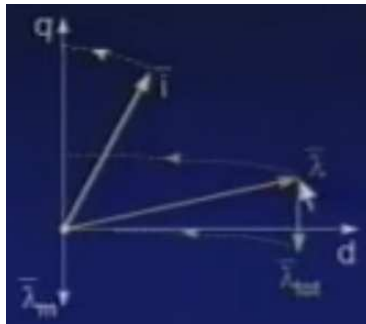


Fig 1.11: vector diagram flows and currents PMASR

The vector diagram would be the same as simple reluctance motors, but with the addition of magnetic flux we will have a different vector and $\bar{\lambda}_{rel} \rightarrow \bar{\lambda}_{tot} = \bar{\lambda} + \bar{\lambda}mq$.

The trajectories in the figure are those that are maintained by the constant current, that is:

$$id^2 + iq^2 = constant \quad (1.13)$$

$$\frac{\lambda d^2}{Ld} + \frac{\lambda q^2}{Lq} = constant \quad (1.14)$$

The second equation represents an ellipse, the first a circumference.

Ideally, following the trajectories shown in the figure, $\bar{\lambda}_{tot}$ never meets the bisector of the first quadrant, point at which the maximum voltage value would be to a certain speed and after which the machine will no longer be a feature $\frac{V}{f}$ constant, the flow will have to go down to keep the voltage constant, as well as the current, in front of a further increase of speed. Ideally, therefore, the speed range of the reluctance motor assisted is *infinite*. In truth, the *phenomena of thermal drift* of the ferrites limit this hypothesis and the deflection range will be about the same as the induction motors. These statements are anticipations of what will be described later when it comes to control trajectories but that help to understand the vector diagram.

1.4 Control Trajectories

The following discussion does not have the purpose of studying in detail the control loops for an assisted reluctance motor, but it is intended to provide the basis to the reader about the trajectories of control according to the mechanical angular velocity of the rotor, thus justifying the course of the electromechanical torque delivered according to the angular velocity.

The key places for a vector control are three:

- MTPA (*maximum torque per amp*)
- MTPV (*max torque per volt*) or MTPF (*maximum torque per flux*)
- LM (*loss minimization*)

These three trajectories always identify a characteristic of current in a dq plane and the switching from one to the other is detected by physical states, such as the maximum value of voltage reached by the converter or the achievement of the maximum current.

It is important to note that, as they are defined, the MTPA feature is the one that minimizes the Joule losses, while MTPV is the one that minimizes losses in iron; the LM trajectory itself will find the two closest to one rather than to the other depending on the motor rotor speed.

Below you can see a vector diagram in dq axes that highlights the first two features, speed-independent.

NB: the figure refers to the convention where the magnets are directed towards the axis in quadrature.

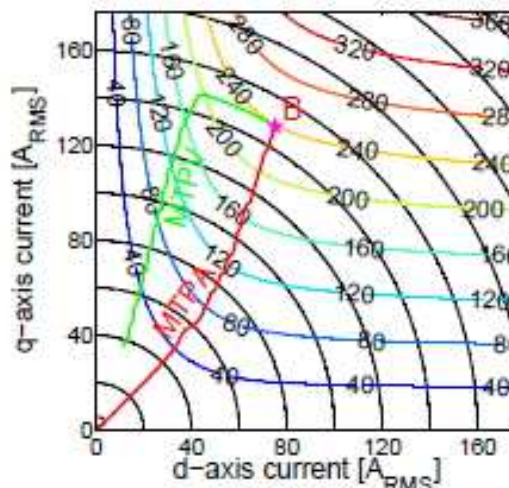


Fig 1.12: motor control trajectories

The current and torque constant locations are also highlighted.

1-MTPA ($0 < \omega < \omega_1$)

From 0 to ω_1 , for any torque required above 240Nm, the drive checks the motor MTPA characteristic for which torque is required for the motor, the current is controlled in module and phase so that it lies on the characteristic MTPA. The torque stays constant and the speed rises. The power consequently rises.

2-FLUX WEAKENING ($\omega_1 < \omega < \omega_2$)

By increasing the speed, reaching the maximum power that can be delivered, it increases the voltage up to become the maximum for the driver. You will no longer be able to work second constant flux logic ($V \cong j\omega\lambda$, neglecting the stator resistance) and it must be decreased entering in flux weakening control region. During this phase, the module of the current is kept constant and the voltage is maximum. The torque, as seen from the figure, will drop in particular with hyperbolic trend, proportional to ω^{-1} and the power will remain constant, making the coarse hypothesis that the PF of the machine does not vary and it keeps constant throughout the feature. Keeping these conditions would lead to enormous iron losses and almost an instantaneous falling of mechanical feature.

3-MTPV ($\omega_2 < \omega < \omega_{max}$)

This phase coincides with the maximum point of the machine static feature, which corresponds to the voltage that you would have to maintain the maximum torque depending on the speed of the motor, that corresponds to the best magnetic flux condition, in module and phase. During this phase, the voltage remains high but the current module lowers inversely proportional to the angular speed of the machine; the torque trend is inversely proportional to the square of the angular velocity of the torque and consequently lowering power.

1.5 Performance comparison between AC motors

The comparison in terms of performance is done based on the torque density of the machine, that is, referring to a current, considered equal to the required torque, the dimensions of the machine and the cooling conditions, the ratio between the torque identifying currents for the various types of motors. All this is equivalent to making comparisons in terms of efficiency in delivering torque under stalled conditions.

$$\eta = \frac{P_m}{P_m + W_d} = \frac{\omega_m}{\omega_m + \frac{W_d}{T_0}} \quad (1.16)$$

The maximum performance condition will be:

$$\max \eta \rightarrow \max \frac{T_0}{W_d}$$

Let us analyze the machines to be compared, first considering the stator differences, then those rotor.

The *stator* is identical for all types of AC motor (induction, brushless, synchronous reluctance and synchronous reluctance assisted); saying that the stator is the same for all, means to say that the induction peak at the air gap B_{max} is common to all. But this doesn't mean having the same flux! This is because the presence of magnets or less influence the waveform of the air gap induction, making it more or less wide (Brushless have in fact the higher flux in the gap via the use of rare earth magnets, tracing the characteristic waveform of flux helmet under the gap).

For this reason, simple coefficients are defined:

Brushless: $T_b \sim k_b * i_{qb}$ (1.17)

Induction: $T_i \sim k_r * i_{qi}$ (1.18)

Reluctance: $T_r \sim k_{dq} * i_{qr}$ (1.19)

The three coefficients are:

- $1 < k_b < 2/\sqrt{3}$
- $k_r < 1 \sim \sqrt{0.94}$
- $k_{dq} < 1 \sim 0.9$

The *rotor*, on the other hand, is not equal for everyone and it is responsible for a different formulation for the torque T:

$$T_b = \frac{3}{2} * p * \lambda_m * i_{qb} \quad (1.20)$$

$$T_i = \frac{3}{2} * p * k_r * \lambda_r * i_{qi} \quad (1.21)$$

$$T_r = \frac{3}{2} * p * (\lambda_d * i_{qr} - \lambda_q * i_{dr}) \sim \left(1 - \frac{L_d}{L_q}\right) * \lambda_d * i_{qr} \rightarrow T_r = \frac{3}{2} * p * k_{dq} * \lambda_d * i_{qr} \quad (1.22)$$

Let us assume now that all the motors produce the same power lost Wd:

$$Wd = \begin{cases} W_b = \frac{3}{2} * R * i_{qb}^2 \\ W_r = \frac{3}{2} * R * (i_{qr}^2 + i_{dr}^2) \\ Wi = \frac{3}{2} [R * (i_{qi}^2 + i_{di}^2) + R_r * (k_r * i_{qi})^2] \end{cases}$$

In fact, the brushless does not require a direct axis current because it is already excited by his surface mounted magnets; the induction motor, in addition to the stator windings, also has rotor motors and the dissipated power is distributed between the rotor and the stator.

To continue the discussion, empirical values will be used that make sense of the comparisons that we want to do; generally, it will be assumed the $\frac{i_d}{i_q}$ ratio; as the radial dimension increases, i_d proportionally decrease and therefore the ratio $\frac{i_d}{i_q}$ will do the same: this ratio for reluctance machines is supposed to be 0.4. In addition to the ratio between currents, the relationship between rotor and stator resistance of the asynchronous will be assumed as $\frac{R_r}{R}$ 0.8, which can be justified by averaging between starting values and nominal values.

$$\underline{W_b = W_r}$$

$$i_{qb}^2 = i_{qr}^2 + i_{dr}^2 = (1 + 0.4^2) * i_{qr}^2 \rightarrow i_{qb} = \sqrt{1 + 0.4^2} * i_{qr} \rightarrow i_{qr} \cong 0.93i_{qb}$$

$$\underline{W_b = W_i}$$

$$i_{qb}^2 = i_{qi}^2 * \left(1 + \frac{Rr}{R} * kr^2\right) + i_{di}^2 = i_{qi}^2 * \left(\left(1 + \frac{Rr}{R} * kr^2\right) + 0.4^2\right) \rightarrow i_{qi} = 0.7i_{qb}$$

This means that, to have the same losses that would occur in a brushless motor by a current path of 1 Ampère, 0.93A would be enough for a reluctance motor or even 0.7A for one by induction. For assisted reluctance motors, the only disadvantage that they have with respect to Brushless is the presence of the magnetizing current, however with a ratio lower than 0.4 between the currents of two axes in quadrature. Ultimately, it would take about **0.97A** to have the same losses of brushless paths by 1A.

The considerations made so far are indicative, of course, of the machine returns. Below, we see a table that also highlights the costs and range of flux weakening:

	T_0	Deflux $\left(\frac{kVA}{kW}; \frac{\omega^2}{\omega_1}\right)$	Affordability	Applications
NdFeB	1	/	--	Assi
Ferrite	0.7	/	+-	Assi
Induction	0.55/0.6	2;4	++	Mandrini
Reluctance	0.7/0.75	3;4	++	Assi/Mandrini
PMASR	0.9	<2;4	+-	Mandrini

Table 1.1

Chapter 2

ABB

Industrial context and programs used

In this chapter we will make a general statement of the industrial context in which the document was created, both programs were used. This is to allow the reader to have an idea of the tools necessary to do an analysis similar to the one that it will be in the second part of the elaborate to give knowledge about how a large company like ABB will arrange for meet European development targets.

2.1 R&D team

The team of R & D (research and development) is a team that aims to keep pace with today's technology, developing innovative design of electric machines and testing them in view of a possible industrial production.

The team receives ABB internal orders for special applications, in this case all the motors are developed for low-voltage applications (220 / 380V), with various power range, from hundred W to nearly a hundred kW.

2.2 Used program

The programs used are essentially two, one used for FEM simulations, in turn internally composed of multiple programs that carry out separate phases of processing and post-processing, and the other used for the processing of the data, MATLAB; as well as for data processing, MATLAB was also used to invoke external programs doing in a loop some callout according to precise logics, manipulating the input data to the simulation. About MATLAB and its use, see the website of Mathworks, readily available from any search motor.

2.2.1 Adept for FEM simulation

The simulation program used is internal ABB.

Great potential of this software tool is being able to automatically generate the geometry for analysis by providing only a few key dimensions of the stator and rotor structure to be studied with the finite element analysis.

The screen interface is simple and intuitive, here you can modify the simulation data, being able to vary the supply voltage, the mechanical power output and the target frequency, but not only: you can vary the geometry, the rotor temperature and stator system, you can select a time dependent simulation or static depending on the output of the useful simulation.

Below you can see a flow chart of how Adept works.

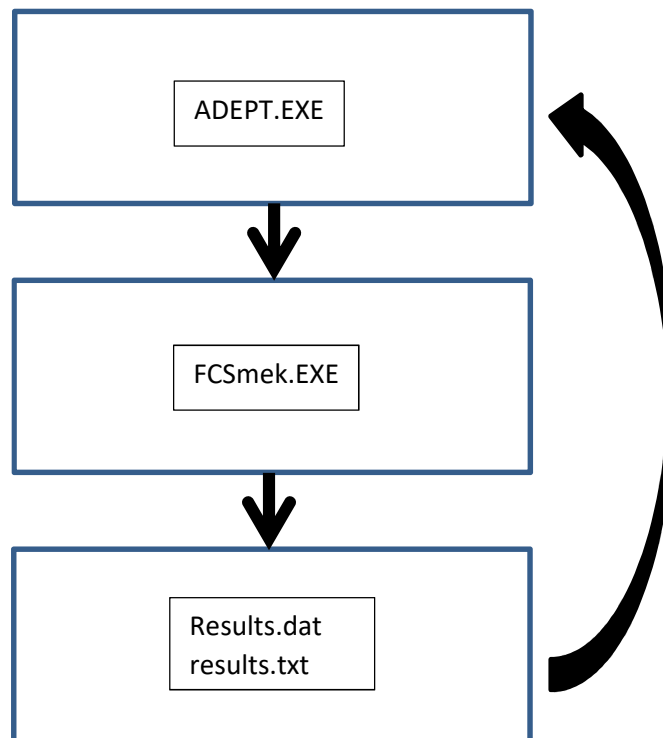


Fig 2.1: ADEPT flow chart

Looking the image above, we should focalise our attention to the FCSMEK blocks. This is the core program about ADEPT FEM simulations.

2.2.2 FCSmek input

The FCSmek calculation profile in Adept is divided into four groups of parameters; operating points, geometry parameters, calculation parameters and time stepping parameters.

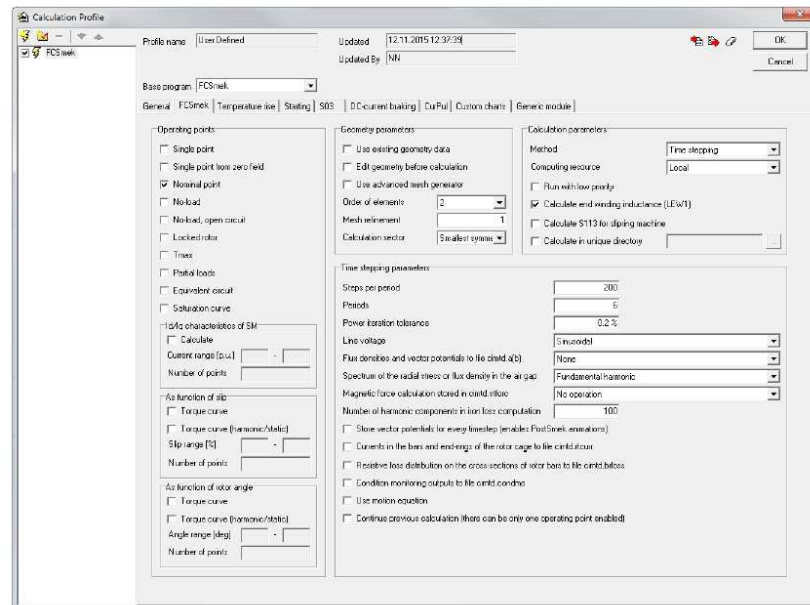


Fig 2.2: Calculation profile of FCSmek

Operating points

Single point

Single point from zero field: This can be used for example to calculate dynamic start of a motor with time stepping analysis using motion equation.

Nominal point

No-load

No-load open circuit: current supply with zero current. Current supply with zero current.

Locked rotor: operating point where slip is 100 %

Tmax: operating point which gives maximum torque

Partial loads: operating points for 25 %, 50 %, 75 % and 125 % of nominal power.

Saturation curve: for induction machines this means no-load current and power as function of supply voltage. For synchronous machines this means open-circuit voltage and short-circuit current as function of field current curves.

Id/Iq characteristics of SM: table of direct and quadrature axis flux as a function of direct and quadrature axis currents is calculated. This task is valid only for synchronous machines and its main use is to provide parameters to people who tune frequency converter parameters.

Torque curve as function of rotor slip

Torque curve as function of rotor angle

Geometry parameters

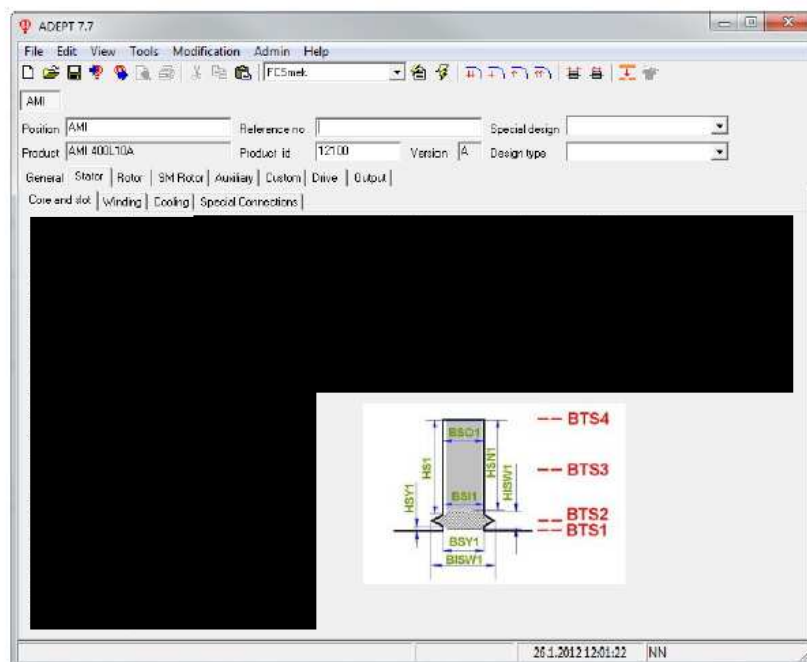
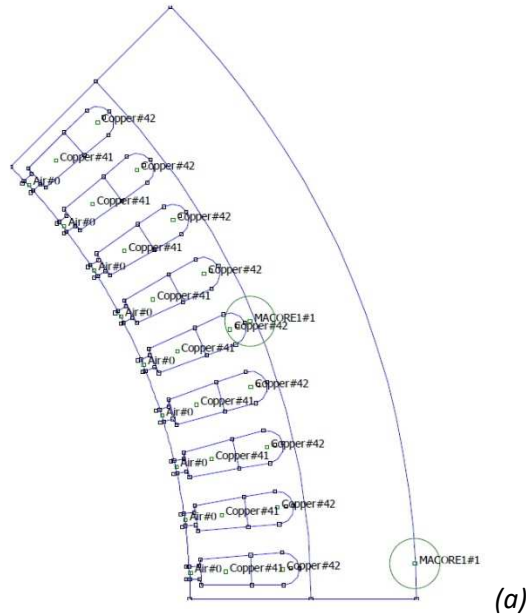
Use existing geometry data: It is so that after each calculation Adept reads from calculation folder FCSmek geometry definition files to Adept as parameters. If this option is enabled Adept will write those files to calculation folder before next calculation. This is useful behaviour if user has modified the geometry manually and wishes to use the same geometry also for next calculation. See next option for more details on geometry modification.

Edit geometry before calculation

Use advanced mesh generator

Order of elements: This defines the order of the elements to be used in the simulation. The recommended selection is to use second order elements. Experience has shown that by using third order elements one does not gain much in accuracy but loses a lot in simulation time

Mesh refinement: Factor for increasing the mesh density near air-gap region.



(b)

Fig 2.3: (a) output geometry (b)input data for auto generation of geometry

Calculation parameters

That parameters control the calculation process.

Method: This defines the simulation type, time harmonic or time stepping

Computing resource: This defines where the calculation is done. Default option is to do the calculations in the local computer; there is the option that can use remote environment in order to not use the local CPU and run more process in parallel.

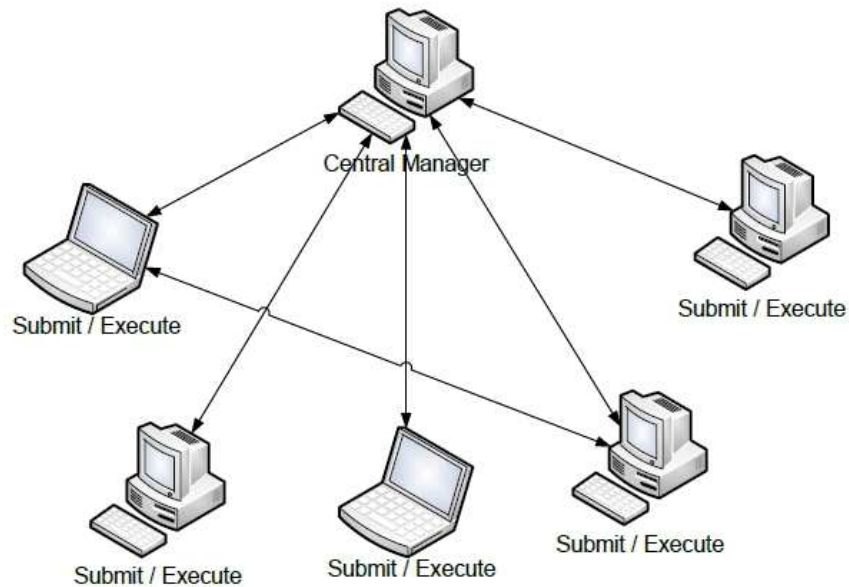


Fig 2.4: Condor: remote CPU usage

Time stepping parameters

Steps per period: the number of time steps used per every period of supply. is important to specify here high enough number to catch all phenomenas user is interested. This number for example directly how high frequencies are available after FFT spectrum analysis.

Periods: this defines how many supply periods the simulation is run

Power iteration tolerance: This value is used to determine how accurately the power iterations will be done. Maximum allowed power error as percentages of nominal power

Line voltage: this option defines what kind of supply will be used.

Spectrum of the radial stress or flux density in the air gap

Magnetic force calculation

Number of harmonic components in iron loss computation: the default value here is 100 harmonics in iron loss components.

2.2.3 FCSmek output

The outputs of the program are derived from processing and post processing practices and they depends on the request made as input for the program. They are organized into text files and Excel files, each containing different information, output from the magnetostatic simulation or those of the simulation time stepping. The following images are going to show some standard outputs that allow us to do both evaluations snapshots or data processing.

SPECIAL 160ML4 G Base program: Fcsmek-cimtd 10.04.2017 - 14:59:22																																													
OUTPUT (mech):	1.497 kW	LOAD(%)	EFF(%)	CURRENT(A)	cosf																																								
INPUT:	1.612 kW	100 :	92.88	3.43	0.9087 ind																																								
VOLTAGE:	298.0 V	75 :	0.00	0.00	0.0000																																								
FREQUENCY:	100.00 Hz	50 :	0.00	0.00	0.0000																																								
CONNECTION:	Star	25 :	0.00	0.00	0.0000																																								
CURRENT:	3.43 A	125 :	0.00	0.00	0.0000																																								
COSFI:	0.9087 ind	0 :		0.00	0.0000																																								
TORQUE:	4.77 Nm	start:		0.00	0.0000																																								
SPEED:	3000.00 rpm																																												
POLES:	4																																												
<table border="1"> <thead> <tr> <th></th> <th>TORQUE(Nm)</th> <th>SPEED(rpm)</th> <th>DELTA(deg)</th> </tr> </thead> <tbody> <tr> <td>Tn</td> <td>4.77</td> <td>3000.00</td> <td>65.505</td> </tr> <tr> <td>Tmax</td> <td>0.00</td> <td>0.00</td> <td>0.000</td> </tr> <tr> <td>Tmin</td> <td>0.00</td> <td>0.00</td> <td>0.000</td> </tr> <tr> <td>Ts</td> <td>0.00</td> <td></td> <td></td> </tr> <tr> <td colspan="4">STARTING</td> </tr> <tr> <td>Ts/Tn</td> <td>0.00</td> <td></td> <td></td> </tr> <tr> <td>Tmin/Tn</td> <td>0.00</td> <td>TRUN1: 20.0</td> <td>K</td> </tr> <tr> <td>Tmax/Tn</td> <td>0.00</td> <td>TRUN2: 20.0</td> <td>K</td> </tr> <tr> <td>Is/In</td> <td>0.00</td> <td>Amb: 25.0</td> <td>C</td> </tr> </tbody> </table>							TORQUE(Nm)	SPEED(rpm)	DELTA(deg)	Tn	4.77	3000.00	65.505	Tmax	0.00	0.00	0.000	Tmin	0.00	0.00	0.000	Ts	0.00			STARTING				Ts/Tn	0.00			Tmin/Tn	0.00	TRUN1: 20.0	K	Tmax/Tn	0.00	TRUN2: 20.0	K	Is/In	0.00	Amb: 25.0	C
	TORQUE(Nm)	SPEED(rpm)	DELTA(deg)																																										
Tn	4.77	3000.00	65.505																																										
Tmax	0.00	0.00	0.000																																										
Tmin	0.00	0.00	0.000																																										
Ts	0.00																																												
STARTING																																													
Ts/Tn	0.00																																												
Tmin/Tn	0.00	TRUN1: 20.0	K																																										
Tmax/Tn	0.00	TRUN2: 20.0	K																																										
Is/In	0.00	Amb: 25.0	C																																										
200 steps/period, 2 periods. Supply: sinusoidal																																													

(a) results-1

Fig 2.5: output for immediate analysis

Numerous other output will be used to do frequency dependent analysis of electrical, mechanical and magnetics quantities, that are also useful to build the flux matrix, also considering the cross-saturation effects and the possible thermal drift of the permanent magnets.

Here are some plots resulting from these outputs:

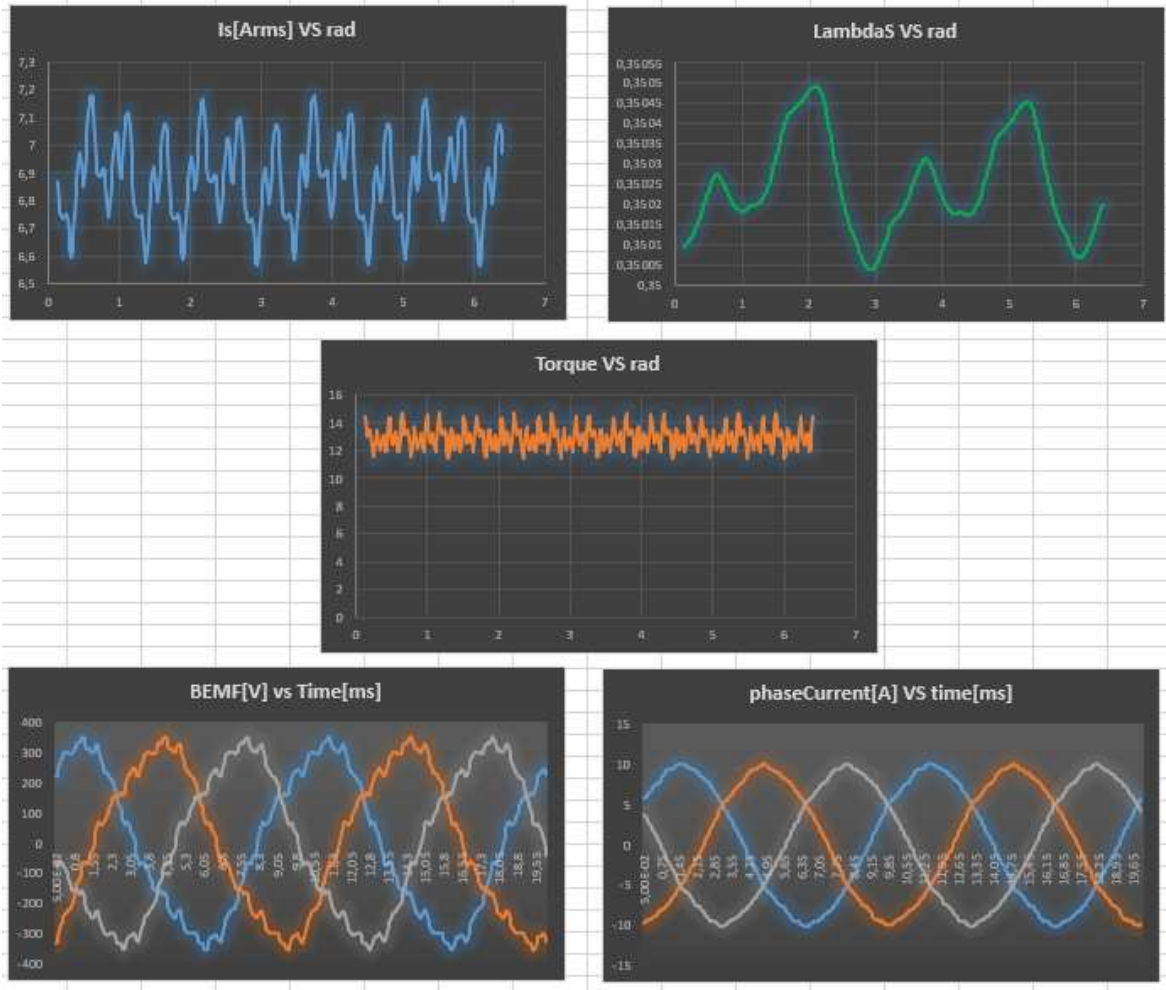
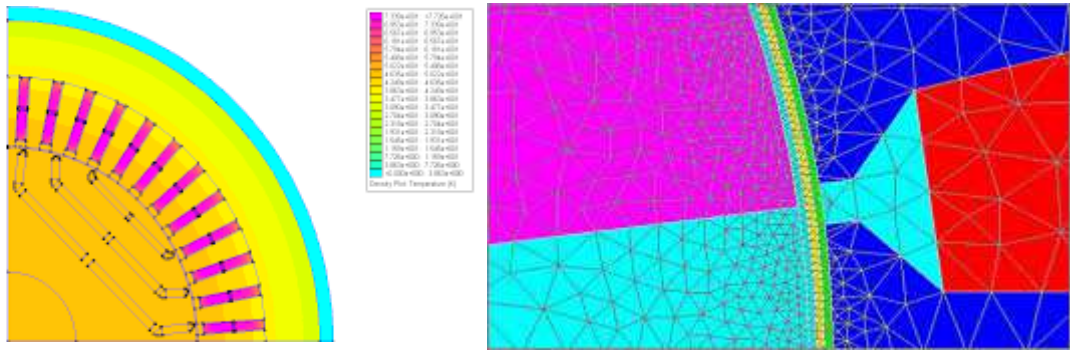


Fig 2.7: Output that evidence the harmonic distortions

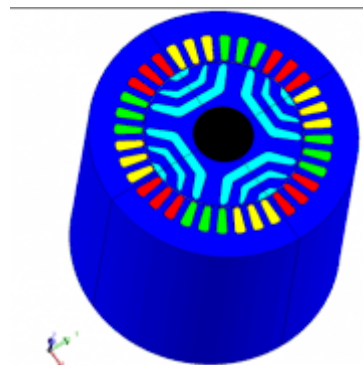
Another useful tool that FCSmek provides is the *PostFCSmek* ; it graphically illustrates the geometry highlighting the characteristics of both mesh and physical. It shows precisely, using chromatic scales, the density of the losses on the motor geometry, the one of the magnetic flux, the temperature distribution, the geometry and the division into areas for the study FEM, the current density on the cables in the stator slots etc.

The following images are going to show some outputs examples from PostFCSmek.



(a) Temperature distribution

(b) mesh result



(c) Complete machine materials

Fig 2.8: (a) (b) (c) PostFCSmek output

2.2.4 Adept optimization tool

One of the most powerful tools, is surely the one for the optimization phase.

Following optimization techniques according to genetic algorithms and using for example the Pareto method (which will be mentioned on the third chapter), this tool is able to optimize objective functions building an extremely high number of individuals and generations.

Of course, the output of the optimization tool can be varied depending on how you are going to set the optimization parameters; it shows an example in the picture, which anticipates in part the third chapter, but it is useful to understand this practice.

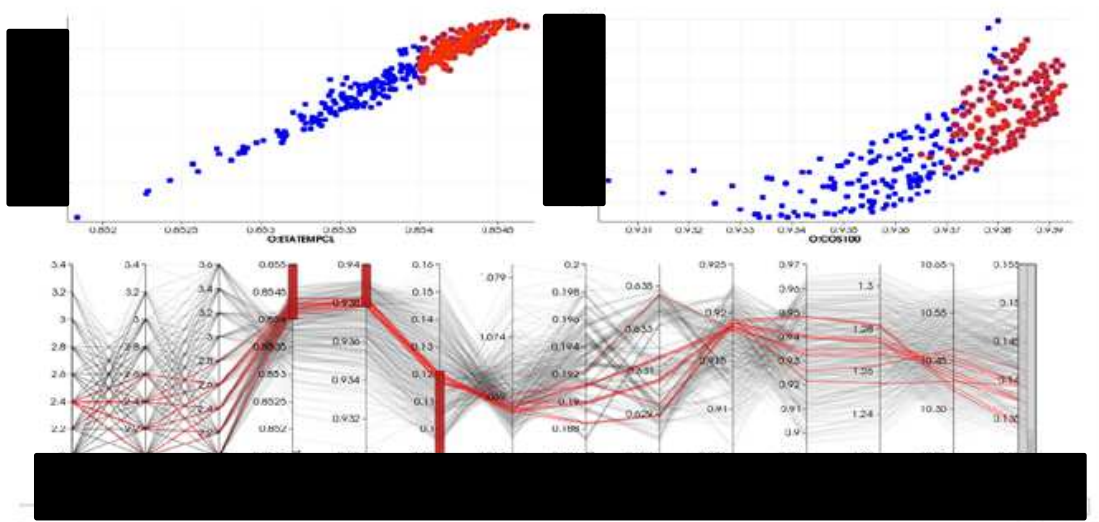


Fig 2.9: optimization tool output

In the picture the target to which the simulation aims are vertically highlighted, the lines that continue horizontally represent the best individual of each generation. In the upper figures, the points in blue and red represent the population of a generation, the red ones are the individuals who exceed a certain level of fitness in the environment set where they "live" (with environment we intent a complex system of inter-related functions).

2.2.5 Limitations

The limitation that I have encountered in using this powerful software is the fact that it can't carry out simulations to find the feature that maximizes the torque for the same current module (MTPA) or other characteristics like that. It is not thought to control studies on the motor, but to make as easier as possible the construction of the electric motor.

The search for that kind of features has been made, therefore, manually, searching the points of interest by doing simulations in groups between two limit supply voltages, with a certain discretization of the voltage set.

Despite the speed of single simulation, this type of research activity was too slow.

A second limitation of the program, is that the output of the magnetostatic simulations, to define the matrix of the machine flows, don't mediate the effects that teeth and stator slots have on the state of flows. The simulation can't provide, in addition, a complete matrix of flows but leaves some elements at zero when there is a high level of saturation of the iron.

This function also doesn't make possible to customize the range of currents you want. In Chapter 7 will be described how to solve all these problems, because the processing of the provide data makes possible to find all the machine control trajectories.

Furthermore, there is no correspondence between the matrix of inductances and those of the flux from the same simulation. It must be a program bug.

Another bug concerns the direct axis detection for the simulations time stepping and magnetostatic; it will be seen in chapter 5 how this error can be easily remedied using a simple spreadsheet.

Chapter 3

SynRM2

Objective, design and optimization phase

This chapter will describe the different stages faced by the R & D team for the development of high-efficiency motors, passing from mechanical considerations to energy considerations, as well as the quality in the torque developed. It will then be taken, for example, a prototype, following each procedure in detail. ABB calls the reluctance motors assisted by magnets SynRM2 instead of PMASR.

Firstly, it will be clarified what we mean when we talk about efficiency classes, in particular regarding the IE4 and IE5 ones. It will also be made an introduction about the used optimization technique.

As we know, the energy efficiency of an electric motor is very important, considering that about 75% of the electric energy consumed in the industrial sector is due to deliver the power to the electric motors.

The standard EN 60034-30 determines a classification of the performance of motors according to the IE code (*International Efficiency*):

1. IE1 *Standard*;
2. IE2 *High*;
3. IE3 *Premium*;
4. IE4 *Super Premium*;

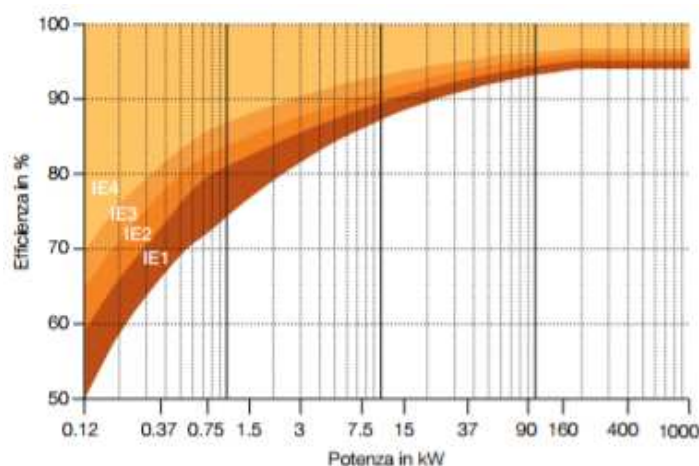


Fig 3.1: Efficiency class for a 4 poles motor, 50 Hz

It is expected the introduction of IE5 level in a forthcoming edition, with the aim of further reducing losses by 20% compared to IE4 class.

But what are the motors that fit the standard?

The new standard includes a wider range of products. The power range has been extended and starts from 120 W up to 1000 kW. All types of electric motors in AC fall in the standard if they are dimensioned for direct operation by the network. This includes the following types:

- electric motors with single speed (mono and three-phase), 50 Hz and 60
- 2, 4, 6 or 8 poles
- nominal power PN from 0.12 kW to 1000 kW
- nominal voltage UN exceeding 50 V up to 1 kV
- motors capable to operating in continuous service to the respective nominal power with over temperature value within the limits of the specific thermal insulation class
- marked motors with an ambient temperature range between -20 °C and + 60 °C
- marked motors with a maximum altitude of 4000 m above sea level.

The following motors are not included in the standard IEC / EN 60034-30-1

- single speed motors with 10 or more poles or multi-speed motors
- totally integrated motors in a machine (for example, pumps, fans or compressors) that can't be tested separately from the machine
- electric motors self-brake, if the brake can't be dismantled or separately power supply.

How is it marked a class IE?

The lowest efficiency value of voltage combinations listed and the relative IE class are marked in the motor nameplate.

Reported below is the table according to IEC / EN 60034-30-1: 2014 regarding the efficiency of the motor based on the number of poles and the output power:

Potenza	IE1				IE2				IE3				IE4			
	2 poli	4 poli	6 poli	8 poli	2 poli	4 poli	6 poli	8 poli	2 poli	4 poli	6 poli	8 poli	2 poli	4 poli	6 poli	8 poli
0.12	45.0	50.0	38.3	31.0	53.6	59.1	50.6	39.8	60.8	64.8	57.7	50.7	66.5	69.8	64.9	62.3
0.18	52.8	57.0	45.5	38.0	60.4	64.7	56.6	45.9	66.9	69.9	63.9	58.7	70.8	74.7	70.1	67.2
0.25	54.6	58.5	47.6	39.7	61.9	65.9	58.2	47.4	67.2	71.1	65.4	60.6	71.9	75.8	71.4	68.4
0.37	63.9	66.0	59.7	49.7	69.5	72.7	67.6	56.1	73.8	77.3	73.5	69.3	78.1	81.1	78.0	74.3
0.40	64.9	66.8	61.1	50.9	70.4	73.5	68.8	57.2	74.6	78.0	74.4	70.1	78.9	81.7	78.7	74.9
0.55	69.0	70.0	65.8	56.1	74.1	77.1	73.1	61.7	77.8	80.8	77.2	73.0	81.5	83.9	80.9	77.0
0.75	72.1	72.1	70.0	61.2	77.4	79.8	75.9	65.2	80.7	82.5	78.9	75.0	83.5	85.7	82.7	78.4
1.1	75.0	75.0	72.9	66.5	79.6	81.4	78.1	70.8	82.7	84.1	81.0	77.7	85.2	87.2	84.5	80.8
1.5	77.2	77.2	75.2	70.2	81.3	82.8	79.8	74.1	84.2	85.3	82.5	79.7	86.5	88.2	85.9	82.6
2.2	79.7	79.7	77.7	74.2	83.2	84.3	81.8	77.6	85.9	86.7	84.3	81.9	88.0	89.5	87.4	84.5
3	81.5	81.5	79.7	77.0	84.6	85.5	83.3	80.0	87.1	87.7	85.6	83.5	89.1	90.4	88.6	85.9
4	83.1	83.1	81.4	79.2	86.8	86.6	84.6	81.9	88.1	88.6	86.8	84.8	90.0	91.1	89.5	87.1
5.5	84.7	84.7	83.1	81.4	87.0	87.7	86.0	83.8	89.2	89.6	88.0	86.2	90.9	91.9	90.5	88.3
7.5	86.0	86.0	84.7	83.1	88.1	88.7	87.2	85.3	90.1	90.4	89.1	87.3	91.7	92.6	91.3	89.3
11	87.6	87.6	86.4	85.0	89.4	89.8	88.7	86.9	91.2	91.4	90.3	88.6	92.6	93.3	92.3	90.4
15	88.7	88.7	87.7	86.2	90.3	90.6	89.7	88.0	91.9	92.1	91.2	89.6	93.3	93.9	92.9	91.2
18.5	89.3	89.3	88.6	86.9	90.9	91.2	90.4	88.6	92.4	92.6	91.7	90.1	93.7	94.2	93.4	91.7
22	89.9	89.9	89.2	87.4	91.3	91.6	90.9	89.1	92.7	93.0	92.2	90.6	94.0	94.5	93.7	92.1
30	90.7	90.7	90.2	88.3	92.0	92.3	91.7	89.8	93.3	93.6	92.9	91.3	94.5	94.9	94.2	92.7
37	91.2	91.2	90.8	88.8	92.5	92.7	92.2	90.3	93.7	93.9	93.3	91.8	94.8	95.2	94.5	93.1
45	91.7	91.7	91.4	89.2	92.9	93.1	92.7	90.7	94.0	94.2	93.7	92.2	95.0	95.4	94.8	93.4
55	92.1	92.1	91.9	89.7	93.2	93.5	93.1	91.0	94.3	94.6	94.1	92.5	95.3	95.7	95.1	93.7
75	92.7	92.7	92.6	90.3	93.8	94.0	93.7	91.6	94.7	95.0	94.6	93.1	95.6	96.0	95.4	94.2
90	93.0	93.0	92.9	90.7	94.1	94.2	94.0	91.9	95.0	95.2	94.9	93.4	95.8	96.1	95.6	94.4
110	93.3	93.3	93.3	91.1	94.3	94.5	94.3	92.3	95.2	95.4	95.1	93.7	96.0	96.3	95.8	94.7
132	93.5	93.5	93.5	91.5	94.6	94.7	94.6	92.6	95.4	95.6	95.4	94.0	96.2	96.4	96.0	94.9
160	93.8	93.8	93.8	91.9	94.8	94.9	94.8	93.0	95.6	95.8	95.6	94.3	96.3	96.6	96.2	95.1
200	94.0	94.0	94.0	92.5	95.0	95.1	95.0	93.5	95.8	96.0	95.8	94.6	96.5	96.7	96.3	95.4
250	94.0	94.0	94.0	92.5	95.0	95.1	95.0	93.5	95.8	96.0	95.8	94.6	96.5	96.7	96.3	95.4
315	94.0	94.0	94.0	92.5	95.0	95.1	95.0	93.5	95.8	96.0	95.8	94.6	96.5	96.7	96.3	95.4
355	94.0	94.0	94.0	92.5	95.0	95.1	95.0	93.5	95.8	96.0	95.8	94.6	96.5	96.7	96.3	95.4
400	94.0	94.0	94.0	92.5	95.0	95.1	95.0	93.5	95.8	96.0	95.8	94.6	96.5	96.7	96.3	95.4
450	94.0	94.0	94.0	92.5	95.0	95.1	95.0	93.5	95.8	96.0	95.8	94.6	96.5	96.7	96.3	95.4
500-	94.0	94.0	94.0	92.5	95.0	95.1	95.0	93.5	95.8	96.0	95.8	94.6	96.5	96.7	96.3	95.4
1000																

Fig 3.2: efficiency value based on poles number and mechanical power output (from ABB web site)

3.2 SynRM2 ABB

This range of motors is classified according the size identifiable through the rotor height from the ground.

They are distinguished in 6 sizes:

- H71
- H80
- H90
- H100/112
- H132
- H160

For the following discussion, reference will be made about one of these sizes; for industrial confidentiality reasons and copyright ABB, we will focus only on the procedure used and some engineering techniques used to address specific problems, omitting images or darken parts and results for which this document is not authorized to show information about.

3.2.1 Preliminary mechanical evaluation

This section aims to make a preliminary analysis with the purpose of dimensioning the critical parts of the lamination of the rotor, i.e. the iron bridges. All assessments were made referring to electrical datasheet of magnetic sheet steel M400-50A; below some basic properties, as well as some design assumptions about the mechanical bridges:

Max Speed	5400 RPM
Stack Length	Max possible, from M3AA frame designs
Magnet Size	Max possible, from lamination design
Lamination Material	M400-50A
Targeted Safety Factor (on max yield stress)	2

(a)

Material	Property	Value
M400-50A	Yield strength	325 N/mm ²
M400-50A	Young's modulus	210 000 N/mm ²
M400-50A	Poisson coefficient	0.3
M400-50A	Density	7700 Kg/m ³
Ferrite	Yield strength	185 N/mm ²
Ferrite	Young's modulus	1.7 E11 Pa
Ferrite	Poisson coefficient	0.3
Ferrite	Density	4700 Kg/m ³

(b)

Fig 3.3: (a) main hypotheses for mech evaluation (b) materials properties

Let's see how proceeds the mechanical assessment of the preliminary section of the rotor, H80 SynRM2;

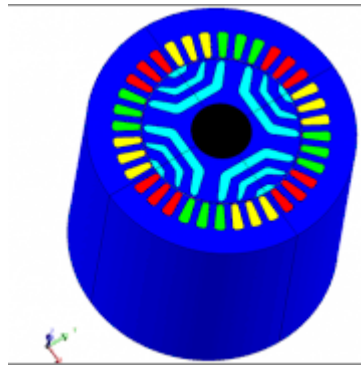
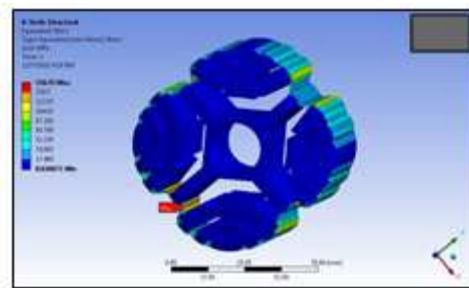


Fig 3.4: preliminary cross section – example

Simulation results are summarized in the following table, for different dimension of the bridges:

Bridge dimension [mm]	Max Stress [MPa]	Safety Factor (Yield)
	125.64	2.59
	171.09	1.90
	156.93	2.07

(a)



(b)

Fig 3.5: (a) Simulation max stress results (b) simulation output figure

It is here fixed the initial geometry once obtained a safety factor greater than 2.

3.2.2 Optimization phase

Abstract - Genetic Algorithm

The optimization method used by ABB for this phase is the genetic algorithm, for which will make a brief introduction; for the insights, refer to bibliographical notes.

The genetic algorithm is heuristic, and it's based on the principle of natural selection and biological evolution theorized in 1859 by Charles Darwin. The "genetic" adjective comes from the fact that the evolutionary model is Darwinian explanations of a branch of biology, called genetics, and genetic algorithms implement similar mechanisms of choice to those of biochemical processes discovered by this science.

To apply it to our case, without going into the heart of algorithm, for which reference should be made to the bibliographical notes where you can find both the genetic operators, as well as the various definitions, one must understand how this algorithm meanwhile reasons.

The genetic algorithm, involves the construction of an *environment*, a generation composed by

The following are some of the design constraints adopted:

- Stator lamination geometry and mechanical parts are inherited from M3AA H80 motor of the ABB induction motor catalogue.
- Single layer winding
- Supply line to line voltage = 370V
- Operating temperature range: [-20÷105°C]
- Overloadability = 1.5
- RE free PMs; Br = 400mT
- Minimum fillet radius = 1mm
- Maximum acceptable value of the torque ripple (TTHD) is to be determined.

Some details on the FE simulation settings are listed as follows:

- Order of the elements 2
- Mesh refinement 1
- Steps per period 180
- Periods of run 2

Two different optimization studies will done.

1. Two filled flux barriers and one empty flux barrier

Population size set: 600;

Parameter description	Adept symbol	Unit	Target
Efficiency	ETATEMPCL		Maximize
THD of the torque waveform	TTHD	[%]	Minimize
Power factor	COS100		Maximize

(a)

Parameter description	Adept symbol	Min	Max	Step
Thickness of the 1 st barrier (inner barrier)	BM1			0.2
Thickness of the 2 nd barrier	BM2			0.2
Thickness of the 3 rd barrier (outer barrier)	BM3			0.2
Position of the 1 st barrier	B21			0.1
Position of the 2 nd barrier	B22			0.1
Position of the 3 rd barrier	B23			0.1
Number of effective turns per slot	ZN1			1

(b)

Fig 3.7: (a) optimization objectives; (b) optimization variables

Below we can see the output of the generic algorithm form Pareto fronts, as well as the identification of the best individual:

OUTPUT (mech):	0.750 kw	LOAD(%)	EFF(%)	CURRENT(A)	cosf
INPUT:	0.852 kw	100 :	87.96	1.40	0.9456 ind
VOLTAGE:	370.0 V	75 :	0.00	0.00	0.0000
FREQUENCY:	50.00 Hz	50 :	0.00	0.00	0.0000
CONNECTION:	Star	25 :	0.00	0.00	0.0000
CURRENT:	1.40 A	125 :	0.00	0.00	0.0000
COSFI:	0.9456 ind	0 :	0.00	0.00	0.0000
TORQUE:	4.77 Nm	start:		0.00	0.0000
SPEED:	1500.00 rpm				
POLES:	4				

	Tn	TORQUE(Nm)	SPEED(rpm)	DELTA(deg)
	Tmax	4.77	1500.00	75.461
	Tmin	0.00	0.00	0.000
	Ts	0.00	0.00	0.000
	STARTING			
	Ts/Tn	0.00		
	Tmin/Tn	0.00	TRUN1: 80.0	K
	Tmax/Tn	0.00	TRUN2: 80.0	K
	Is/In	0.00	Amb: 25.0	C

Fig 3.11: New geometry - working point simulation results

Fig 3.11 shows the main characteristics of the selected candidate. As can be seen, its efficiency exceeds the efficiency target (IE4 level = 85.7%) by a margin of 2.2%. A high value of the minimum flux density in the PMs, at steady state rated operation, can be observed (PMBMIN=220mT). The main issue of such motor might be represented by the high torque ripple: TTHD=16%.

2. Three filled flux barriers with PM

Population size set: 600;

Parameter description	Adept symbol	Unit	Target
Efficiency	ETATEMPCL		Maximize
THD of the torque waveform	TTHD	[%]	Minimize
Power factor	COS100		Maximize

(a)

	Variable	Min	Max	Step
Thickness of the 1 st barrier (inner barrier)	BM1			
Thickness of the 2 nd barrier	BM2			
Thickness of the 3 rd barrier (outer barrier)	BM3			
Number of effective turns per slot	ZN1			

(b)

Fig 3.12: (a) optimization objectives; (b) optimization variables

Below we can see the output of the generic algorithm form Pareto fronts, as well as the identification of the best individual:

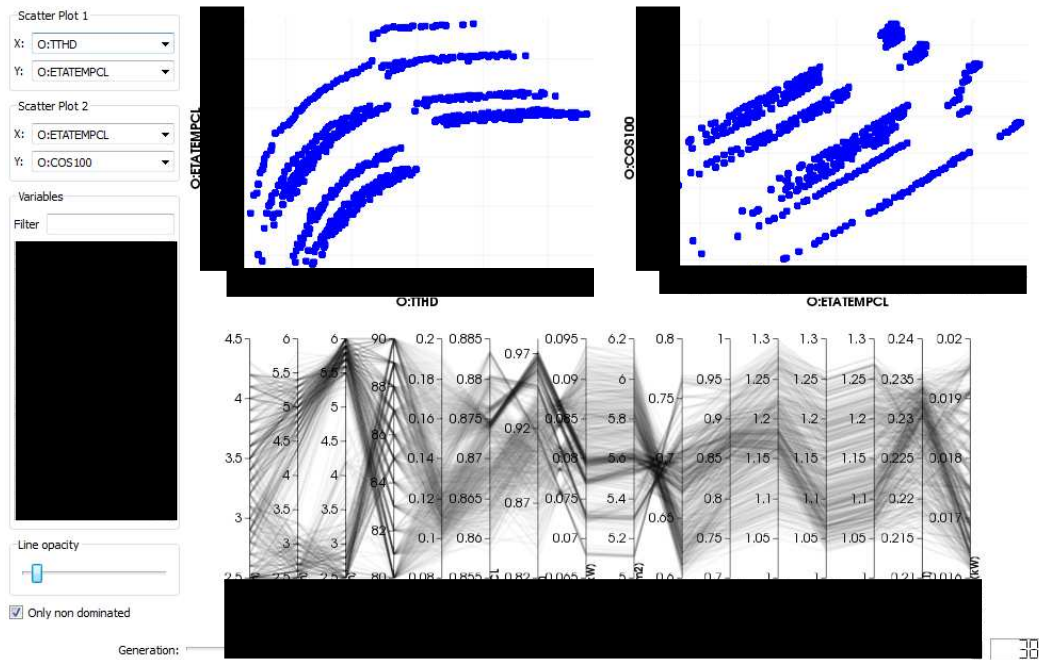


Fig 3.13: optimization output

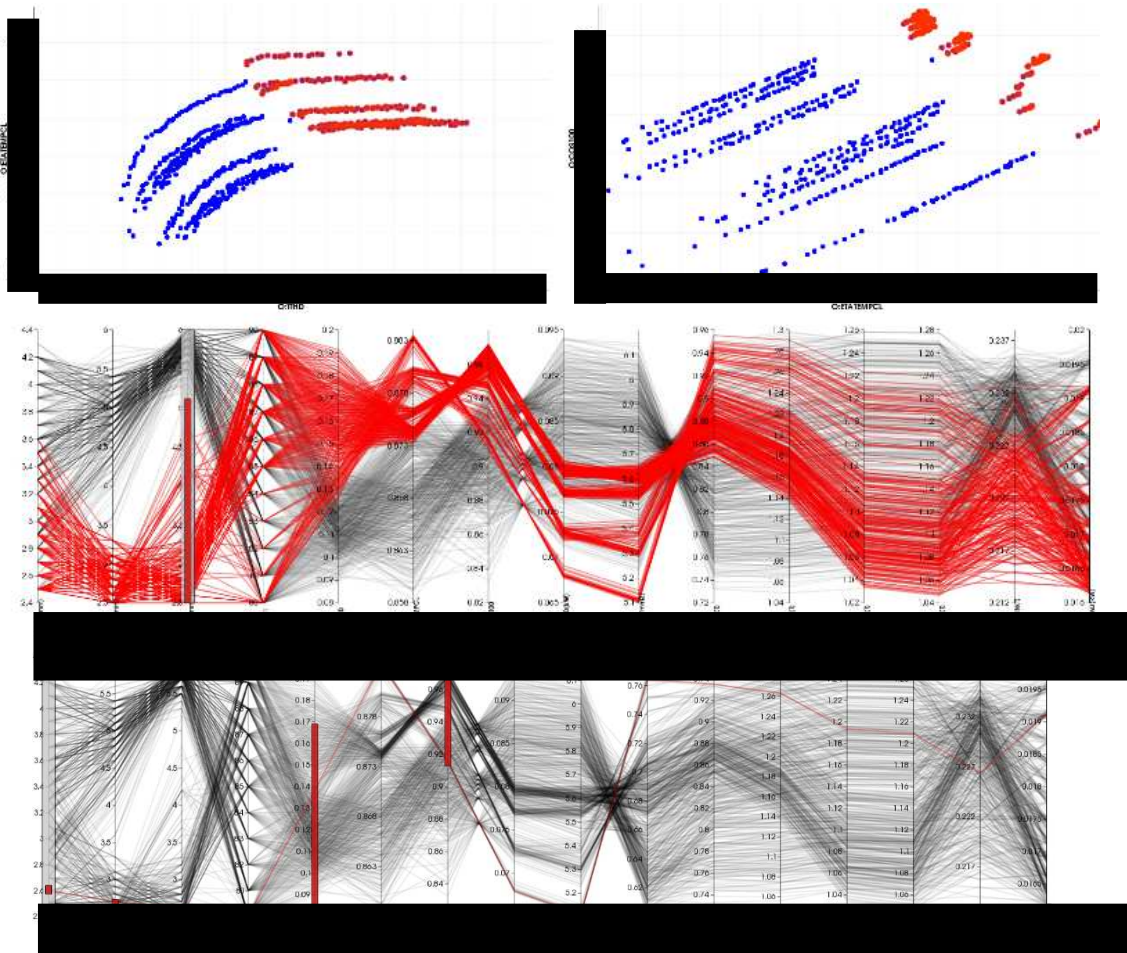


Fig 3.14: procedure of selection of the optimum candidate

OUTPUT (mech):	0.749 kw	LOAD(%)	EFF(%)	CURRENT(A)	cosf
INPUT:	0.848 kw	100 :	88.33	1.44	0.9148 ind
VOLTAGE:	370.0 V	75 :	0.00	0.00	0.0000
FREQUENCY:	50.00 Hz	50 :	0.00	0.00	0.0000
CONNECTION:	Star	25 :	0.00	0.00	0.0000
CURRENT:	1.44 A	125 :	0.00	0.00	0.0000
COSFI:	0.9148 ind	0 :	0.00	0.00	0.0000
TORQUE:	4.77 Nm	start:	0.00	0.00	0.0000
SPEED:	1500.00 rpm				
POLES:	4				
		Tn	TORQUE(Nm)	SPEED(rpm)	DELTA(deg)
		Tmax	4.77	1500.00	76.271
		Tmin	0.00	0.00	0.000
		Ts	0.00	0.00	0.000
		STARTING			
		Ts/Tn	0.00		
		Tmin/Tn	0.00	TRUN1:	80.0 K
		Tmax/Tn	0.00	TRUN2:	80.0 K
		Is/In	0.00	Amb:	25.0 C

Fig 3.16: New geometry - working point simulation results

Figure 3.16 summarizes the performances of the selected optimal motor. The efficiency target (85,7%) is achieved with a high margin, 2.6%. The model shows good values of PMBMIN and power factor, respectively equal to 226 [mT] and 91%. The main issue of such design might be represented by the high torque ripple, TTHD = 14%. Further investigation is to be done to determine the maximum acceptable value of such variable. The figure 3.15 shows the geometry and the field solution at rated operation.

3.2.3 Final design

You can see below the two results derived from the optimizations compared on the main features:

Shaft Height [mm]	H80	H80
Stack Length [mm]	100	100
Voltage [V]	370	370
Current [A]	1,42	1,42
Frequency [Hz]	50	50
Torque [Nm]	4,77	4,77
PF	0,94	0,94
Eta [%]	87,21	87,26
Margin to IE4 [%]	1,5	1,6
Current density [A/mm ²]	5,79	5,77
Flux density in the teeth [T]		
THD of airgap torque [%]	15,4	14,32
N° of Flux Barriers	2	3
PM Type	Hitachi NMF5D	
PM Weight [g]	520	510

Fig. 3.17: main characteristics of the optimized H80 motors

In this case, both solutions are valid from every point of view. For this reason, we can't prefer one over the other and continue the discussion with both optimized geometries because from the electrical point of view are equivalent.

Analysis of demagnetization in worst condition

In order to determine the worst condition for the magnetic state of the PMs, the load angle at which the minimum of PMBMIN occurs has been searched for several different values of current amplitude, above the rated value. For each position of the current vector in the dq plane, a time-transient simulation of the motor has been performed. This analysis is reported only for the motor with three filled barriers.

The worst condition corresponding to:

- $i_{max} = 5A$, i.e. 2.5 times the amplitude of the rated current, at $-20^{\circ}C$
- $i_{max} = 7A$, i.e. 3.5 times the amplitude of the rated current, at $20^{\circ}C$.

A complete plot of the maximum current capability against rotor temperature can be traced, on the basis of more detailed characteristics of the PMs material, to be requested to the manufacturer.

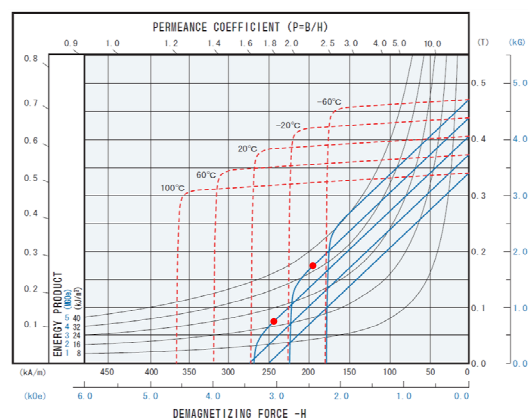


Fig. 3.18: BH characteristic - working point in worst condition

Additional considerations are made in conditions of overload at high temperatures rotor to assess any effects of PM demagnetization.

Comment on possible reduction of inertial mass

The two architectures summarized are equivalent from the electrical design point of view. The saturation level is the only discriminant, as can be seen in Figure 3.X and Figure 3.X, where the colour maps of the flux density in the cross sections of the two architectures are shown. There can be seen that the architecture with three filled barriers shows a more uniform flux density distribution. On the other hand, the architecture with two filled barriers might have lower manufacturing costs and higher speed capability. To the aim of this work, a choice between the two solutions is not necessary.

Mechanical revision

After completing the optimization phase and the various considerations on the demagnetization of the magnets worst condition, must mechanically review the output geometry, in addition to consider the working conditions in other work points, different from the one considered for the optimization.

The results of mechanical stress simulations are summaries in the following results table, we have to hide the real results for confidential reasons.

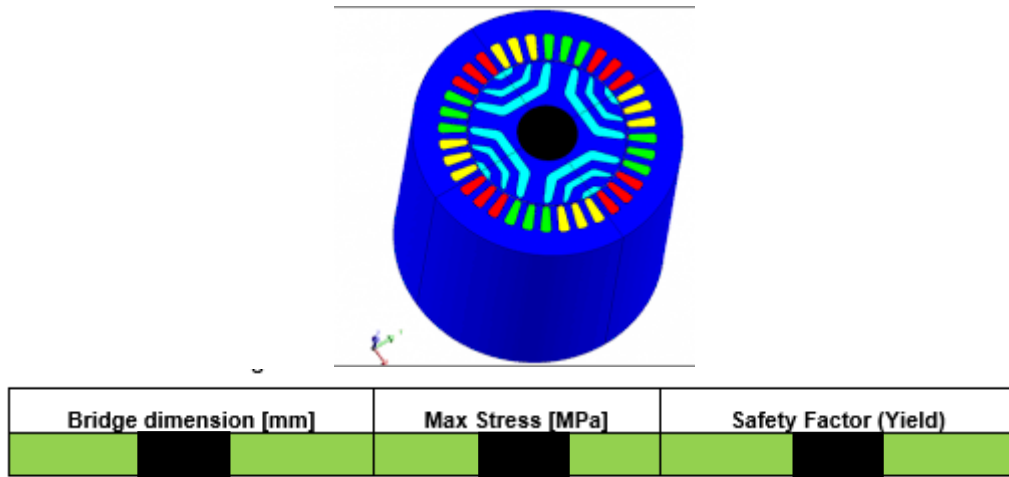


Fig. 3.19: mechanical simulation – stress results of the optimate geometry

Part II

Chapter 4

Thesis proposal

This chapter is introductory for the second part of this paper.

It helps to understand the topic of thesis work in relation to the questions that the company poses herself in relation to various themes, for example about the ABB drivers that they use in their laboratory.

4.1 ABB

ABB is a company organised by matrix structure for organizational matters.

In addition to the "mechatronic" field, which sees robotics as protagonist, in Vittuone their work regards also middle and low voltage converters and electric motors.



Fig. 4.1: ABB motors drive

4.2 Thesis proposal

Considering the use of assisted reluctance motors, as the technology is not yet mature status of the control development is improvable. The purpose of this thesis is to support the development of the control with a description as accurate as possible of the characteristics of the motor from the point of view of control, and then check whether the ABB drivers follow or not the control strategy, in this case the MTPA one.

To do this, basically we're going to follow three steps:

1. Research of the MTPA feature by time stepping simulation;
2. Research of the characteristic by analytical model that manipulates data provided by magnetostatic simulations;
3. Trace the control characteristic in the laboratory through constant torque demand.

Lastly, we will compare the three characteristics by assuming time to time the reasons for the various divergences between these, trying to predict the techniques of the ABB drives.

4.3 Grade of access to the motor drive

The R & D team has several motor test benches, each with two inverters. However, there is no way to pleasure handle the power supply voltage of the motor in the laboratory.

This restricts the third part of this work, as also the data that drives releases to the PC: they can't be selected but the data are some standard outputs.

Lastly, the ABB control for PMASR motors is one modified control existing for SMPM, and therefore it doesn't consider many things. But we will see along the third part of the elaborate what this fact implies regarding the max torque per current characteristic.

Chapter 5

MTPA trajectory

Time-step simulations

Let's go to show how to extrapolate the characteristic MTPA through the output of a time dependent simulation using ADEPT.

The discussion will follow each step and will attach to the appendix all the scripts and spreadsheets used commented in each part.

It will be briefly treated what is meant by finite element simulation (FEM) on the electric motors application.

5.1 FEM - theory overview

The FEM study consists essentially of 5 steps:

- Portion of domain (dA), where the portion of the mesh gives the domain;
- Choice of interpolation function;
- Formulation of the system (in that case, flux equations to solve);
- Solution of the problem;
- Post processing.

For the solution of the problem and the formulations annexes to the magnetic flux, it is necessary to provide boundary conditions that follow more or less strong assumptions.

The hypotheses that we make are two, periodic, and provide the domain boundary conditions (mesh) studied:

- *Dirichlet*
- *Neumann*

These hypotheses provide immediate considerations regarding the magnetic potential on the surface.

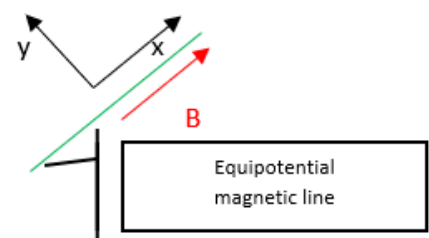
Stator windings are characterized by the distribution of unitary FMM for whose theory reference is remanded to bibliographic notes.

What actually studies a simulation of finite elements is the value of the magnetic potential between two surfaces so, as the magnetic potential (defined below less than two variables) is defined, we need two contour conditions.

To draw flux lines, the following formulations are used:

$$B_x = \frac{\partial A_z}{\partial y} \quad (5.1)$$

$$B_y = -\frac{\partial A_z}{\partial x} = 0 \quad (5.2)$$



For any surface,

$$\phi = \iint \vec{B} \cdot \vec{n} dS = \iint \text{rot}(A) \cdot \vec{n} dS = \oint A \cdot l dl \quad (5.3)$$

$$\phi = (Az1 - Az - (Az2 - Az)) * Lstk \quad (5.4)$$

$$\phi = (Az1 - Az2) * Lstk \quad (5.5)$$

In the case of many conductors, it is considered the average value of A_z on the surface of conductors

$$\phi = \left(\int_{S_{cu+}} A_{z1} dS - \int_{S_{cu-}} A_{z2} dS \right) * \left(\frac{Lstk}{S_{cu}} \right) \quad (5.6)$$

Once found the value of magnetic flux, the concatenated one will be given by the following formula, with n_{qs} as the number of conductors in series for each slot, Q as total number of slot, q the considered slot, p as poles pairs and the unitary distribution of magnetomotive force $N(x)$:

$$\Lambda_j = 2p * Lstk * n_{qs} * \sum_{q=1}^{\frac{Q}{2p}} N(x)_{ij} * A_z(q) \quad (5.7)$$

Consequently, induced electromotive force will be calculated as:

$$Ea = \frac{1}{\sqrt{2}} * \omega * \Lambda_j \quad (5.8)$$

Knowing the voltage, the magnetic field flux and the stator current distribution can be calculated, identifying the rotor position with respect to the rotating axes in quadrature, the axis inductances and dq currents.

Through post processing we can now find all the other quantities of interest.

5.2 MTPA trajectory research

Due to the limitations already seen of the program, multiple working point have been simulated individually for the detection of the minimum current by setting a supply voltage range in which the motor should provide the torque for that working condition. This iterative work was done for 8 speeds and hence different frequencies for 8 torque values, analysing in total 64 physical conditions for the motor, in order to compensate, by mediating, the error deriving from the fact that Adept can't use a continuous function of voltage but a discretization more or less dense from one value of power supply voltage to the next.

The 8 different MTPA features have been mediated, which obviously doesn't depend on the speed as it is defined (minimizes joule losses and hence would be the same, ideally, as blocked rotor), finding the ultimate trajectory.

5.2.1 MTPA research

As anticipated, several points of operation of the machine have been simulated; let see the results of this phase referring to the outputs of the simulation at nominal speed, but not before clarifying the constructive features of the considered machine.

Machine characteristics

SynRM2 H90

Nominal power [kW]	Nominal velocity [rpm]	Nominal Torque [Nm]	Poles pair	Voltage [V]
4	3000	12.73	2	370

MTPA construction at nominal rotor speed

The values above are in p.u. (per unit, normalized) of the nominal torque and, by calculating the power output, we can set the simulation parameters;

Velocity%	Torque %	Power[W]	frequency[Hz]	torque [Nm]
100	12,5	500	100	1,59
100	25	1000	100	3,18
100	37,5	1500	100	4,77
100	50	2000	100	6,37
100	62,50	2500	100	7,96
100	75	3000	100	9,55
100	87,50	3500	100	11,14
100	100	4000	100	12,73

Fig. 5.1: Considered working point

ADEPT inputs for simulations of this type are only three that permit us to change operating point:

- Power [kW];
- Voltage [kV];
- Frequency [Hz];

Regarding power and frequency, these two inputs came directly from the chosen operating point. Regarding the supply voltage, it's necessary to change it to find the point that would minimize the Joule losses until there was a supply voltage value that gives us the minimum value of current in that determinate working point.

The output of the 100% speed simulation, 87.5% torque, gave the results in figure 5.2, where you can see an Excel spreadsheet that relate the effective value of the current to the power supply voltage and therefore sees that the simulation with 395V has given as output the lowest current.

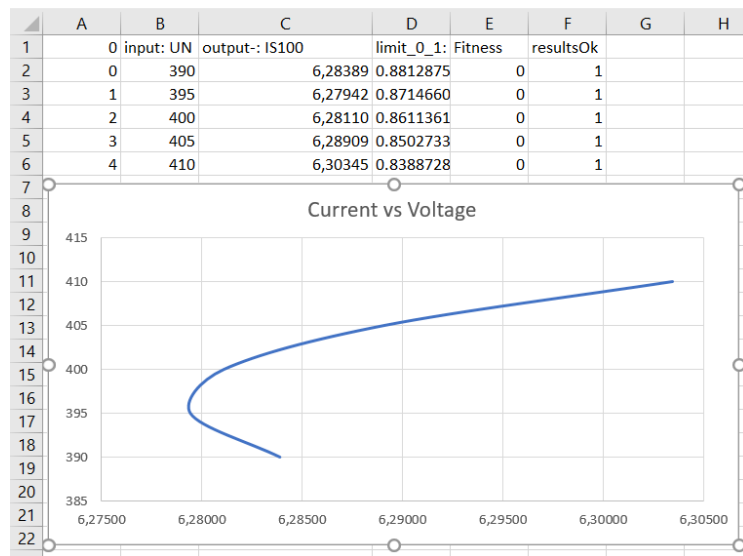


Fig 5.2: simulation output 100%velocity 87.5%torque

In this case, as you can see, a voltage step of 5V was good for our assessments but, in some cases, it had to be investigated up to the step of one Volt.

Identified the simulation that provided the lowest current, we have now to look the other outputs of that, taking note about the current components in the rotating axes and the position of the direct axis as well as the PF.

These considerations are made for all simulated torque values.

All of that is reported on a spreadsheet; the results are illustrated in the figure 5.3.

Power[W]	frequency[Hz]	torque [Nm]		Id	Iq
500	100	1,59		-0,91445	1,889745
1000	100	3,18		-2,206	3,117
1500	100	4,77		-2,86648	3,63645
2000	100	6,37		-4,132	4,158
2500	100	7,96		-4,77568	4,701796
3000	100	9,55		-5,343	5,802
3500	100	11,14		-6,67343	5,43955
4000	100	12,73		-7,810	5,797

Fig. 5.3: Idq MTPA value at nominal velocity

For more precision which determines the MTPA feature, we can make further considerations on the value of the power factor (PF), which for all points may not differ too much. It was then blended a spreadsheet which has as its purpose to refine the search already made recommending in some cases other simulations for which the practice was to decrease the voltage range and using a lower delta for the voltages that we simulate, in a way as to obtain more accurately the module of the lower current.

Now we can plot on a dq plane the MTPA feature found to the considered speed. In section A1 in the appendix you can find the script useful to plot the feature like the one in the figure below.

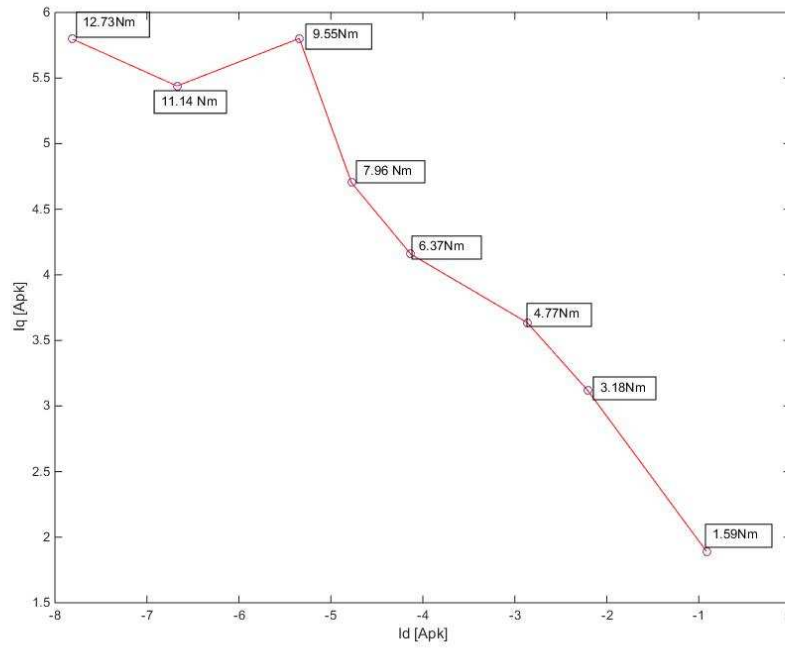


Fig. 5.4: preliminary MTPA at nominal speed

You already see how the point at 9.59Nm is not too consistent with the trend we can expect. The interpolation used was chosen here to highlight aspects of this type.

5.2.2 MTPA mediated from all preliminary characteristics

The operations described above are made for 8 different speeds; then we will get a contest like the type shown in Figure 5.5

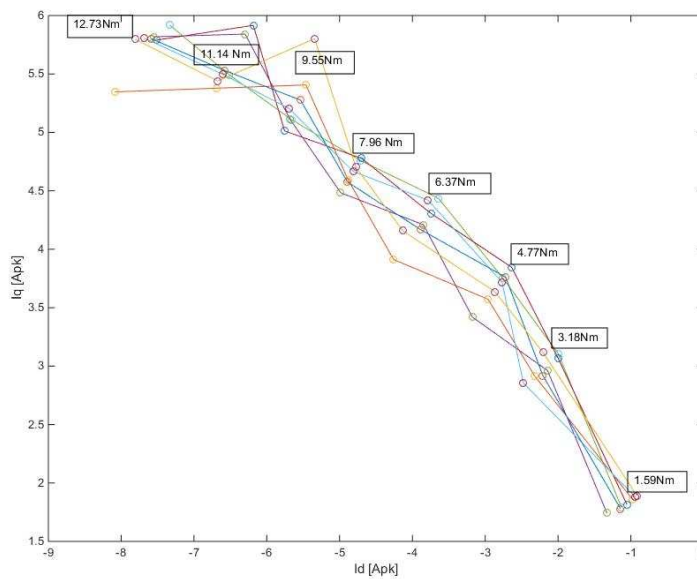


Fig. 5.5: all velocity MTPA characteristic

Now comes the time to mediate the features to find another one as accurate as possible, which compensates gross errors that, as already mentioned, can't find the exact voltage value for which the current is lower.

The script used to mediate and plot the result can be found in appendix to section A2.

The result is shown in Figure 5.6.

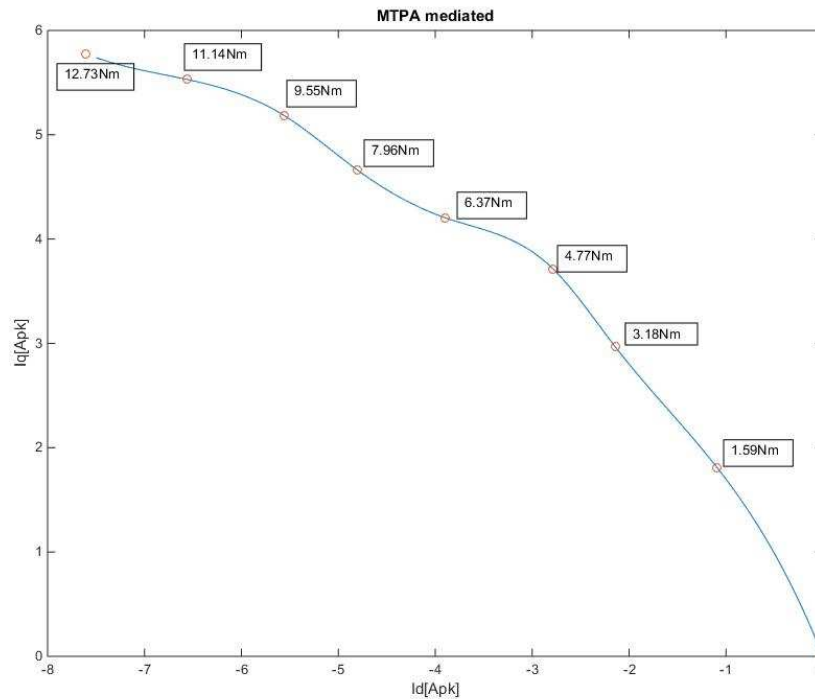


Fig. 5.6: time step MTPA output

Let's look some key characteristics in order to justify its course.

The characteristic starts more inclined to the q axis and, growing the effects of saturation, it falls down the d axis. The effects of saturation and cross-saturation have an effect of this type for this characteristic, the effect that the control that works in MTPA logic must be taken into account.

Let's see the angle of the current angle γ trend in Figure 5.7:

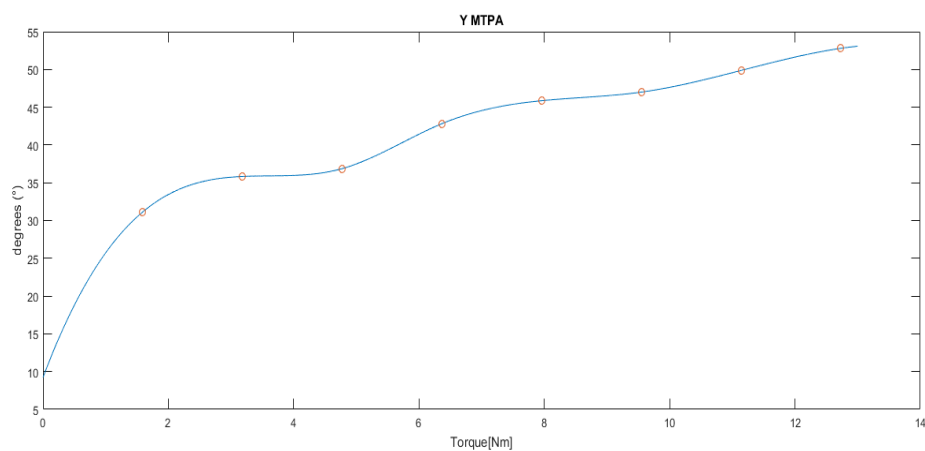


Fig. 5.7: Current angle on the MTPA

These waveforms will then be compared to those resulting from the magnetostatic calculation, topic of the next chapter.

5.2.3 Mediated MTPA supply voltage characteristics

Now the objective is to trace the power supply characteristics for further comparison when the motor will be tested via the ABB drive.

The calculation is simple and depends firstly from the frequency and the effective value of the stator current. The calculation sheet of figure 5.9 was used, repeated for all the speeds that we have analysed.

	100 (Hz)	87.5 (Hz)	75 (Hz)	62.5 (Hz)	50 (Hz)	37.5 (Hz)	25 (Hz)	12.5 (Hz)
PowerOut	3999,1295 [W]	3499,238 [W]	2999,34713 [W]	2499,456 [W]	1999,5648 [W]	1499,6736 [W]	999,78238 [W]	499,89119 [W]
Torque	12,73 [Nm]	12,73 [Nm]	12,73 [Nm]	12,73 [Nm]	12,73 [Nm]	12,73 [Nm]	12,73 [Nm]	12,73 [Nm]
Id	-7,609 [A]picco	-7,609 [A]picco	-7,609 [A]picco	-7,609 [A]picco	-7,609 [A]picco	-7,609 [A]picco	-7,609 [A]picco	-7,609 [A]picco
Iq	5,777 [A]picco	5,777 [A]picco	5,777 [A]picco	5,777 [A]picco	5,777 [A]picco	5,777 [A]picco	5,777 [A]picco	5,777 [A]picco
p.u.D	-0,780057154 [A]rms	-0,78006 [A]rms	-0,7800572 [A]rms	-0,78006 [A]rms	-0,780057 [A]rms	-0,780057 [A]rms	-0,780057 [A]rms	-0,780057 [A]rms
p.u.Q	0,592200881 [A]rms	0,592201 [A]rms	0,59220088 [A]rms	0,592201 [A]rms	0,5922009 [A]rms	0,5922009 [A]rms	0,5922009 [A]rms	0,5922009 [A]rms
Is	6,755539038 [A]rms	6,755539 [A]rms	6,75553904 [A]rms	6,755539 [A]rms	6,755539 [A]rms	6,755539 [A]rms	6,755539 [A]rms	6,755539 [A]rms
fiD	7,06E-02 [wb]	7,23E-02 [wb]	7,121461E-02 [wb]	7,20E-02 [wb]	7,01E-02 [wb]	7,14E-02 [wb]	7,09E-02 [wb]	6,82E-02 [wb]
fiQ	0,515068932 [wb]	0,515406 [wb]	0,52032206 [wb]	0,516473 [wb]	0,4903044 [wb]	0,5154391 [wb]	0,5225843 [wb]	0,5093284 [wb]
fem	326,6438187 [V]	286,1238 [V]	247,474594 [V]	204,7756 [V]	155,5966 [V]	122,60513 [V]	82,836585 [V]	40,358522 [V]
Rs*Is	5,40443123 [V]	5,404431 [V]	5,40443123 [V]	5,404431 [V]	5,4044312 [V]	5,4044312 [V]	5,4044312 [V]	5,4044312 [V]
Alim	396,6833083 [V]linea	347,4893 [V]linea	300,569012 [V]linea	248,7364 [V]linea	189,04794 [V]linea	149,01851 [V]linea	100,79861 [V]linea	49,442986 [V]linea

Fig. 5.9

Repeating the calculation for each torque, we obtain the voltage characteristics that drive the MTPA trajectory at each different power frequency. The results can be seen in Figure 5.10.

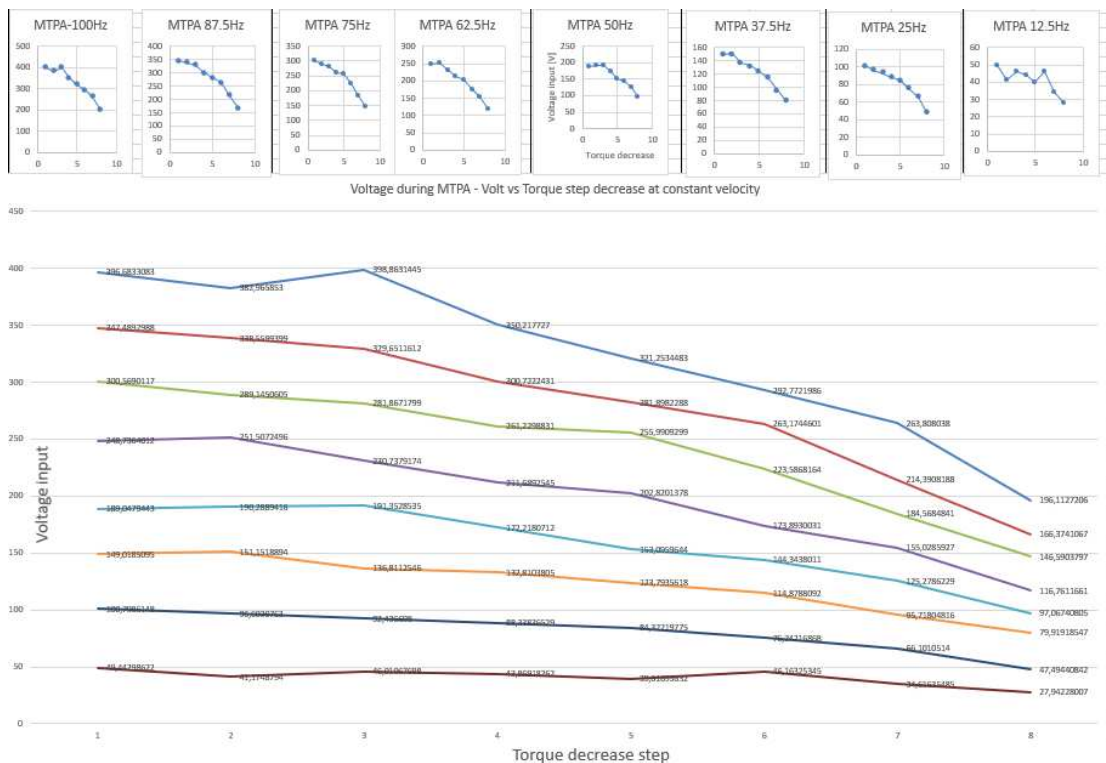


Fig. 5.10

Chapter 6

MTPA trajectory

Magneto-static simulations

Here is explained how to derive the minimum current characteristic through the manipulation of the table of flux resulting from a lot of magnetostatic simulation (each point of the matrix is one magnetostatic simulation).

6.1 Flux tables

The flux table is one of the outputs of the magnetostatic simulation if required; the computing time is high as many working point are simulated; they take into account the cross-saturation effects between the axes.

After finishing the simulation, we will have these data in an Excel file, that is shown in Figure 6.1.



Fig. 6.1: mgt-static simulation output: Flux table

Representing them on a 3D plane, they will appear as in Figure 6.2.

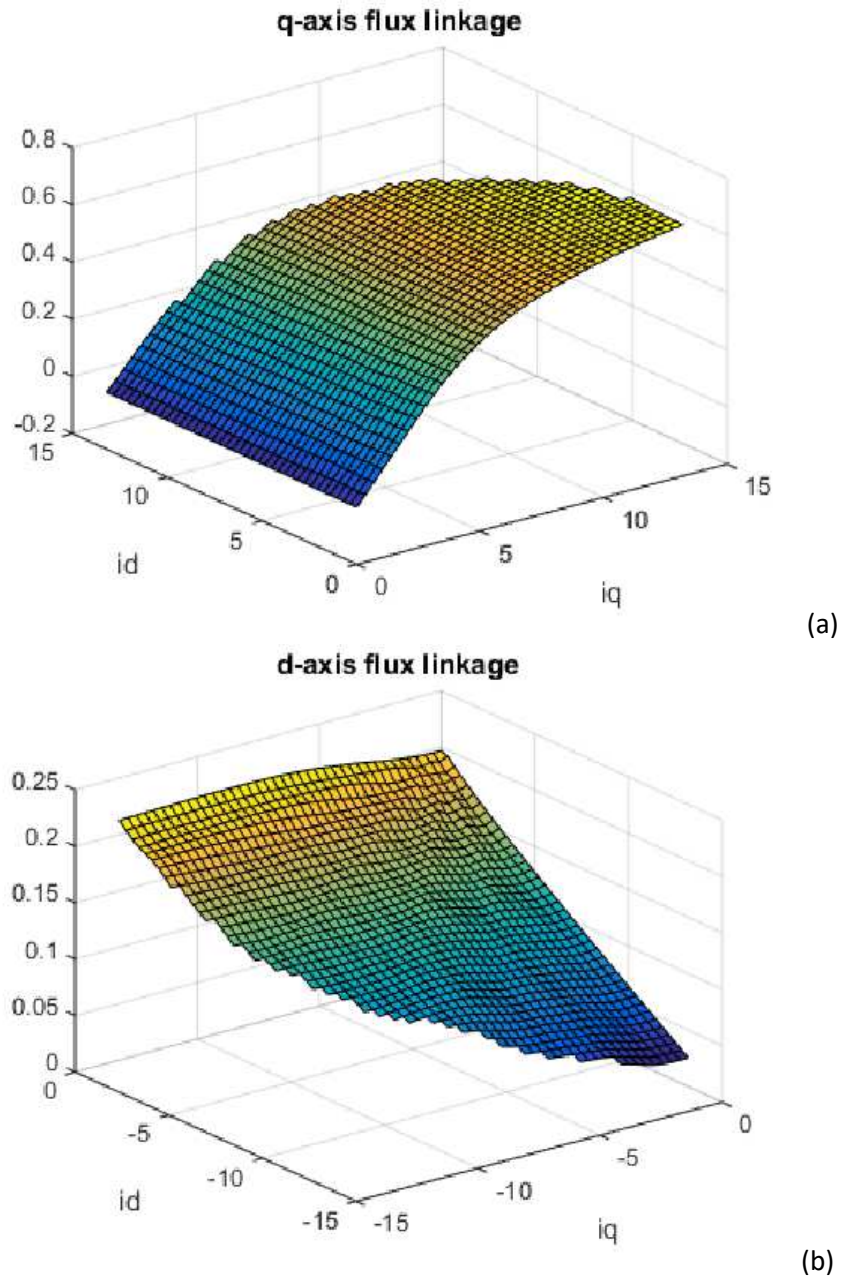


Fig. 6.2: Flux 3D representation

The script used is contained in Appendix A3.

Inline and cross interpolation operations must be made to fitting the amount of data in order to make them as complete and suitable as possible for a post-process analysis. Also this time, the script used is in appendix at section A3.

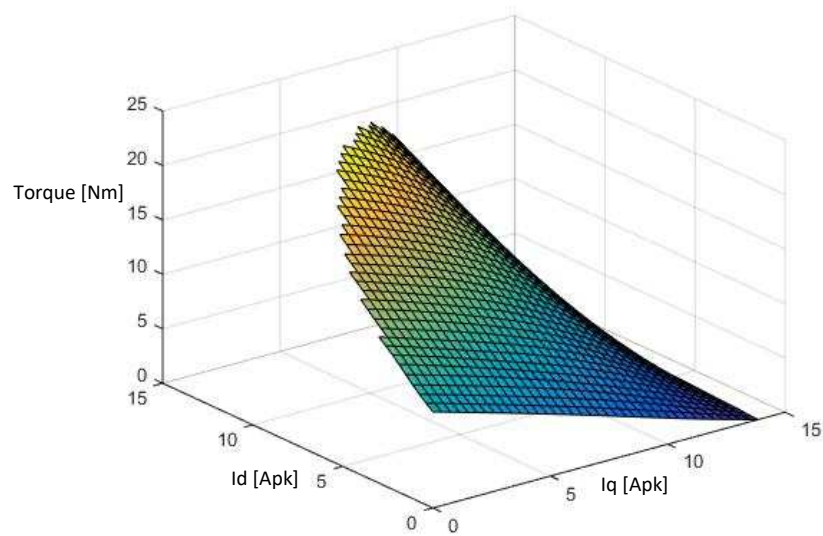
I have to remember that the outputs from a magnetostatic simulation aren't mediated on a period, but it fixes the position of the rotor. For this reason, the stator effects are relevant. You will see in the next chapter how to consider such effects and how to mediate them.

6.2 Search MTPA trajectory by manipulating the flow chart

NB: the following discussion refers to the convention in which the magnets are oriented as the q axis. Please refer to section 1.3.1 and 1.3.3 of this document if this agreement is not yet fully understood.

Handling Flow Charts consist on the use of scripts in appendix A3, fully commented.

To summarize the algorithm used by the script, the manipulation consists in the construction of a torque matrix that contains in its interior all the features iso-torque as a function of d and q axis currents; the formulation of the torque used in this step is the (1.12). We have now current feature resulting from iso-torque characteristics. The point with lowest current corresponds to the searched point; relying on it, the MTPA feature will be built.



(a)

Fig. 6.3: (a) Torque surface

The following figures show the outputs of the script that searches the lowest current point; in section A3 in the appendix, you can find this script and others that do the same, here will be clear inputs and outputs of this, for easy reuse.

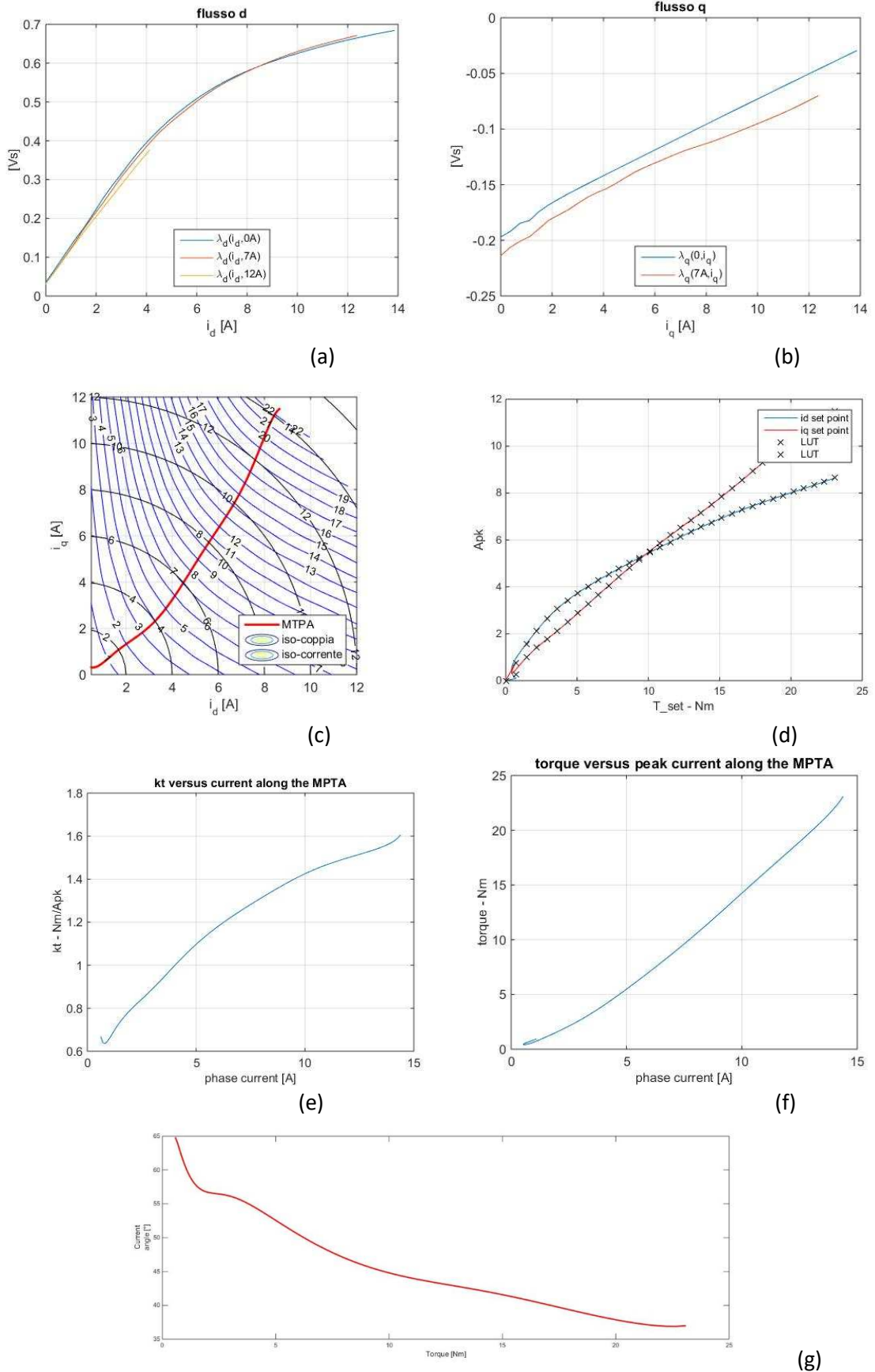


Fig. 6.4: MTPA main characteristics

We're now ready to compare this MTPA with the one found in the previous chapter through time-step simulations.

The problem is, as anticipated, the fact that simulations of this type do not mediate the *stator effects*. In the next chapter we will see how to consider such effects and then finally we will be able to evaluate the differences between one feature and the other.

Chapter 7

Compensation of ripple derived by stator effects

We will scrupulously follow every step of this discussion; then the conceptual approach that has been followed will be explained, as well as how to implement it with the available tools.

7.1 Method

In this section, you will see all the logical process that leads to the hoped result.

7.1.1 Stator effects

The stator effects influence the rotor flux flowing over the air gap. In fact, machine flux can't be the same under the stator tooth (which is iron, $\mu r \rightarrow \infty$), and under the slot, filled with copper and air depending on the slot fill factor. What said is evident in the figure 7.1, where you can see the flux lines under the slots and under the stator teeth.

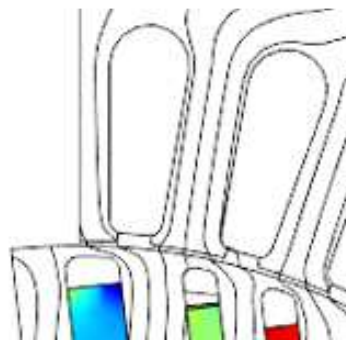
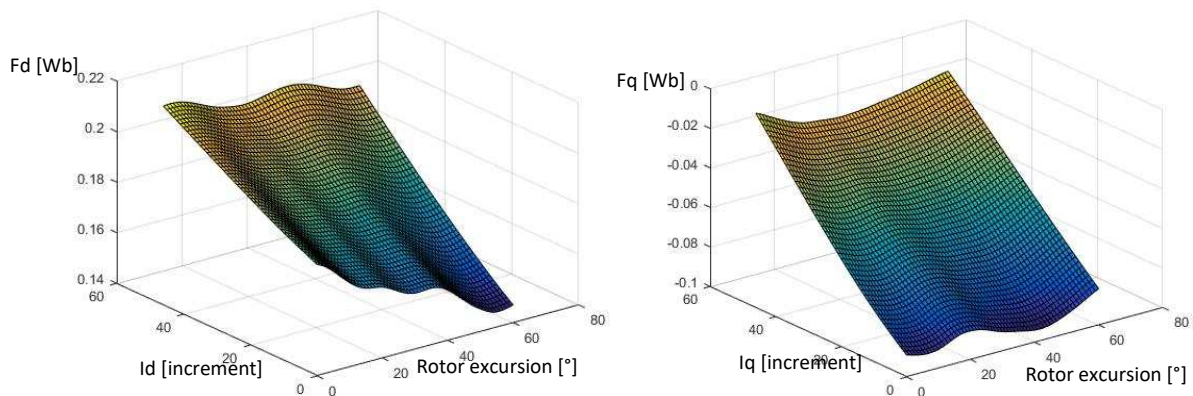


Fig. 7.1

In fact, it is evident the change of density of the magnetic flux lines if it is under a stator cave or under a stator tooth. Above in the figures, it is noted how this influence the waveforms of the magnetic flux.



7.1.2 *Problem solving*

The goal is to build a new flux matrix that has the substantial difference in mediating the effects previously exposed.

This can be done by fixing the currents of rotating axes dq following a rotor travel of 60° with respect to the stator, one degree at a time. The results are sixty flux values for each couple of i_{dq} ; the mediated element will occupy a position in the final flux matrix.

Once the new matrix is built, it will be enough manipulated it to get the new MTPA feature.

7.2 Application

The previous section has described how to fix the problem after identifying it.

In this section we will see how to solve it from a practical point of view.

All the scripts used are in section A4.

7.2.1 *Idea*

The basic idea is to be able to use Adept in order to simulate “ n ” motor conditions imposing the current in the simulations in such a way that the change in the rotor angle doesn’t change anything of it. For each simulation we have to capture the flux resulting from dc.out (output of Adept, mentioned in chapter 2 of this paper) and save it.

To get as much as possible a full flux matrix, we want to simulate the largest number of pairs i_d/i_q and for this reason has been chosen to simulate 66 couples of dq currents that allow to have ample fit results in an extended range.

But let's make two accounts:

only considering the fact that we consider 66 pairs of currents, we will have to run the simulation program for 66x66 simulations; thinking about the fact that for each pair of currents given, we have to make a 60° rotor excursion, by step of 1° , we have to compute a total number of $66 * 66 * 60 = 261.360$ simulations, it is therefore impossible to manually set up the .ini file that contains the information useful to initialize Adept for simulations, doing simulations time to time, and save the results.

It is spontaneous to think of a script that can do everything, recalling the executable of FCSmek and getting the results by elaborating them, but how long?

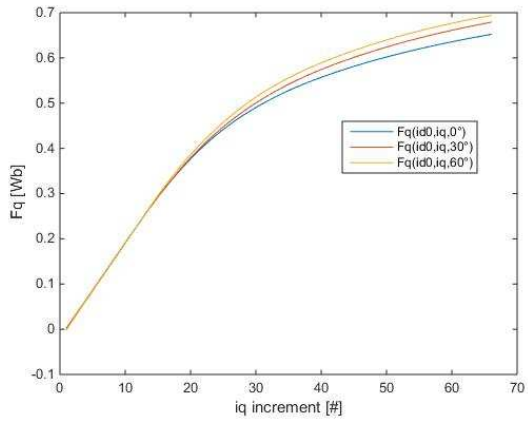
Considering about 3 seconds per simulation, there will be 784,080 seconds of simulation that are expected to match approximately 9 days of computation.

7.2.2 Realization and results

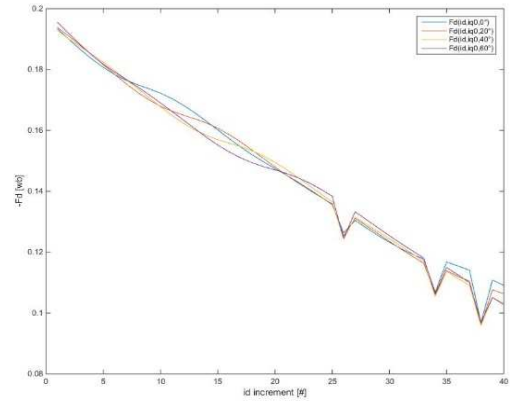
The script can be found in appendix A4.

In practice, it manipulates a .ini file according to the currents to be fixed and the rotor angle, which will then be passed to a function that recalls the FCSmek .exe file; after that it saves the results of the dc.out simulation and process them.

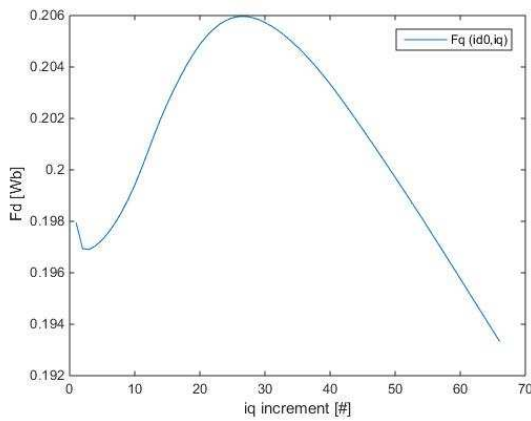
Some outputs of this script are shown in figure 7.2.



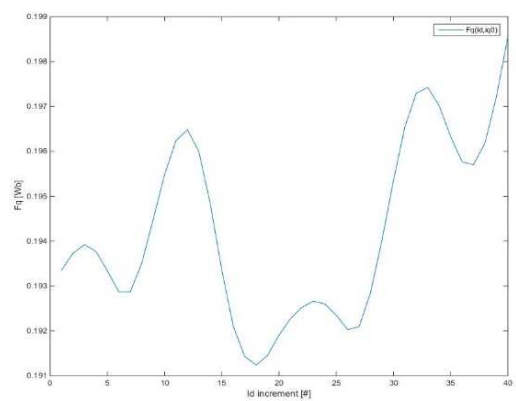
(a)



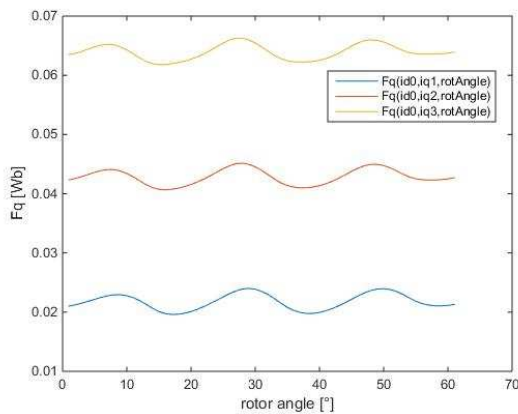
(b)



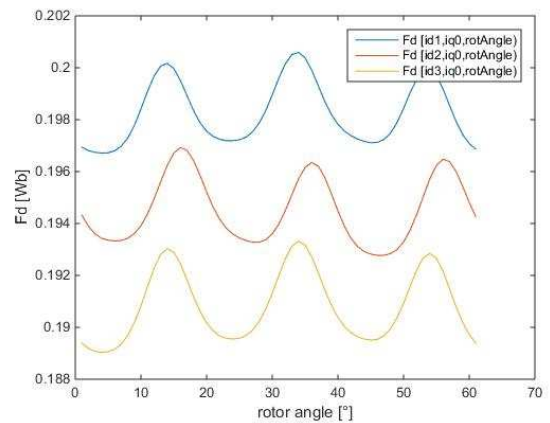
(c)



(d)



(e)



(f)

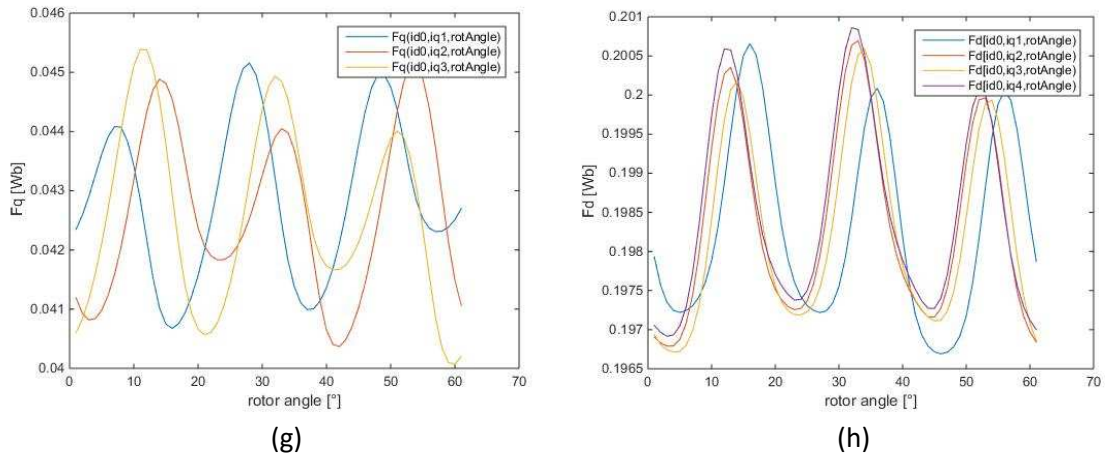


Fig. 7.2

These figures are ordered in pairs depending on what they want to highlight.

The first two, 7.2 (a) and (b), show how flux characteristics change according to the rotor angle only, without considering cross-saturation effects. It's evident that the flux characteristic to be used to make precise calculation data can't be derived from a single magnetostatic simulation that fixes the position of the rotor, because it strongly depends on it.

The figures (c) and (d), give an idea of the effects derived from only cross-saturation, without considering the effects of the stator.

The images (e) and (f), without highlighting cross-saturation effects, want to show stator effects for a 60° rotor mechanical excursion for 3 different current values in the axis considered. The undulation effects on the flux are evident.

The last two, (g) and (h), show how stator effects also vary depending on the cross-saturation phenomenon for a given axis current.

The problem results very complex to be considered and to be predicted. A study like that makes the average of all these effects closely related phenomena; the flux matrix, 66x66 in this case, can be obtained and it allow us to find the most veritable MTPA possible.

7.3 MTPA final

In this section we shall see, always using the scripts, like in Chapter 6, that can be found in the appendix, the construction of the MTPA trajectory with the new matrix of flux just found. It will then be compared to the one obtained without taking into account the stator effects.

7.3.1 Characteristic construction from new flux table

Below you will see all the results from simulations that mediate stator effects.

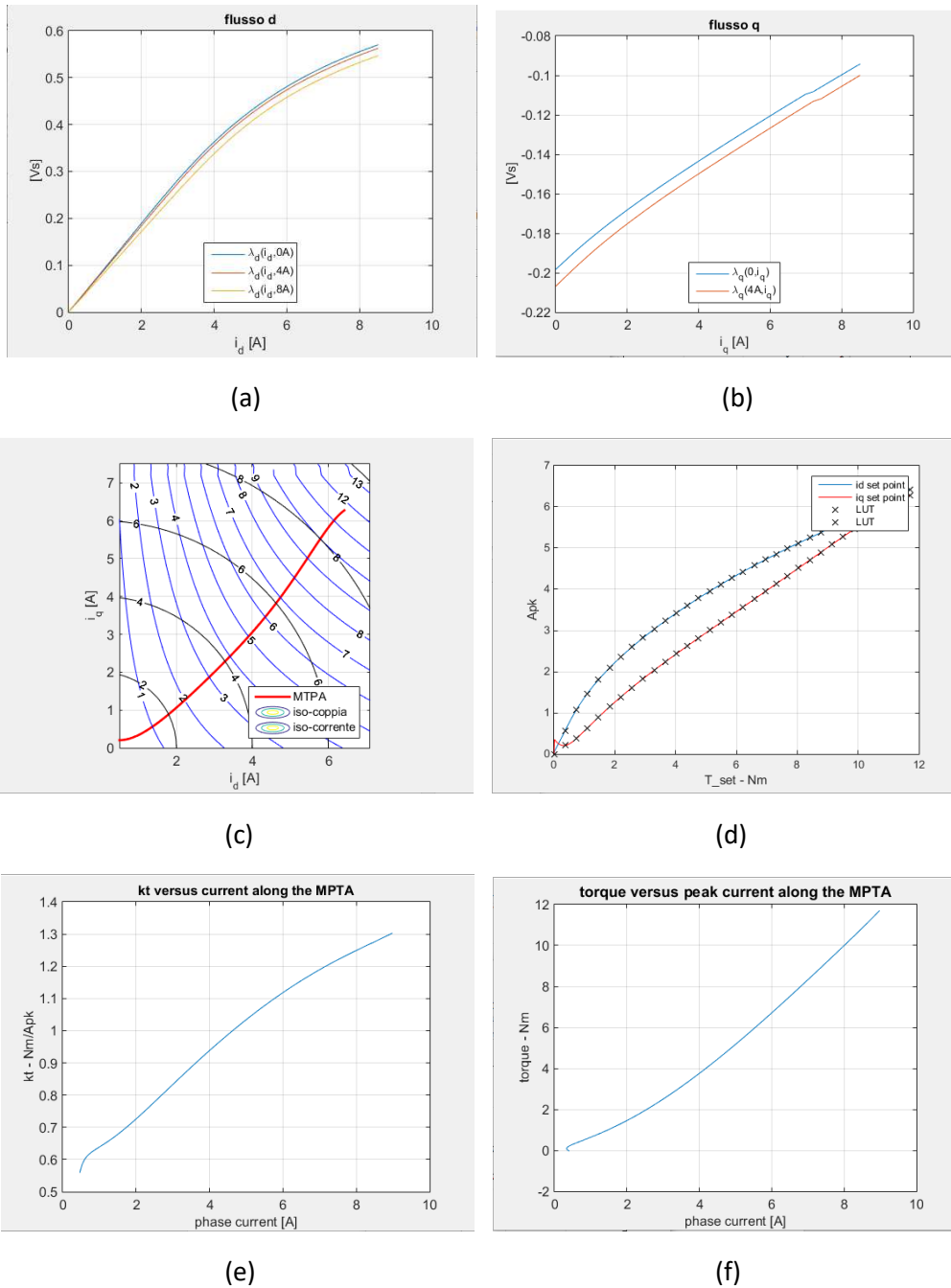


Fig. 7.3: main MTPA characteristics with mediated stator effects

7.3.2 Comparison between the two magnetostatic simulations

In this section we will compare outputs from the two magnetostatic simulations, pointing to agreement and disagreements points between the two.

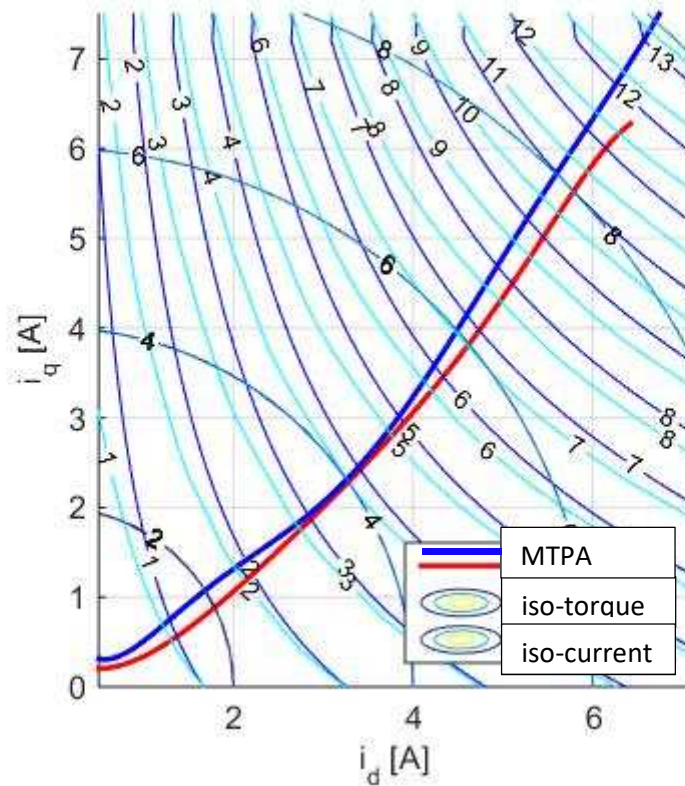


Fig. 7.4

Before commenting on the trajectories, let's observe the different curves iso-torque; in light-blue, the old iso-torque curves, in blue the MTPA trajectory derived by time step simulation found in the chapter 5, associated with the trajectory that mediate stator effects, the one just found (in red). In fact, you will see that the new iso-torque MTPA are correct, once you will compare this with the trajectory output from time step simulations discover in Chapter 5.

In spite of this substantial difference, the features are similar, but in a control perspective, where accuracy is essential for a good drive technique, this error becomes sensitive and unacceptable.

Then, looking at the characteristics of fluxes, you can immediately notice differences that justify the concern about the effects of the stator; in the first magnetostatic simulation in which the stator effects were not mediated, the d-axis flux characteristic considered that cross-saturation effects with $i_q=7A$, crosses and exceeds that the one with $i_q=0A$ starting by i_d approximately 6A.

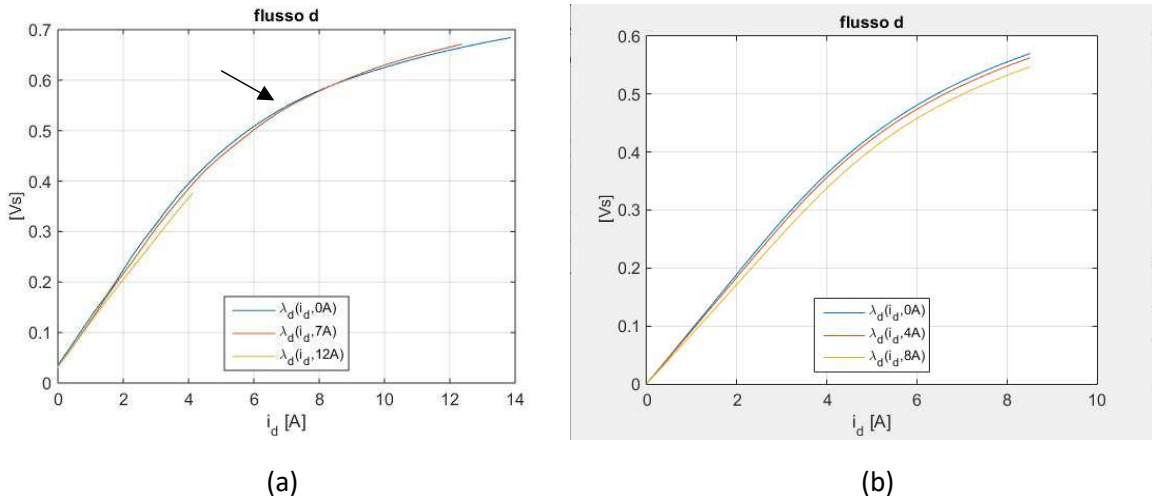


Fig.7.5: (a) Fd characteristics with stator effects; (b) new Fd characteristics

Obviously, such a situation should not occur: in fact, it should be against the principle of energy and coenergy described by the formula (1.10.1) in Chapter 1.

As expected, mediating the stator effects, these problems disappear, as seen in Figure 7.5 (b).

Other considerations can be made about the axis q. You can see how the cross-saturation effect follow a more consistent behaviour with respect to the theory.

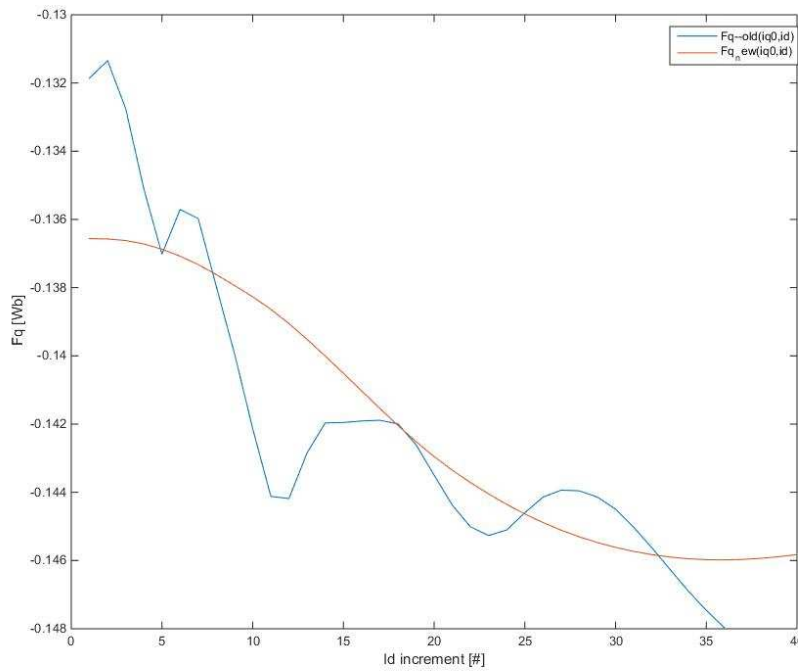


Fig. 7.6: cross saturation effects compare

Chapter 8

Dependence on temperature of MTPA and maximum efficiency characteristics

The characteristics just found are referred to the same temperature of environment, rotor and stator. *But how much do these temperatures influence the characteristic at minimum current per torque?* In this chapter the results obtained for different temperatures will be compared and you will see how the temperatures actually affects this trajectory.

As we know, MTPA by definition is the trajectory that minimizes Joule losses, while MTPV minimizes iron losses and parasitic currents. Maximum efficiency characteristics (Loss Minimization - LM) are those that minimize all losses, hence it minimizes a power function that will be the sum of all types of leaks. Therefore, we can say that the MTPA characteristic coincides with that of LM when the rotor's radial velocity is equal to zero, while the MTPV coincides with the LM when the rotor speed is ideally infinite. It can be concluded that all other loss minimization at different speeds will be closer to one or another trajectory depending on whether the speed is close to zero or to speed limit of rotor. Let's see the results of time-step simulations to highlight what's just said.

8.1 MTPA at different temperature

Time-step simulations have been made to search the MTPA characteristic at two different temperatures; the case called "A" refers to 25°C ambient temperature, with a rotor temperature regime of 120°C, and 80°C the stator temperature; the case B, on the other hand, at 0°C ambient temperature, 80°C rotor and 40°C stator at regime.

The method used to find the characteristics is the same as the one seen in chapter 5, via time-step simulations.

Before displaying the results, let's see what we can expect and how the temperature can affect the electrical and magnetic parameters of the machine.

First of all, we have to consider the thermal drift of the ferrite, for which we see features from the datasheet of the magnets used for that motors, in Figure 8.1.

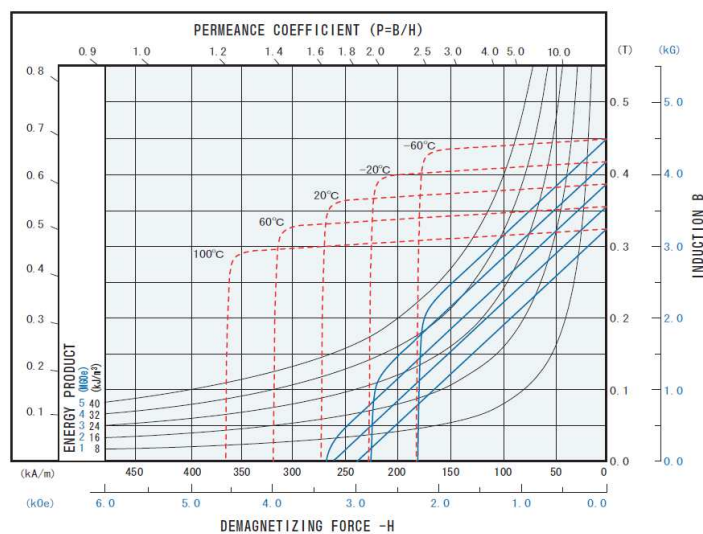


Fig. 8.1: demagnetization characteristics

Secondly, there is the combined effect between the resistances of the windings and the $Bemf$ (back electro-motive force); the temperature decrease so:

- Stator resistance drops
- $Bemf$ increase

The effect on the stator current will be affected in positive or in negative depending on whether one or the other effect prevails.

8.1.1 Case A vs case B

In the first analysis, it was seen how much the different temperatures in the two cases changed the inductances. It was initially calculated the percentage difference between inductances, output of the magnetostatic simulation, through a script that can be viewed in Appendix A5, whose outputs are given in Figure 8.2.

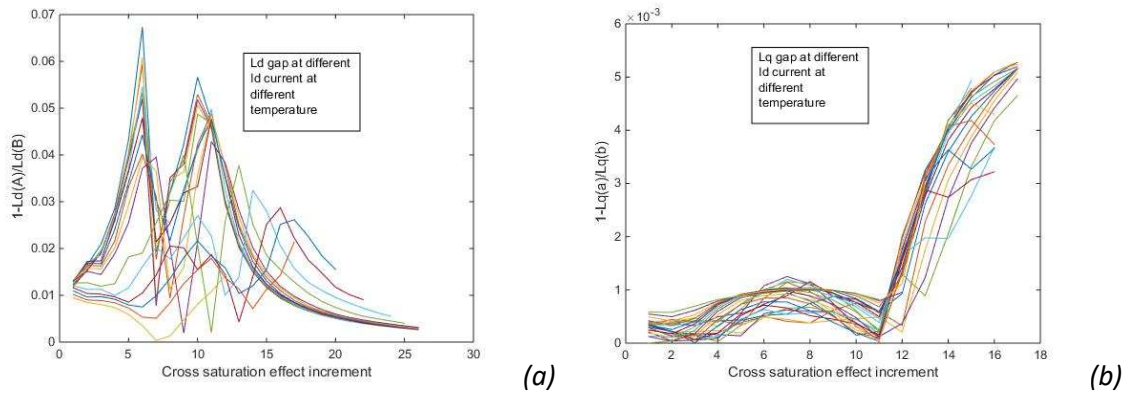


Fig. 8.2: percent deviations between inductances

You see how the percent deviation effects follow discordant trends as the cross-saturation effect increases.

It should also be noted that the inductance in the direct axis were more influenced then the other in the q axis by temperature; this is justified by the presence of the magnets in this axis (temperature drift of ferrite).

The MTPA of the two cases, A and B, are shown in Figure 8.3. It's evident that these two actually don't differ too much, although the temperature is very different in the two cases considered. This is because the temperature effects already mentioned tend to compensate each other.

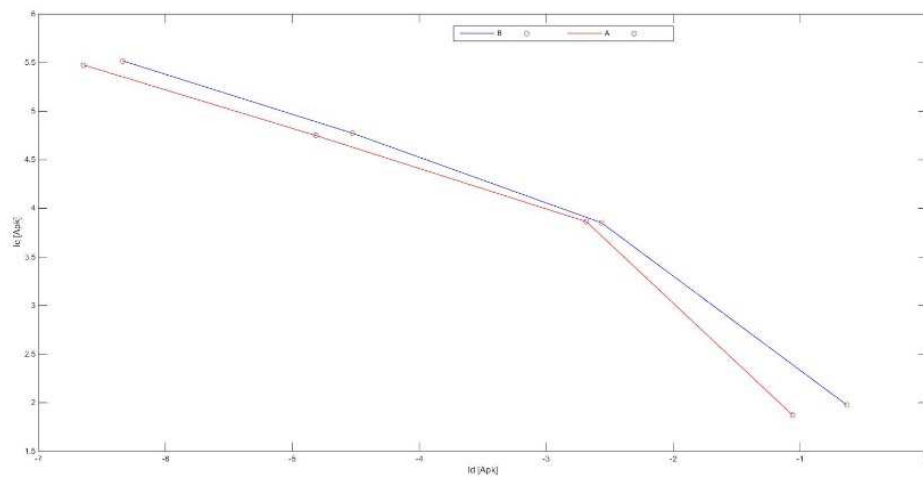


Fig. 8.3

The results are shown in Figure 8.6. It is noted, as predicted, that the distance between the LM feature from the MTPA increases as the speed increases.

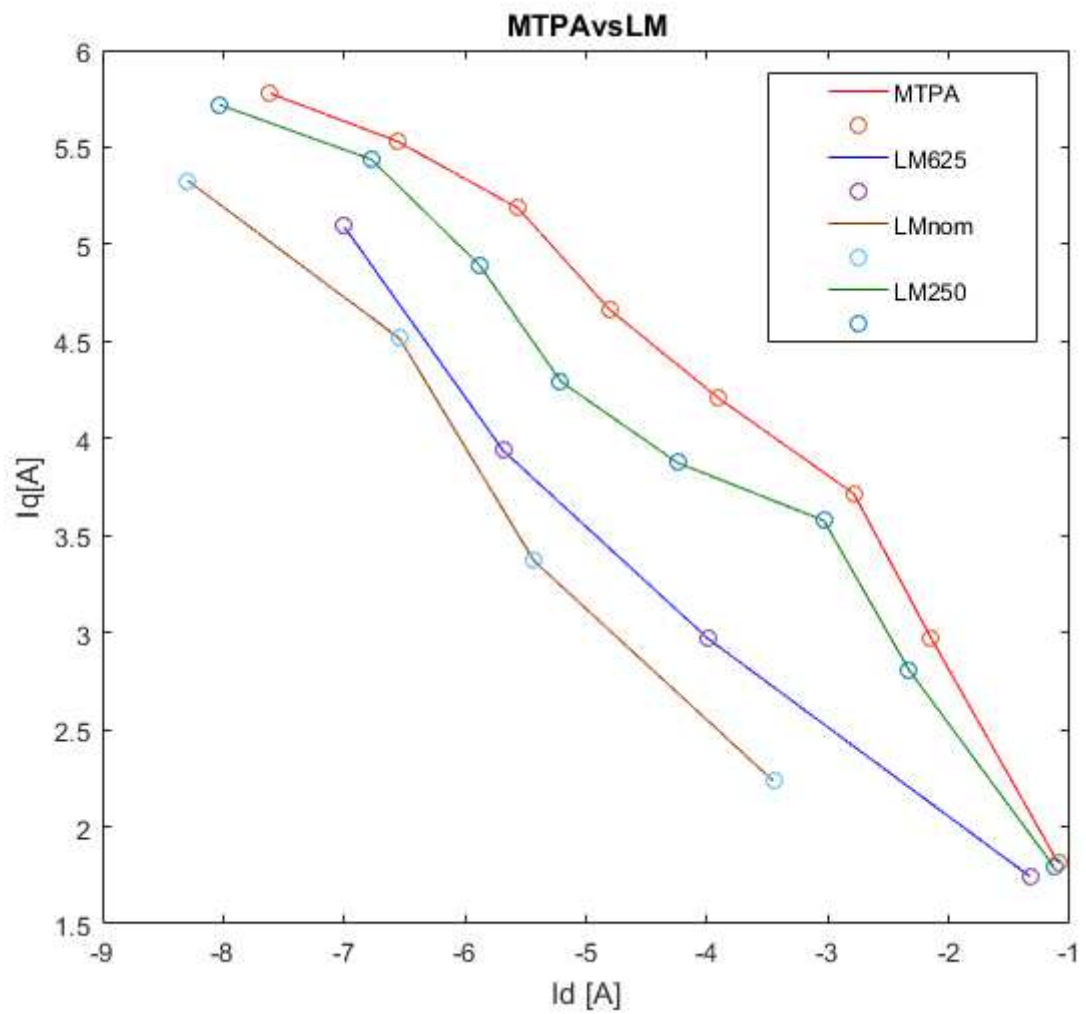


Fig. 8.5: LM characteristics at different frequency

Chapter 9

Cross verify on time step characteristic

Comparison between different MTPA derived by FEM studies

Let's make a further check on the MTPA founded during the use of time step simulations, identifying an error of assessment regarding the position of the axis d by FCSmek. It will be useful to see how an error like that can affect the control's trajectory.

Subsequently, the two MTPAs derived from FEM simulations will be compared, hypothesizing what may be the reasons for any discordance.

9.1 Cross-check – MTPA from time-step correction

To be able to verify the characteristic obtained in time step, a cross-check is made between the outputs of the magnetostatics simulations with the flux table and the outputs in torque, currents and flux showed by time-step simulation.

9.1.1 Problem individuation

To find out any problems, a spreadsheet was built; that can be seen in every part in Figure 9.1.

NOMINAL POINT - TORQUE OUTPUT					
time-stepping simulation results					
simulation parameters:			Output:		
Rs	0,8 [Ohm]		S	4400 [W]	
Pout	4000 [W]		P	4104,3 [W]	
Valim	370 [V]		Q	1585,7 [W]	
Ibase	6,875 [Arms]		Is	6,88 [Arms]	
			cosfi	0,9328 ind	
			Ldd	17,189 [mH]	
			Ldq	-2,13 [mH]	
			Lqq	90,58 [mH]	
			Ld	18,43 [mH]	
			Lq	94,24 [mH]	
			Id	-8,41 [Apk]	-0,865 p.u.
			Iq	4,9 [Apk]	0,504 p.u.
			Fd	0,073 [Wbpk]	
			Fq	0,462 [Wbpk]	
			efficien	0,9328	
			FPM	0,1943 [Wbpk]	
mgt-stat simulation - cross check					
ip.u. fixed like time-step output, the flux as to be the follow:					
Fd	0,10317 [Wbpk]		apparent inductances:		
Fq	0,405 [Wbpk]		Ld	12,26 [mH]	Lq 82 [mH]
flux fixed like time step output, the current in p.u. value as to be the follow:					
Id	-1,04 p.u.		apparent inductances:		
Iq	0,6 p.u.		Ld	7,135 [mH]	Lq 80,2 [mH]
Using the mgt-stat output that give directly the inductance:					
Ld	8,6 [mH]				
Lq	94,3 [mH]				
OUTPUT IN COPPIA:					
extended formula (1,9)	12,729	11,734749	15,292		[Nm]
explicit formula (1,12)				13,45	[Nm]

Fig. 9.1

In practice, a check was made to compare torque outputs according to formula (1.9) and (1.12). The time-step simulation was taken into account at the nominal point and the outputs were taken (highlight in yellow); fixing once the currents (highlight in green), once the fluxes (highlight in orange) of this simulation, it has been read in the fluxes table how effectively the currents and the corresponding fluxes are valid or how much the currents set the values of flow. Further verification was made using the inductance matrix, this time fixing the currents (highlighted in blue). The latter is a further output of the magnetostatic simulations that also provided fluxes tables, but didn't match the simple formula that sees the relationship between flux and current in the respective axes, so it was taken as a third part of the comparison.

The torque was compared to the nominal value and between themselves. As it can be seen from the spreadsheet, the cross-checking has highlighted a problem that is certainly greater than the fact that magnetostatic simulations don't mediate the stator effects. The torque values coming out of the various tests, differentiated by the different colours, are very far from the nominal value.

9.1.2 Problem solution

The possible causes of the problem are essentially two:

- Error in identifying the direct axis position with respect to the peak of the voltage in the phase 'a' of the triad;
- not very high precision of the interpolation method of the flux matrix;

The entities of the error let us assume that the first hypothesis is the one responsible for the error. This fact plays to our advantage because an incorrect direct detection axis does not affect the current module, but only its angle, and then the components i_d and i_q . Therefore, it is necessary to test with a current simulation set at the same value of module already obtained, and manually change the rotor angle to achieve concordant results between the two simulations.

Direct axis detection

For assisted reluctance motors, it is easy to locate the direct axis angle once the stator reference position is known. Let see the Figure 9.2.

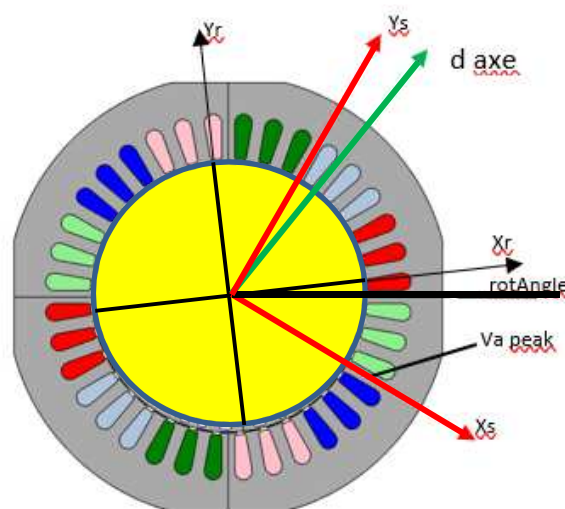


Fig. 9.2: axes position on the complete geometry of a four poles machine

As we know, considering the pole shown in the figure, the straight axis is at 45° precise mechanics. Adept fixes the stator reference coincidentally with the peak of the phase voltage and considers always fixed angle 0° of the stator, as shown in the figure.

Considering an angle of 0° rotor, we will have that the position of d axis with respect to the Xs axis is 75° mechanical degrees, which, for a 2 pole pairs motor, corresponds to 150 electrical degrees.

Constant current simulations with fixed d axes position of 150°

This kind of simulation brought the reconciliation between outputs as desired. The results are shown in Figure 9.3. In yellow the results of the simulation with current imposed, which can be done by modifying the .ini file in the dedicated section.

The torque output of the flux matrix checkout, as we see, approaches far to the nominal value, as desired. The result is not exactly the same, but this is justified by the fact that interpolation can lead to minimal errors and also that the flux matrix used derives from a single magnetostatic simulation and that, therefore, it doesn't mediate of the stator effects widely discussed in the previous chapters.

Nominal point - results of the simulation at fixed current and a axes angle fixed									
nuovo angolo di rotore			62,16015921 //65		interpol of the flux table		rispetto a d(0.78):	Fd'=Fd(0.78,0.54)+(idp.u-0.78)/(0.84-0.78)*(F0.84-F0.78)	
							rispetto a q(0.54):	Fq'=Fq(0.54,0.78)+(idp.u-0.54)/(0.6-0.54)*(F0.6-F0.54)	
id	-7,9702 [Apk]		-0,819750177 p.u.						
iq	5,58075 [Apk]		0,573990716 p.u.						
Fd	0,11011 [Wbpk]			>>>>	Fd(-0.84,0.54)	0,10646 [Wbpk]			
Fq	0,455 [Wbpk]			>>>>	Fq(-0.84,0.54)	0,44266 [Wbpk]			
					Fd(-0.78,0.54)	0,11306 [Wbpk]			
Torque	12,72281215 [Nm]				Fq(-0.78,0.54)	0,4437 [Wbpk]	Fd=	0,10954 [Wbpk]	
					Fd(-0.84,0.6)	0,10836 [Wbpk]	Fq=	0,45973 [Wbpk]	
					Fq(-0.84,0.6)	0,47622 [Wbpk]			
					Fd(-0.78,0.6)	0,11455 [Wbpk]			
					Fq(-0.78,0.6)	0,47633 [Wbpk]			
							TORQUE OUTPUT	12,8265 [Nm]	

Fig. 9.3

9.1.3 MTPA adjustment

After a focus of the problem, we know that Adept, for an unidentified reason, missed the direct axis direction and, therefore, we are ready to correct all the points of the MTPA feature in addition to the nominal point, working point taken into account to check the problem.

But using or not the process seen so far that use imposed current simulations? The answer is, of course, no: it is not necessary to re-perform all the simulations, we will need to locate and calculate the error made by the simulation, and because the current module isn't affected by the detection of this angle, it's only necessary to recalculate the components of the MTPA feature.

To do this, it's enough to create a spreadsheet. In fact, knowing the PF, the electrical rotation of the rotor (rotAngle_e = p x rotAngle) and taking into consideration the fact that the voltage is concatenated, while the voltage vector is a phase vector (we will have another 30 electrical

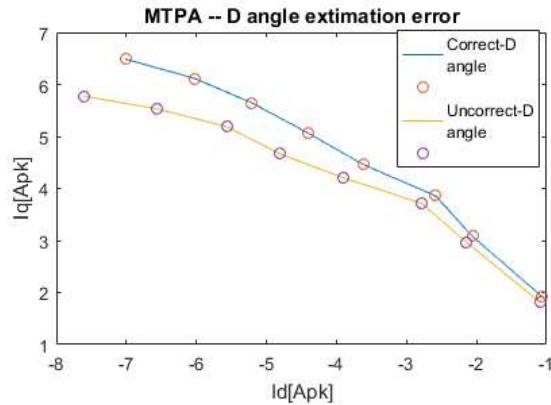
degrees to be added), we can find the current angle with respect to the axis d and then we can correct the components by the following formulas:

$$\gamma = 150 + 30 + \arccos(PF) + \text{rotAngle} \quad (9.1)$$

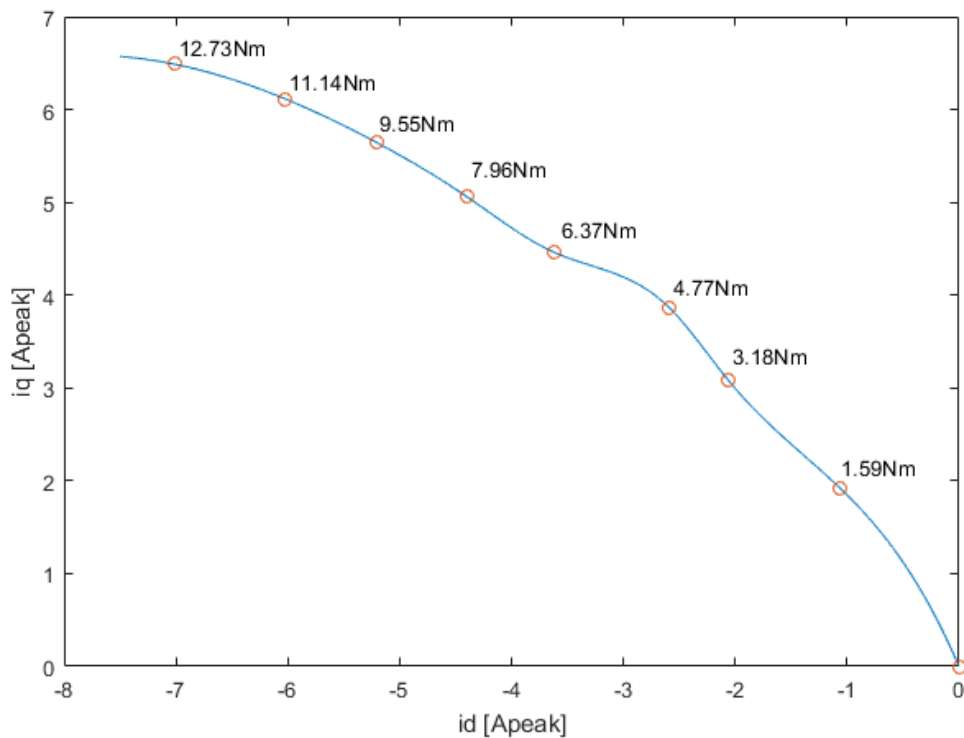
$$i_d = \sqrt{2}I_s * \cos(\gamma) \quad (9.2)$$

$$i_q = \sqrt{2}I_s * \sin(\gamma) \quad (9.3)$$

The results of these adjustments can be seen in figure 9.4; as you can see, the after characteristics differ in a greatly way, despite the axis detection errors not exceeding 5°. This let us know how the identification of the direct axis position is a subject that requires a lot of precision, because of the strong impact it has on control trajectories.



(a)



(b)

Fig. 9.4: (a) evidence the difference from the correct and the previous MTPA (b) new MTPA from time-step simulation

9.2 MTPA from FEM simulations compare

NB: for the subsequent considerations, reference will be made to the convention which consider the flux of the permanent magnets in ferrite is oriented as the axis in quadrature. Refer to section 1.3.3 if it's not clear for the reader at this time.

Figure 9.5 puts the outputs from all FEM simulations made up to date on the same graph. We will refer to this for all subsequent considerations.

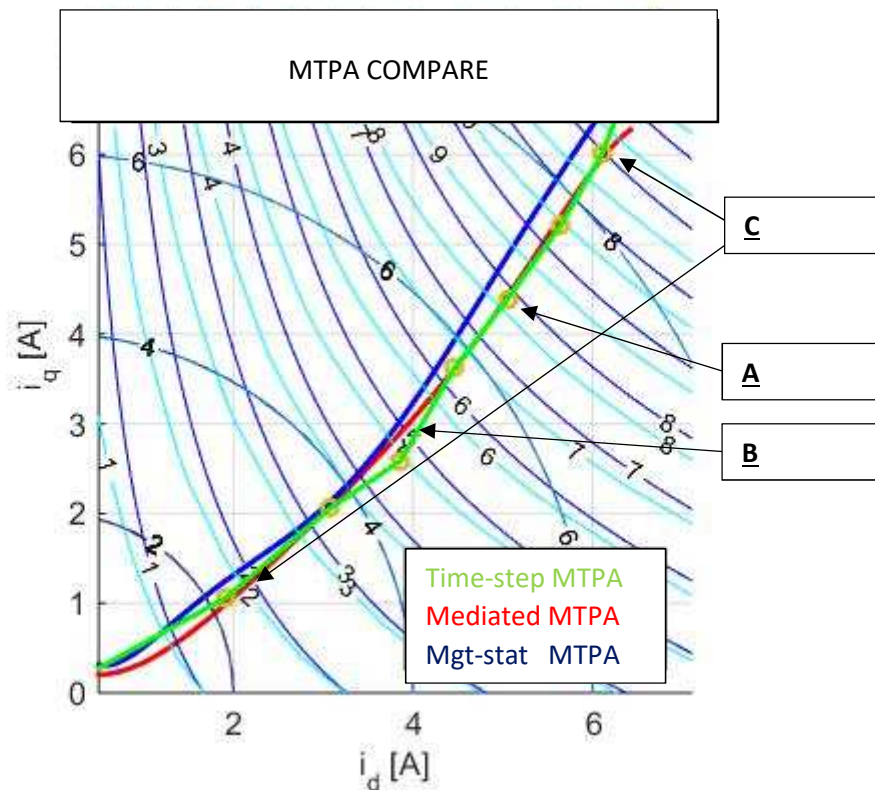


Fig. 9.5

Focus our attention on the 3 points indicated in the figure.

A

The indicated point is that in orange which indicates a torque of 7.96Nm, as by time dependent simulation.

This point makes easily observable which iso-torque curves, if those blue or azure, are the correct ones. Pausing on the fact that 7.96Nm is a value just less than 8Nm, you can easily become aware of the fact that, considering the azure curves, this point should correspond to a torque of about 8.2Nm; referring instead to the blue iso-torque curves, or those deriving from MTPA found in the seventh chapter of this paper, the indicated point is slightly below the characteristic iso-8Nm, as expected.

This speech reinforces and confirms what was said when discussing this previously (Chapter 7), confirming once again the correctness of the MTPA feature that considers the effects on the magnetic flux of the stator.

B

The area indicated by the arrow shows a zone (around the point which indicates 4.77Nm) of strong disagreement between the red (without stator effects) and the green trajectory resulting from time-dependent simulations.

In the other points, the two simulations agree, except for the start and end portions, which we will comment below.

Why is this point in disagreement?

It is noted in the meantime as this point is not in disagreement with the curves iso-torque. In fact, it is exactly where you expect to find it. This means that, in addition to strengthening again what is said in the step **A**, the time-step simulation was not wrong to identify the operating point, is simply far the current vector identified in this case.

However, as mentioned in Chapter 5, the fact that the detection of the minimum current points was made by means of finite power supply voltage step, or, by modifying this, the minimum current point was noted, thus making a mistake from this finished step of voltage, more or less serious; this fact was mediated on 8 different points that united the torque, but not the speed. In this case, however, the error consists and is evident.

C

The areas indicated by the arrows show divergence between the characteristics, despite the fact that the orange points (which are typical of the MTPA time-step feature) almost fit the MTPA in red.

The reason for this is the choice of two different types of interpolation in Matlab, one making use of the *spline* method, the other a linear interpolation method *interp01*.

Part III

Chapter 10

Test bench and tests description

The test bench is always located at the ABB in Vittuone (Milan). Let's describe the tools used to carry out the tests on the motor under test and then will be described the actions that the test involves in order to obtain the desired feature.

10.1 Test bench overview

The test bench, figure 10.1, is composed by:

- 1 computer
- 1 power analyser
- 1 torque transducer and its reader tool
- 1 current sensor
- 1 thermocouple bench
- 2 drivers
- 1 motor / generator
- 1 bench for mechanical coupling
- 1 plexiglas structure for protection

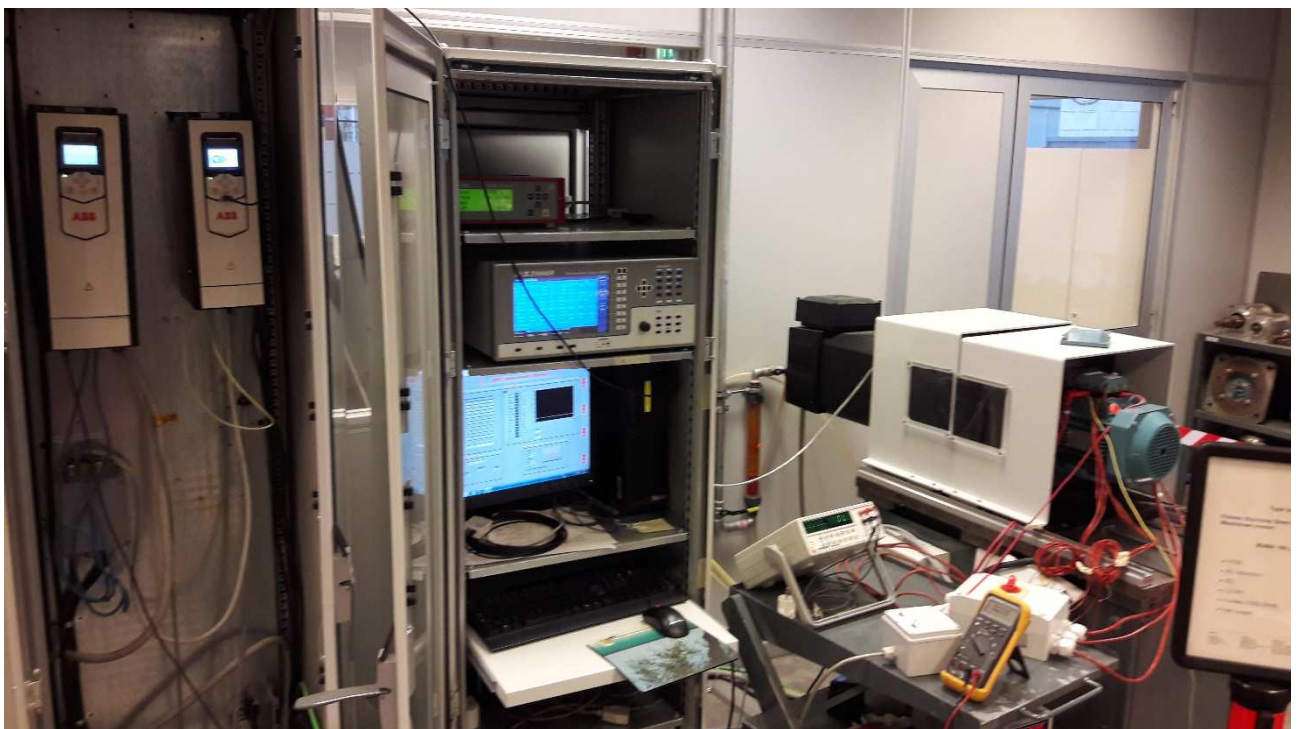


Fig. 10.1: ABB test bench

Referring to Figure 10.2, you can better understand the functionality of the tools.

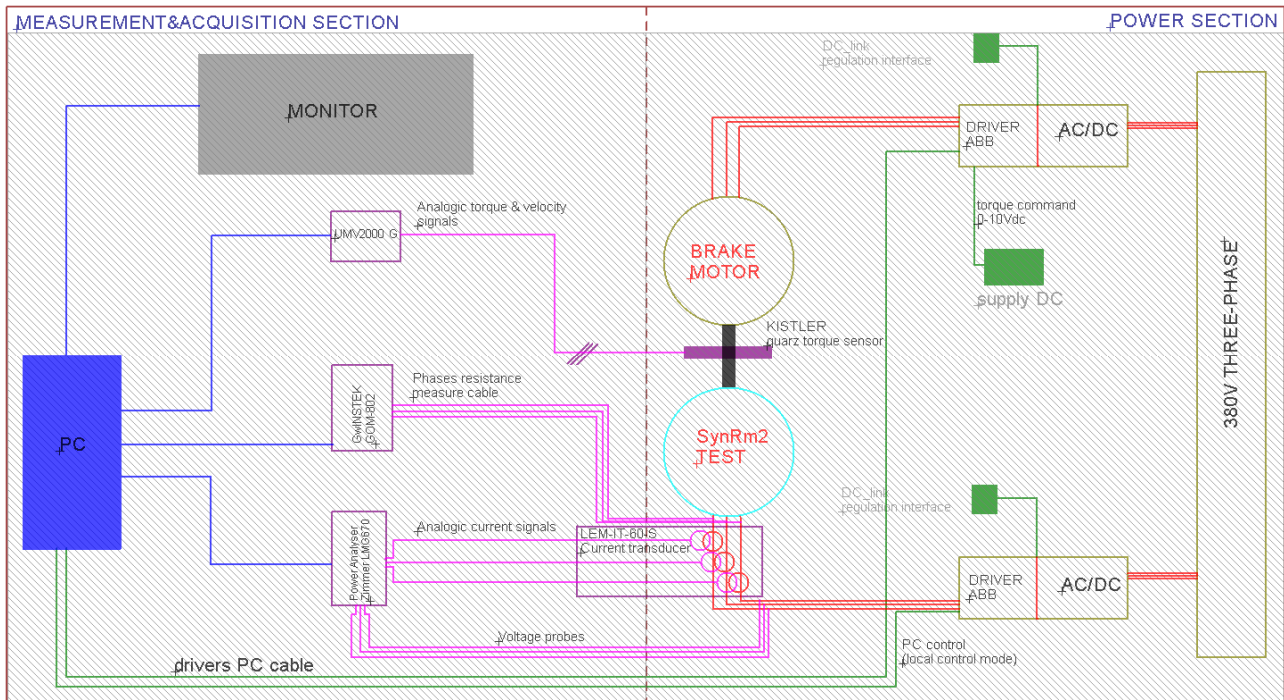


Fig. 10.2: LAB functional scheme

Power analyser

The power analyser provides real-time measurements of all electrical quantities. Thanks to the computer, you can real-time logging these measures to accumulate process data.

The figure 10.3 shows the interface screen and the power analyser used.



Fig. 10.3

Due to the high sampling frequency, the instrument allows precious analysis to the harmonics of the waveforms measured.

Kistler torque transducer

The torque transducer used have a high precision and allow us to know the real working point of the motor as well as to centre it during tests.

The torque sensor consists of two steel disks, between which a ring is fitted which contains several shear-sensitive quartz plates. The crystal axes of the quartz plates are oriented tangentially to the peripheral direction and therefore yield a charge exactly proportional to the applied torque.

The quartz set is protected by the tightly welded and rustproof steel case. The sensor is oil- and splashproof if a tightly fitted cable connector is used.

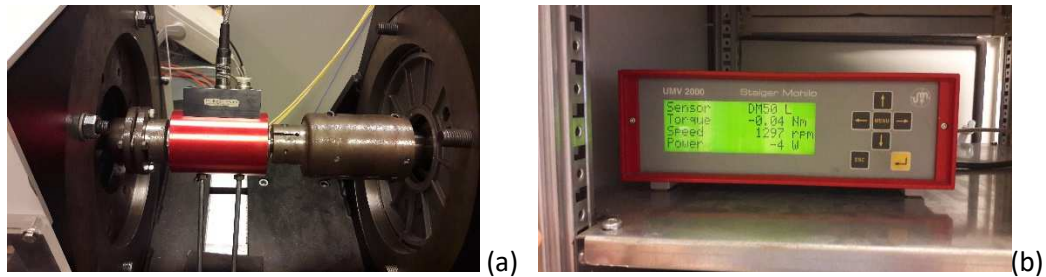


Fig. 10.4: (a) torque sensor; (b) torque reading tool

Inverters

The access to the drivers, though limited, allows us to know the actual values of control (measurements of the DC side voltage, AC output voltage, effective current measurement, speed in rpm etc ...), the current values of direct-axis and quadrature and the control loop gains of the DT and also allows us to act on the appointed parameter "voltage reserve "; this parameter will allow us to change the AC output voltage from the drive. All through an easy interface program.

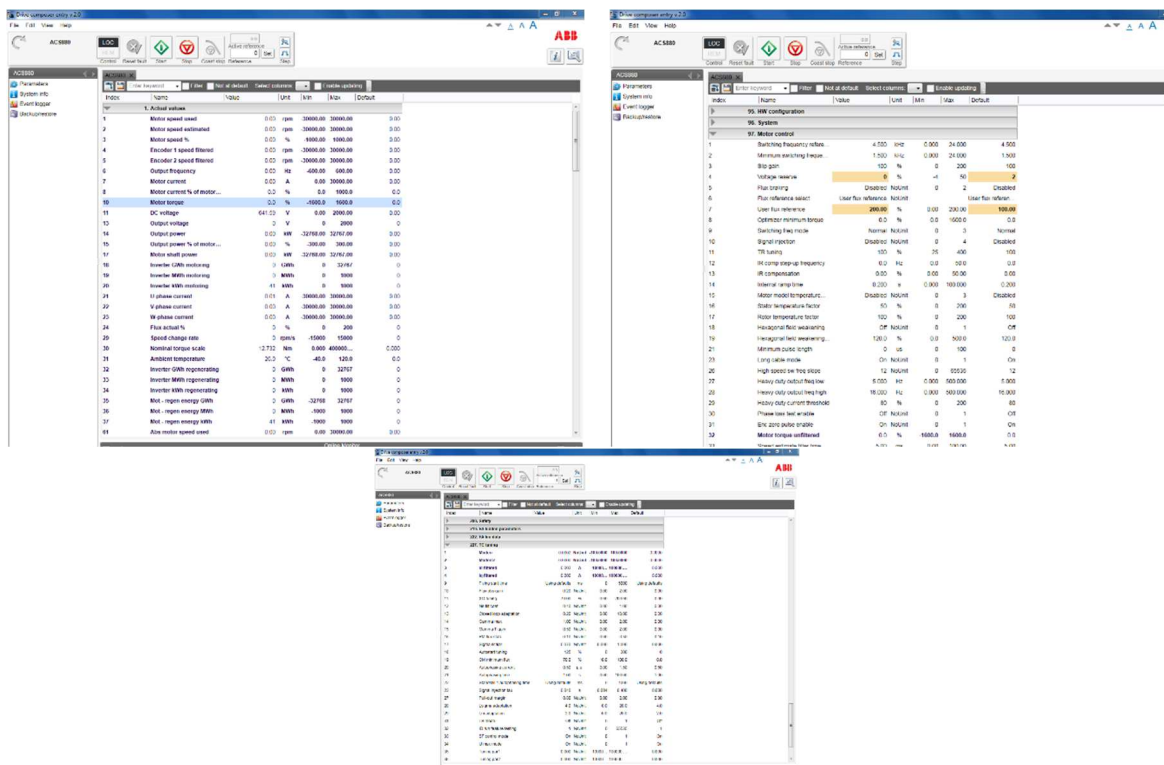


Fig. 10.5: driver program interface

10.2 Experiment description

The tests are essentially two, the first with the stator at ambient temperature (25-30°C) and the second one at a higher temperature (60-70°C).

By observing the measurements at different working points of the motor under test, we can trace the drive control trajectory.

Having a direct torque drive, it always works in MTPA; our aim is to discuss how, in fact, the drive would centre this feature in different operating conditions.

The brake motor is torque driven, with an open speed loop. The one tested, however, is driven in speed and responds to the torque disturbance given by the brake because they are mechanically coupled. By setting the SynRm2 speed at the rated speed (3000rpm), it is possible to observe several working points of this motor by setting the braking torque provided by the brake motor through a simple DC power supply.

The torque is known through the measurement of the torsionmeter, which also provides the speed measurement.

Once set the operating point, we take note of the supply voltage output from the drive, the *rms* current of the fundamental (measured by the power analyser and from the drive via LEM sensor) and the direct axis current and in quadrature estimated and filtered from the drive, viewable in real-time interface screen. The control feature set by the drive is now traceable.

But how do you figure out if the current we measured is actually the minimum for that torque or is the best point that the drive can do with the actual DC voltage? Is that enough?

The supply voltage has to be varied: in fact, at slightly higher or slightly lower voltages, there are noticeable changes of the current; if you had to find the lower current than the one you initially had, the drive was not actually working on the lowest current feature.

On the output voltage of the drive we can act on the "voltage parameter reserve", a parameter that affects the characteristics of field weakening of the motor (the amplitude of the range at constant power, in fact, depends greatly on the DC voltage available), and not only. The voltage reserve is a parameter that operate on the output voltage giving a value under the maximum theoretically possible as output for the motor to be drive. As known, the relationship between DC-link voltage and maximum output voltage from the drive (ignoring losses by switching and conduction) is:

$$V_{out} = \frac{V_{dc}}{\sqrt{2}};$$

The parameter influences the value of V_{dc} . lowering up to 50% of its initial value and increasing it by 4% maximum.

Working on this parameter, it is possible to vary the output voltage from the drive.

Limitations of test bench

The main limitation is basically that it is not possible to increase the output voltage from the drive when it is already at the point of MTPA estimate by the driver control algorithm.

This is a big limitation; in fact, it's not possible to see if there is a lower current for a higher motor supply voltage than the one set by the inverter.

By simulation, the power supply voltage that gives the MTPA was higher than the one estimated and provided by the drive. We can only draw the control characteristic as a result of pure observations, comparing it with the MTPAs derived from FEM simulations.

Chapter 11

Experiment results

In this chapter will be seen and commented the results of the tests described in the previous chapter. Tests are the two made at a different temperature.

11.1 Case A: stator temperature of 35°C

For this test are also considered overload working conditions, not particularly critical due to the low stator temperature of departure; this allow us to guess how the control works and if it changes when the torque is less or greater than the nominal torque.

Between the beginning and the end of the test, which was made from the highest torque value to the lowest torque value, the temperature increased by 7°C between the front and rear of the stator (4 thermocouples are used, two on the front and two on the rear of the stator, inside the carcass). For each point, we were concerned about having enough DC-link voltage so that the inverter wouldn't saturate the live output but actually worked at the estimated MTPA point (DC-link voltage may be from 200V to 750V DC, according to drive datasheet).

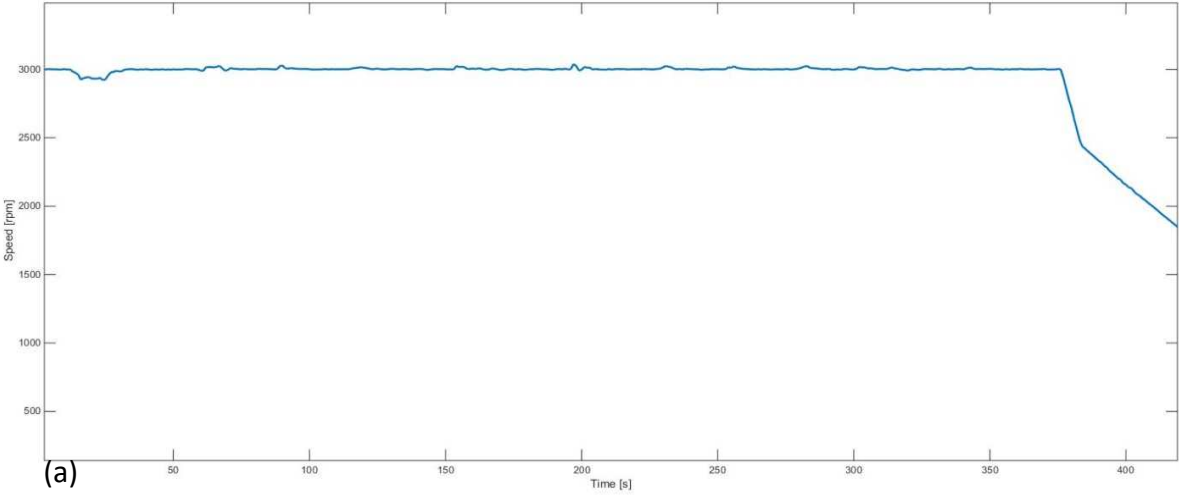
It is recalled that all tests were made at the rated speed of 3000rpm.

Below can be seen the results, in Table 11.1, which will then be shown graphically in Figure 11.1.

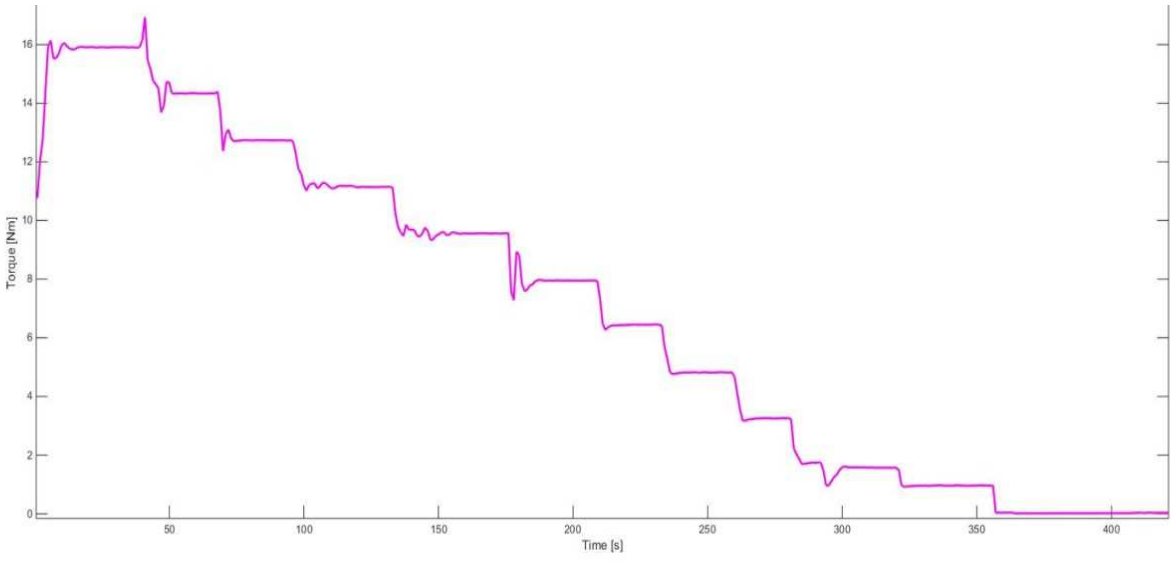
Torque[Nm]	Current[Arms]	Voltage[V]	Id[Apk]	Iq[Apk]
<u>17.5</u>	9.257	450	-11	7.1
<u>15.9</u>	8.34	435	-9.76	7.04
<u>14.32</u>	7.74	419	-8.5	6.94
<u>12.73</u>	7.1	400	-7.28	6.87
<u>11.14</u>	6.45	384	-6.23	6.6
<u>9.55</u>	5.8	365	-5.4	6.11
<u>7.96</u>	5.12	353	-4.53	5.515
<u>6.37</u>	4.46	323	-3.81	4.92
<u>4.77</u>	3.62	286	-2.98	4.17
<u>3.18</u>	2.76	239	-2.07	3.32
<u>1.59</u>	1.68	188	-1.12	2.06

Tab. 11.1

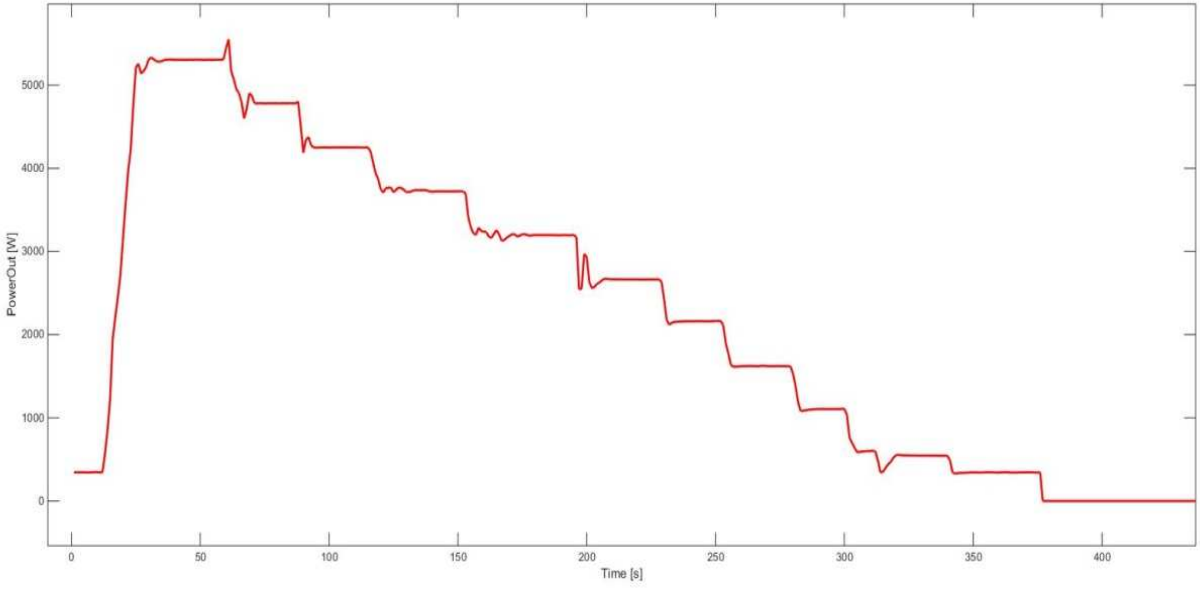
Below, there are the plots of the measures and the derived information during the experiment and then the MTPA plot.



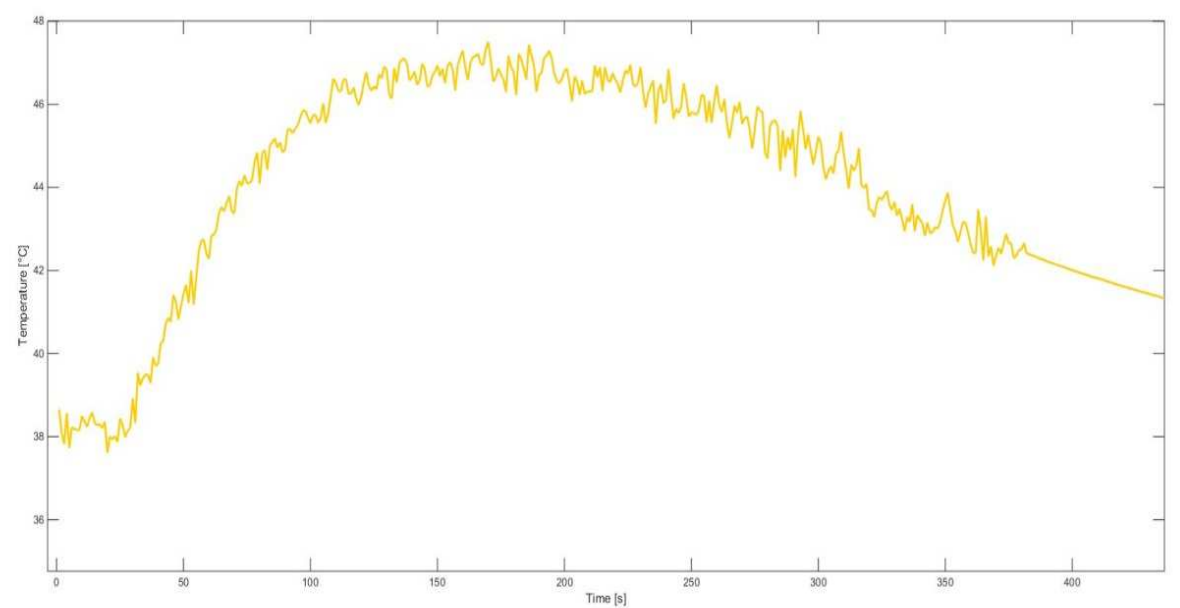
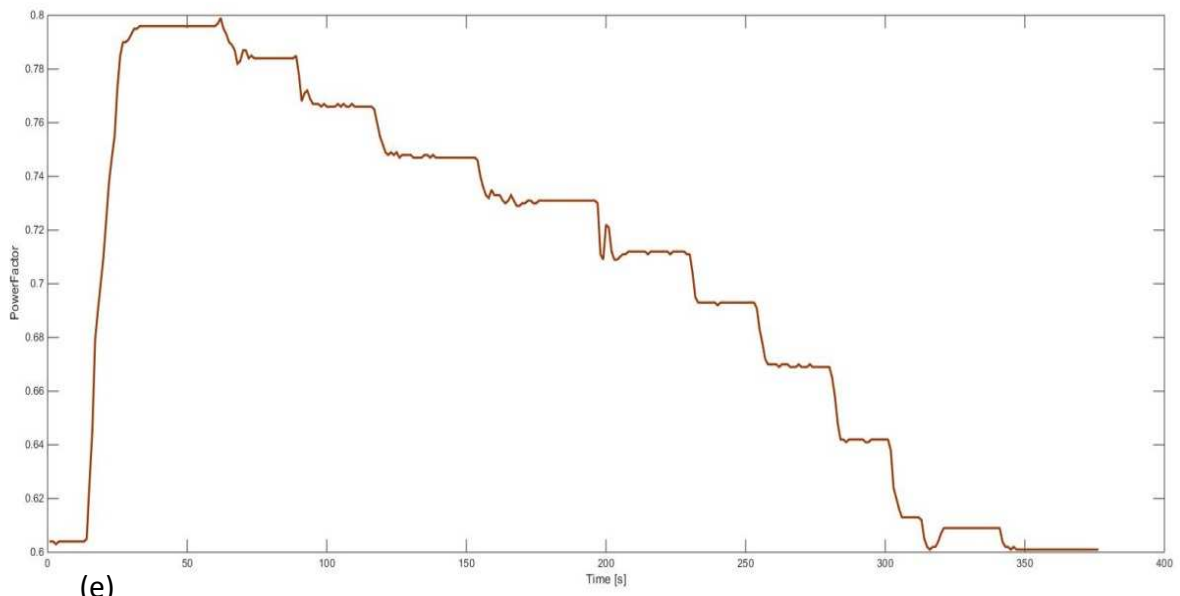
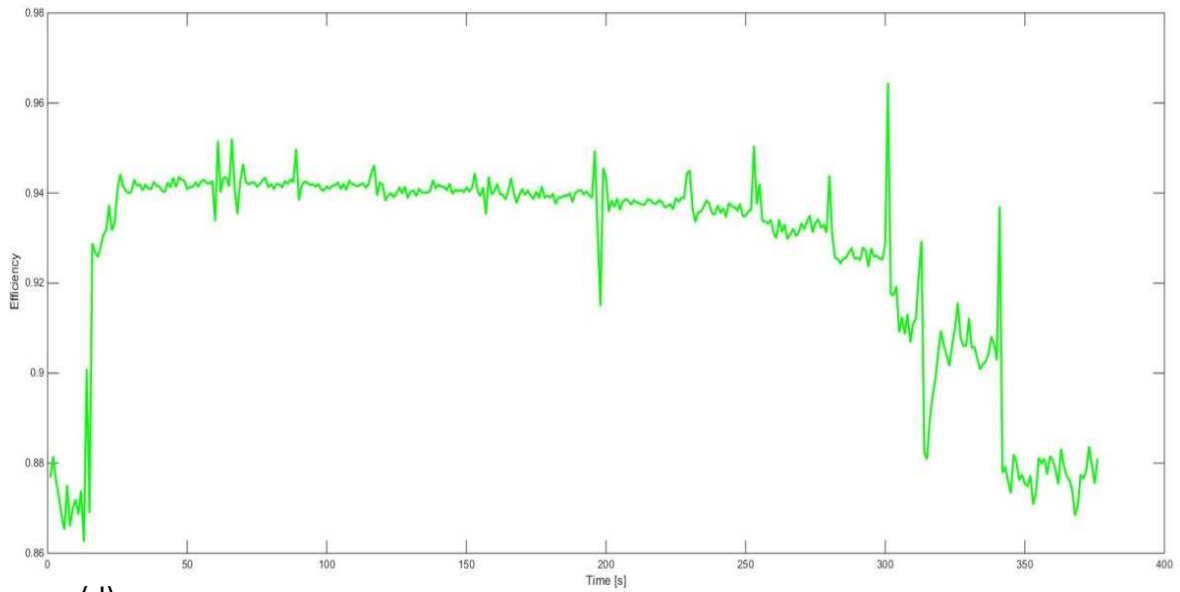
(a)

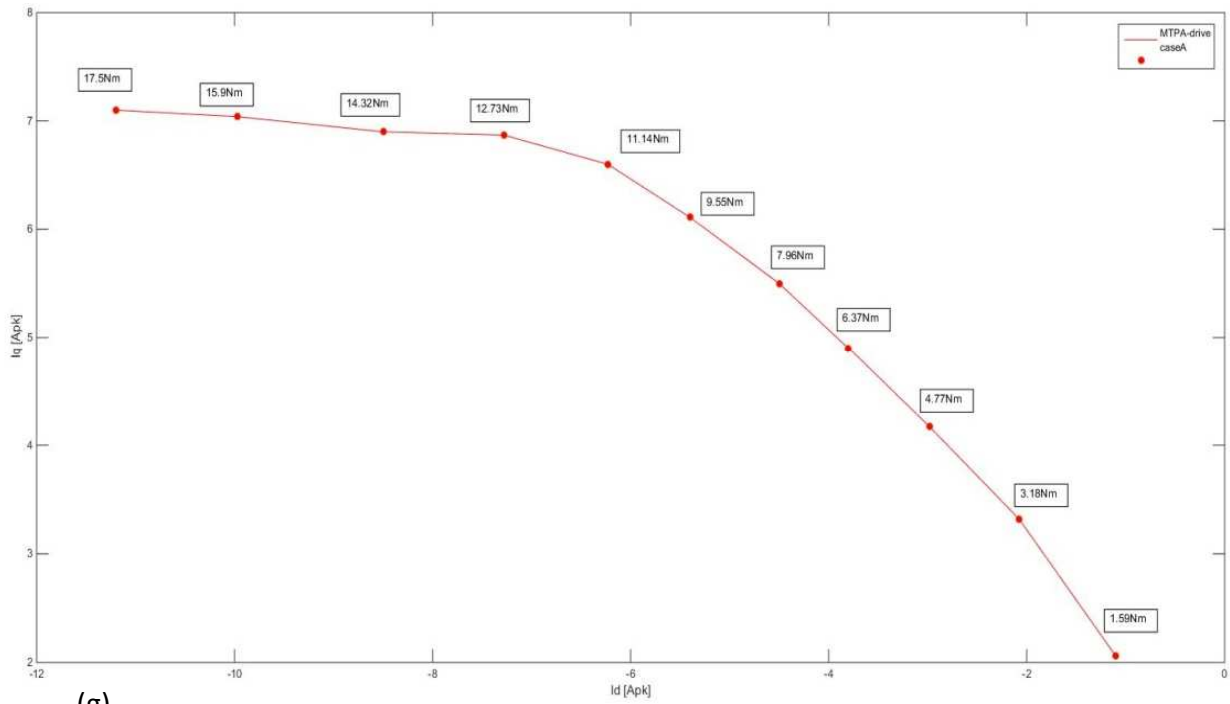


(b)



(c)





(g)

Fig. 11.1: experiment results – caseA

There is a strong saturation of the axis q when the nominal torque is exceeded.
We represent the current control angles, knowing the points of this characteristic (Fig. 11.2).

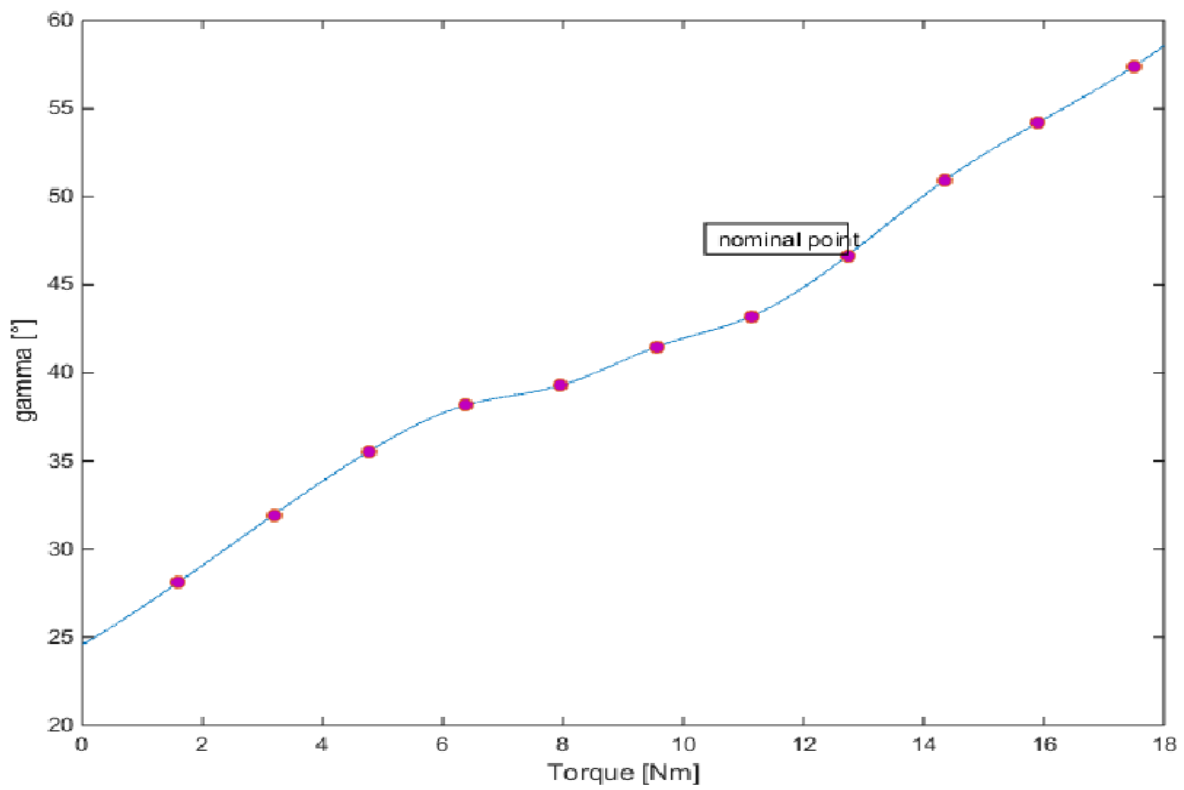


Fig. 11.2

There is a strange change in convexity in the characteristic when the torque exceeds the nominal value.

A comment that can be made is about how the driver drives the motor under test; in fact, this changes completely when the nominal torque is exceeded and it saturates all the axis q. In fact, what may seem like a inflection point at the rated torque point of the current angle control feature (from literature, the current angle should touch a peak and then go down again).

11.2 Case B: stator temperature of 65°C

For this test, differently from the first, we will stop at the nominal point for evaluating the piloted feature.

The temperature between the start and end of the test has dropped by about 5 ° C.

Torque[Nm]	Current[Arms]	Voltage[V]	Id[Apk]	Iq[Apk]
<u>12.73</u>	7.12	408	-7.08	7.15
<u>11.14</u>	6.47	390	-6.26	6.63
<u>9.55</u>	5.84	378	-5.43	6.14
<u>7.96</u>	5.09	356	-4.6	5.6
<u>6.37</u>	4.42	326	-3.85	4.99
<u>4.77</u>	3.39	288	-2.87	4.16
<u>3.18</u>	2.71	239	-2.06	3.32
<u>1.59</u>	1.69	190	-1.04	2.15

Tab. 11.2

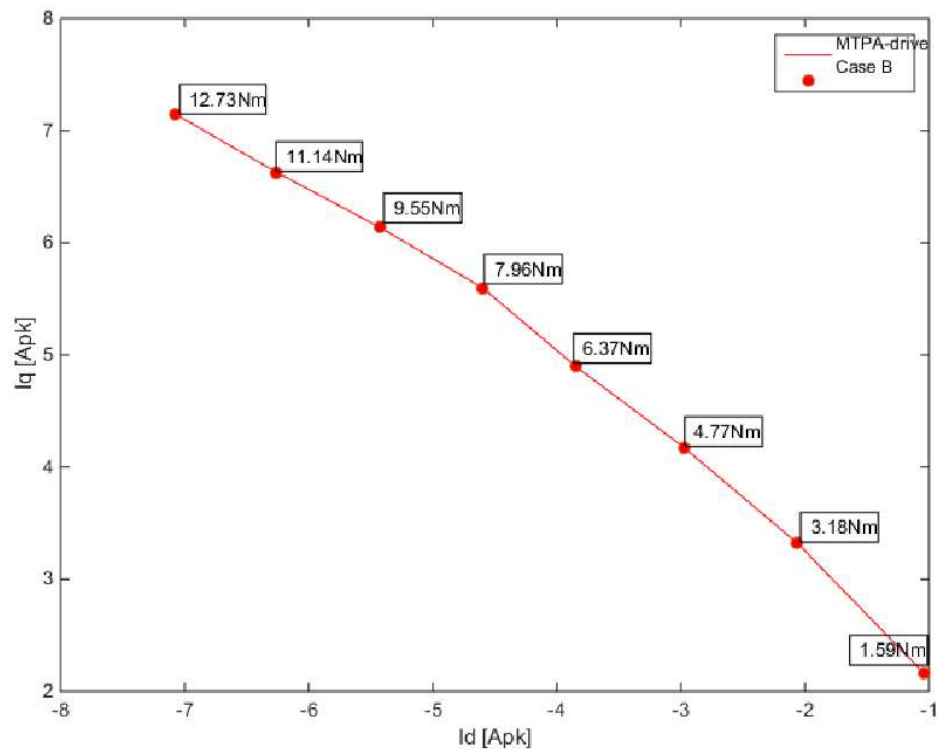


Fig. 11.3: MTPA from drive – caseB

11.3 Case A and case B compare

It has been already sensed from the Fig.11.3 what we're going to say: the control does not consider changes in temperature as the system variables for the determination of a minimum current characteristic.

In fact, they are identical (except for measurement errors or small scraps), as shown in Figure 11.4.

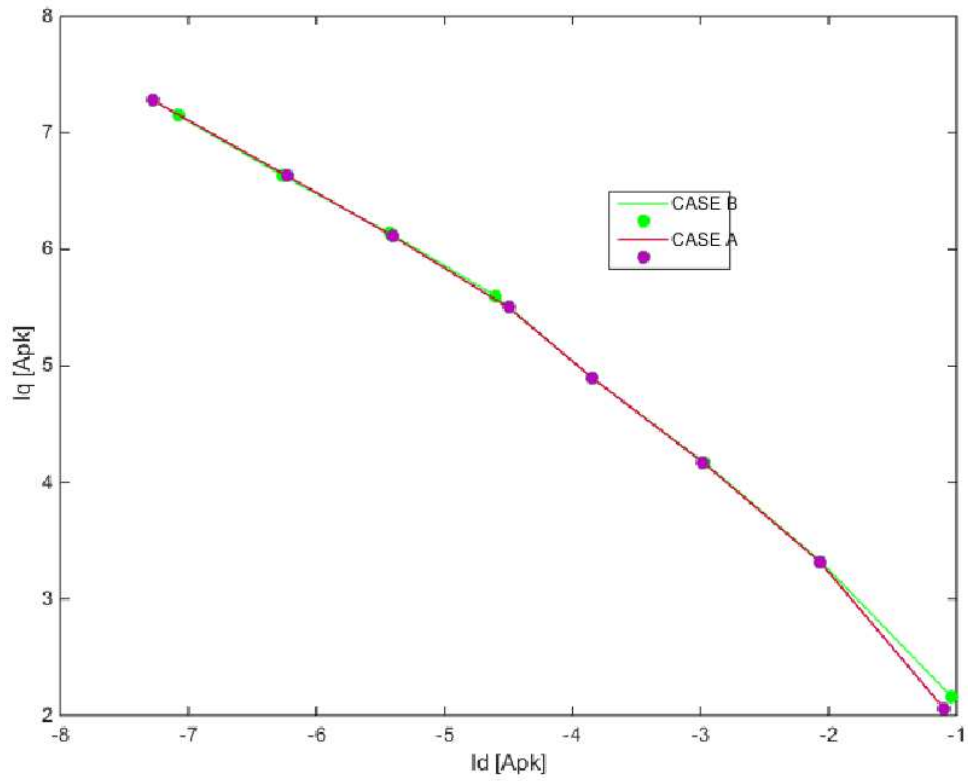


Fig. 11.4: MTPA comparison

Conclusions

In conclusion, we can compare the simulation outputs with the MTPA obtained in the laboratory, highlighting its primary characteristics.

Remember that it was not possible to check the actual MTPA in the lab because of the lack of drive accessibility, as the output voltage could not be raised by the inverter.

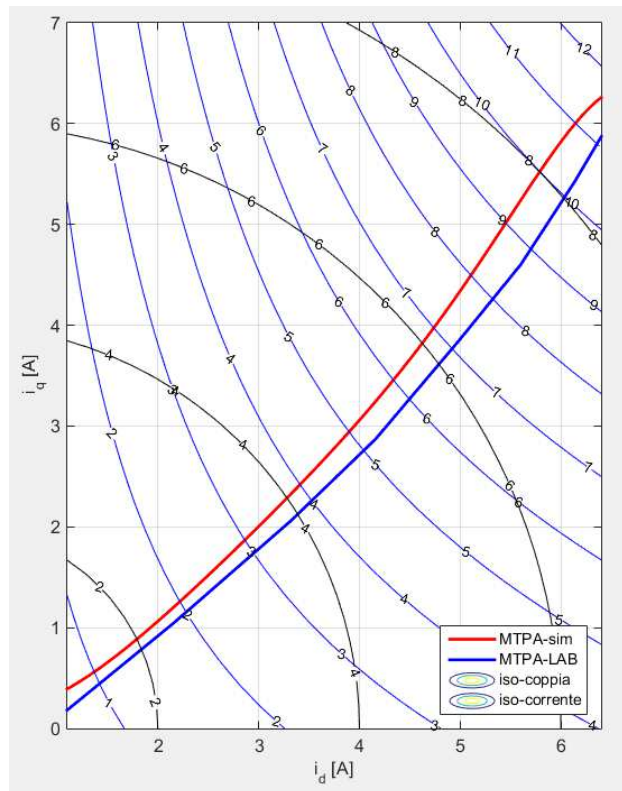


Fig. C.1

From the lowest torque, the two MTPAs are quite far.

In conclusion, we can't focus on the correctness of neither of the two characteristics for simple reasons:

1- also if the red characteristic resulting from FEM simulations have until now centered every point of investigation, this comes still from FEM calculations which, of course, comply with the mathematical model of the motor and for this reason it follows very well the literature; but the mathematical model as we know it's approximated in a more or less strong way, the errors of such simulations can start from the initial data, due to material imperfections, of the magnets etc ... which however in reality matter in a modest way. Finite element analysis is much more useful in terms of machine dimensioning, which gives the idea of current and voltage values so that the entire motor can be dimensioned electrically and mechanically. This thesis shows the difficulty encountered using FEM analysis for control applications that requiring much accuracy and field measurements and direct or indirect derivations of other quantities.

2- the control characteristic traced by the drive can't be questioned due to the fact that that does not allow us to search for a lower current point raising the motor supply voltage, thing that very easily occurs: from simulation, the power supply voltages of the motor to have minimum current were higher than the drive supplied to the motor. Also, by lowering 1% of the supply voltage to the motor, there were significant changes of current value, which suggests that the point is not actually MTPA, since, around this point, the current varies very little. Figure C.2 shows this fact, result obtained by simulations in Chapter 5 and here again to reinforce the thesis.

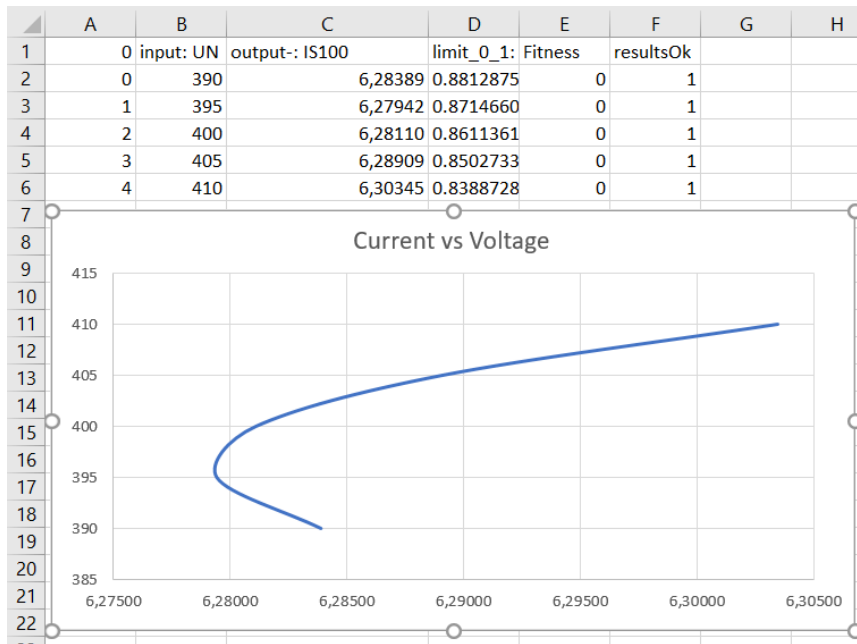


Fig. C.2

Figure C.2 shows the power supply voltages on the abscissa axis and the effective phase currents related to the working point at 3000rpm, 11.14Nm.

With a 5V delta, the current changes in the order of a few thousandths of an ampere. This does not happen when you move away from the lower current point (here at 395V), for example, going from 405V to 410V, the current module changes by 2 cents.

In the lab, the same workstation was driven by the drive with a current of 6.47Arms and a voltage of 390V. By varying the tension of 1%, with about 386V of power supply voltage, the current increased by 4 cents Ampere, arriving at 6.51Arms value. This sensitive rise of current lets us assume that we are not close to the lowest current point, despite the fact that this is the minimum value of current we can obtain in the laboratory. Probably, increasing the voltage in this case we can obtain a lowest current value than the first. But all this has not been demonstrated because of lack of drive accessibility.

3- An observation which criticizes the accuracy of the FEM simulations is the fact that the points highlighted in the figure in the trajectory followed by the drive in green, are those considered up to now. These are not completely in agreement with the iso-torque curves arising from FEM simulations.

Since the torque was measured by a torque transducer in the laboratory, we can be sure that those points are to the specific torque, so the level curves in Figure C.1 are incorrect.

This does not mean, however, that the MTPA traced in the lab is right, but only that the points found are right with respect to the measured torque, ignoring the accuracy of the instrument.

Bibliographical references and sitography

- [1] UNINETTUNO-Azionamenti elettrici 2, prof. Vagati; available at: <https://www.youtube.com/watch?v=buLnfofSOU&list=PLzz3KcpmIGDxhTVg5zqilQAanFUTHQypG>
- [2] UNINETTUNO-Azionamenti elettrici 1, prof. Profumo; available at: <https://www.youtube.com/watch?v=Mmp5-FI7h18&list=PLzz3KcpmIGDwhpUgTWdlgu49vmsbzbvBva>
- [3] Genetic algorithms – The nature of the code; available at: <https://www.youtube.com/watch?v=9zfeTw-uFCw&list=PLRqwX-V7Uu6bJM3VgzjNV5YxVxUwzALHV>
- [4] Basics of finite element analysis; available at: <https://www.youtube.com/watch?v=pB9DqY1bYtk&index=2&list=PLb960prooJQ9wSdJKPwvj6ZTjJojz5jx7>
- [5] FEM figures; available at: <http://belmans.what-when-how.com/numerical-modelling-and-design-of-electrical-machines-and-devices/electromagnetic-and-electrostatic-devices-electrical-machine-part-1/>
- [6] ABB drivers figures; available at: http://new.abb.com/docs/librariesprovider53/about-downloads/d-amp-m-cat-2017_v17.pdf?sfvrsn=2
- [7] Power analyzer datasheet; available at: <https://www.zes.com/en/Products/Precision-Power-Analyzer/LMG670>
- [8] UMV2000 datasheet; available at: <http://guemisa.com/mohilo/docus/UMV2000G.pdf>
- [9] Current transducer datasheet; available at: <http://www.newtons4th.com/wp-content/uploads/2014/07/LEM-IT-60-S.pdf>
- [10] "FCSmek in Daily Use", Tommi Ryyppö, Technology Development, BU Motors and Generators, ABB, November 2015
- [11] "Esempi di riprogettazione di macchine in cui i magneti permanenti in terre rare sono sostituiti da ferriti", Dario Broggi, Master thesis at Politecnico di Milano, relator Prof. Giovanni Maria Foglia, AA 2013/2014
- [12] "Analysis, Design and Optimization of Innovative Electrical Machines Using Analytical and Finite Element Analysis Methods", Michele Degano, Master thesis at Università degli studi di Padova, faculty advisor Prof. Nicola Bianchi, 2014
- [13] "Design of light hybrid vehicles suited to urban and sub-urban mobility", Marco Ferrari, Master thesis at Università degli studi di Padova, faculty advisor Prof. Silverio Bolognani
- [14] "Note sull'analisi e sull'ottimizzazione dei sistemi elettrici di distribuzione", course material "Distribuzione dell'energia elettrica" at Politecnico di Torino, Prof. Gianfranco Chicco
- [15] "Calcolo delle macchine elettriche col metodo degli elementi finiti", Nicola Bianchi, CLEUP 2001 Padova
- [16] "Design, analysis, and control of interior PM synchronous machines", Nicola Bianchi-Thomas M. Jahns, CLEUP 2006 Padova
- [17] European regulation 2005-32-CE; available at: https://it.wikipedia.org/wiki/Direttiva_2005/32/CE

- [18] EU 327-2011 - Fan Ecodesign; available at: <http://efficient-products.ghkint.eu/cms/assets/Fans-Implementing-Measure-Guidance-Notes.pdf>
- [19] Premium efficiency; available at: https://en.wikipedia.org/wiki/Premium_efficiency
- [20] <http://new.abb.com/motors-generators/energy-efficiency>
- [21] ABB internal Energy efficiency IEC standards; available at: https://library.e.abb.com/public/1018a82e36b29462c1257d41002b3470/TM025%20EN%2008-2014%20IEC60034-30-1_lowres.pdf
- [22] Energy efficiency indicators; available at: <http://new.abb.com/drives/ecodesign>
- [23] Matlab command 'dos'; available at: <https://it.mathworks.com/help/matlab/ref/dos.html>
- [24] Matlab command 'surf'; available at: <https://it.mathworks.com/help/matlab/ref/surf.html>
- [25] Matlab command 'interp1'; available at: <https://blogs.mathworks.com/videos/2008/06/30/matlab-basics-interpolating-data-with-interp1/>
- [27] Matlab command 'spline'; available at: <https://it.mathworks.com/help/matlab/ref/spline.html>
- [28] Matlab command 'contour'; available at: <https://it.mathworks.com/help/matlab/ref/contour.html>
- [29] Matlab command 'curve'; available at: <https://it.mathworks.com/products/curvefitting.html>
- [30] How to create .bat files; available at: <http://www.makeuseof.com/tag/write-simple-batch-bat-file/>

Appendix

A1

Plot characteristic MTPA

```
-----  
x=[  
-0.914454201  
-2.866478651  
-4.775681896  
-6.673433699  
-2.206  
-4.132  
-5.343  
-7.810  
]; %% d axis current  
  
y=[  
1.889744937  
3.636449975  
4.701796473  
5.439550032  
3.117  
4.158  
5.802  
5.797  
]; %% q axis current  
xx=[-10:0.001:0];  
MTPA_interpl=interp1(x,y,xx);  
plot(xx,MTPA_interpl,x,y,'o')  
hold on  
  
legend  
  
-----
```

This simple code is used to plot a MTPA characteristic found at a set speed; the couples (x,y) derive from the simulations done. A linear interpolation is then done between them and the result will be plotted.

Code inputs

-x
-y
from simulation results

Code outputs

-MTPA_interpl
a vector composed by 10000 value that follow the xy point
-a plot of MTPA_interpl with a legend

A2

MTPA average

```
%% MTPA-meshed
%% linearly weighted point in an iso-torque locus
id159=0;
iq159=0;
id318=0;
iq318=0;
id477=0;
iq477=0;
id637=0;
iq637=0;
id796=0;
iq796=0;
id955=0;
iq955=0;
id1114=0;
iq1114=0;
id1273=0;
iq1273=0;

for j=1:8           %for loop in order to give us the sum of all data

    id159=id159+T159(j,1);
    iq159=iq159+T159(j,2);

    id318=id318+T318(j,1);
    iq318=iq318+T318(j,2);

    id477=id477+T477(j,1);
    iq477=iq477+T477(j,2);

    id637=id637+T637(j,1);
    iq637=iq637+T637(j,2);

    id796=id796+T796(j,1);
    iq796=iq796+T796(j,2);

    id955=id955+T955(j,1);
    iq955=iq955+T955(j,2);

    id1114=id1114+T1114(j,1);
    iq1114=iq1114+T1114(j,2);

    id1273=id1273+T1273(j,1);
    iq1273=iq1273+T1273(j,2);

end

%filter the sum from the minimum and the maximum value at the corresponding
%Torque output and then, give the mean. 6 because 8 value minus 2 removed from
%the filter operation

id159=(id159+abs(min(T159(:,1)))+abs(max(T159(:,1))))/6;
iq159=(iq159-abs(min(T159(:,2)))-abs(max(T159(:,2))))/6;

id318=(id318+abs(min(T318(:,1)))+abs(max(T318(:,1))))/6;
iq318=(iq318-abs(min(T318(:,2)))-abs(max(T318(:,2))))/6;
```

```

id477=(id477+abs(min(T477(:,1)))+abs(max(T477(:,1))))/6;
iq477=(iq477-abs(min(T477(:,2)))-abs(max(T477(:,2))))/6;

id637=(id637+abs(min(T637(:,1)))+abs(max(T637(:,1))))/6;
iq637=(iq637-abs(min(T637(:,2)))-abs(max(T637(:,2))))/6;

id796=(id796+abs(min(T796(:,1)))+abs(max(T796(:,1))))/6;
iq796=(iq796-abs(min(T796(:,2)))-abs(max(T796(:,2))))/6;

id955=(id955+abs(min(T955(:,1)))+abs(max(T955(:,1))))/6;
iq955=(iq955-abs(min(T955(:,2)))-abs(max(T955(:,2))))/6;

id1114=(id1114+abs(min(T1114(:,1)))+abs(max(T1114(:,1))))/6;
iq1114=(iq1114-abs(min(T1114(:,2)))-abs(max(T1114(:,2))))/6;

id1273=(id1273+abs(min(T1273(:,1)))+abs(max(T1273(:,1))))/6;
iq1273=(iq1273-abs(min(T1273(:,2)))-abs(max(T1273(:,2))))/6;

%creation of the matrix 8x2 that contain the average value at considered Torque
%[Nm*10-3]

MTPA_average=[id159 iq159;id318 iq318;id477 iq477;id637 iq637;id796 iq796;id955
iq955;id1114 iq1114;id1273 iq1273;];

for i=1:8

x(i)=MTPA_average(i,1);
y(i)=MTPA_average(i,2);

end
%interpolate function - spline method
xx=[-10:0.001:0];
MTPA_interpl=spline(x,y);
figure (8);
plot(MTPA_interpl,x,y,'o')
hold on

```

Code inputs

-Txxx vectors taken by simulations at all the 8 different Torque outputs considered. "xxx" is to be considered in [Nm*10⁻³]

Code outputs

-MTPA_average
-MTPA_interpl
-a plot of the average trajectory

A3

a- 3D flux representation

```
load fdfq_idiq_n32.mat

r1 = 1; r2 = 24;

figure
surf(Id(r1:r2,:),Iq(r1:r2,:),Fd(r1:r2,:))
xlabel('i_d [A]','FontSize',12), ylabel('i_q [A]','FontSize',12),
zlabel('\lambda_d [Vs]','FontSize',12)

figure
surf(Id(r1:r2,:),Iq(r1:r2,:),Fq(r1:r2,:))
xlabel('i_d [A]','FontSize',12), ylabel('i_q [A]','FontSize',12),
zlabel('\lambda_q [Vs]','FontSize',12)

figure
surf(Id(r1:r2,:),Iq(r1:r2,:),Id(r1:r2,:))
xlabel('i_d [A]','FontSize',12), ylabel('i_q [A]','FontSize',12), zlabel('i_d
[A]','FontSize',12)

figure
surf(Id(r1:r2,:),Iq(r1:r2,:),Iq(r1:r2,:))
xlabel('i_d [A]','FontSize',12), ylabel('i_q [A]','FontSize',12), zlabel('i_q
[A]','FontSize',12)
```

Code inputs

-matlab workspace fdfq_idiq_n32.mat

a file that contain a 32x32 matrix of flux value on the two axes and the corresponding vectors of 32 value of currents, data from simulation.

Code outputs

- Four figures that show the flux in a 3D region

b- Flux matrix interpolation

```
-----  
%%D axes  
  
%column fitting  
for i=1:32  
    pos=1;  
    flag=0;  
    for j=2:32  
        if(flag==1)  
            pos=pos+49;  
            flag=0;  
        end  
        delta_row=Fd(j,i)-Fd(j-1,i);  
        step=delta_row/11;  
        for m=0:50  
            Fd_row(pos+m,i)=Fd(j-1,i)+step*m;           %#ok<*SAGROW>  
            if (m==50)  
                flag=1;  
            end  
        end  
    end  
end  
  
%row fitting  
  
for i=1:length(Fd_row)  
    pos=1;flag=0;  
    for j=2:32  
        if(flag==1)  
            pos=pos+49;  
            flag=0;  
        end  
        delta_coloumn=Fd_row(i,j)-Fd_row(i,j-1);  
        step=delta_coloumn/11;  
        for n=0:50  
            Fd_frs(i,pos+n)=Fd_row(i,j-1)+step*n;       %#ok<*SAGROW>  
            if (n==50)  
                flag=1;  
            end  
        end  
    end  
end  
end
```

```

%%Q axes

%column fitting

for i=1:32
    pos=1;flag=0;
    for j=2:32
        if(flag==1)
            pos=pos+50;
            flag=0;
        end
        delta_row=Fq(j,i)-Fq(j-1,i);
        step=delta_row/50;
        for m=0:50
            Fq_row(pos+m,i)=Fq(j-1,i)+step*m;           %#ok<*SAGROW>
            if (m==50)
                flag=1;
            end
        end
    end
end

%row fitting

for i=1:length(Fq_row)
    pos=1;flag=0;
    for j=2:32
        if(flag==1)
            pos=pos+50;
            flag=0;
        end
        delta_coloumn=Fq_row(i,j)-Fq_row(i,j-1);
        step=delta_coloumn/50;
        for n=0:50
            Fq_frs(i,pos+n)=Fq_row(i,j-1)+step*n;       %#ok<*SAGROW>
            if (n==50)
                flag=1;
            end
        end
    end
end
end

```

The script interpolates the tables adding 50 linearly interpolated values among the elements of line and those of column of the fluxes matrix.

Code inputs

-fdfq_idiq_n32.mat

Code outputs

-fdfq_idiq_n1600.mat

c- MTPA trajectory from flux matrix manipulation

Iterative method A

```
% input:      fdfq_idiq_n1600

% output:
% 1) MTPA trajectory on id iq plane
% 2) control rulez MTPA idref = f(Tref), iqref = F(Tref)
% 3) tabelle.txt

% close all, clear all

motor_name = 'SynRM2';
p = 2;
Imax = 14;
axes_type = 'SR'; % Synch Rel style

load fdfq_idiq_n1600.mat;

% mgt model
figure(1)
plot(Id(1,:),Fd([33 20 1],:)), grid on
xlabel('i_d [A]'),ylabel('[Vs]','FontSize',12), title('flusso d','FontSize',12)
legend('\lambda_d(i_d,0A)', '\lambda_d(i_d,7A)', '\lambda_d(i_d,12A)', 'Location', 'South')
set(gca, 'FontSize', 12)
figure(2)
plot(Iq(:,1),Fq(:, [1 20])), grid on
xlabel('i_q [A]','FontSize',12),ylabel('[Vs]','FontSize',12), title('flusso q','FontSize',12)
legend('\lambda_q(0,i_q)', '\lambda_q(7A,i_q)', 'Location', 'South')
set(gca, 'FontSize', 12)

% Torque, flux module e current model on matrix Id Iq
id = Id(1,:); iq = Iq(:,1)';
TI = 3/2 * p * (Fd .* Iq - Fq .* Id);
FI = sqrt(Fd.^2 + Fq.^2);
II = sqrt(Id.^2 + Iq.^2);

% PM flux
lm = interp2(Id, Iq, FI, eps, eps);

% contour of torque
TLevel = max(max(TI)) * (0.01:0.01:1);
CurveIsoTI=contourc(id, iq, TI, TLevel);

% contour of current
Imax_interp = max(max(abs(id)), max(abs(iq)));
ILevel = Imax_interp * (0.01:0.01:1);
CurveIsoII=contourc(id, iq, II, ILevel);

% MTPA - ILevel and TLevel curve contact
Curve = CurveIsoII; Level = ILevel;
Tot = 0; Valori = 0; NuovoValore=[];
a = cell(length(Level), 1);
```

```

id_KtMax = []; iq_KtMax = []; T_KtMax = [];

m = 1; finito = 0; count_finito = 0;

while (m<=length(Level) && finito == 0)

    Tot=Tot+Valori+1;
    if Tot > length(Curve)
        break
    end
    Valori = Curve(2,Tot);      %n of points at this level

    if NuovoValore==Curve(1,Tot)
        Tot=Tot+Valori+1;
        Valori=Curve(2,Tot);
    end
    NuovoValore=Curve(1,Tot);

    idIso=Curve(1,Tot+[1:Valori]);
    iqIso=Curve(2,Tot+[1:Valori]);

    T_I = interp2(id,iq,TI,idIso,iqIso);      % T at given I - 1st round
    [Tmax_I, indiceM]=max(T_I);

    id_KtMax(m) = idIso(indiceM);      % max T / I (Nm/A) locus
    iq_KtMax(m) = iqIso(indiceM);

    if ((indiceM == 1) || (strcmp(axes_type,'SR') && (indiceM == length(idIso))))
        count_finito = count_finito + 1;
        id_KtMax(m) = NaN;      % max T / I (Nm/A) locus
        iq_KtMax(m) = NaN;
        Tmax_I = NaN;
    end

    if count_finito == 100
        finito = 1;
    end
    T_KtMax(m) = Tmax_I;

    m = m + 1;
end

% filter Not a Number (non valid solutions)
id_KtMax = id_KtMax(not(isnan(id_KtMax)));
iq_KtMax = iq_KtMax(not(isnan(iq_KtMax)));
T_KtMax = T_KtMax(not(isnan(T_KtMax)));

% polynomial fitting
p_KtMax_i = polyfit(id_KtMax,iq_KtMax,7);
p_KtMax_T = polyfit(id_KtMax,T_KtMax,7);
id_KtMax_p = linspace(0,max(id_KtMax)*1.05,length(id_KtMax));
iq_KtMax_p = polyval(p_KtMax_i,id_KtMax_p);
T_KtMax_p = polyval(p_KtMax_T,id_KtMax_p);

ind = find(abs(iq_KtMax_p + j* id_KtMax_p)>=0.94*Imax,1,'first');

id_KtMax = id_KtMax_p;
iq_KtMax = iq_KtMax_p;
T_KtMax = T_KtMax_p;
I_KtMax = abs(id_KtMax + j* iq_KtMax); %#ok<*IJCL>

```

figure(4)

```

plot(I_KtMax,T_KtMax), grid on
xlabel('phase current [A]','FontSize',12), ylabel('torque - Nm','FontSize',12)
title('torque versus peak current along the MPTA')
set(gca,'FontSize',12)

cut_point = 7;

figure(5)
plot(I_KtMax(cut_point:end),T_KtMax(cut_point:end)./I_KtMax(cut_point:end)),
grid on
xlabel('phase current [A]','FontSize',12), ylabel('kt - Nm/Apk','FontSize',12)
title('kt versus current along the MPTA','FontSize',12)
set(gca,'FontSize',12)

for i=1:length(iq_KtMax)
    if (iq_KtMax(i)<0)
        iq_KtMax(i)=0;
        id_Ktmax(i)=0;
    end
    if (i==1)
        iq_KtMax(i)=0;
        id_Ktmax(i)=0;
    end
end

end

figure(6)

% MTPA
plot(id_KtMax,iq_KtMax,'-r','LineWidth',2), hold on
[c,h]=contour(id,iq,II,[1:1:23],'b'); clabel(c,h,'LabelSpacing',200)
[c,h]=contour(id,iq,II,'k'); clabel(c,h), hold on, axis equal
grid on, xlabel('i_d [A]','FontSize',12),ylabel('i_q [A]','FontSize',12)
axis equal, axis([0.5 7.1 0 7.5])
legend('MTPA','iso-coppia','iso-corrente','Location','SouthEast')
set(gca,'FontSize',12)

motor_name = 'ABB - type SynRM2';
T_KtMax(1) = 0;

% LUT
m = 1; % numero righe
n = 32; % numero colonne (la tabella sarà di dimensione n + 1)

Tmax = T_KtMax(end);
step = Tmax / 32;
T_set = 0:step:Tmax;

id_set = interp1(T_KtMax,id_KtMax,T_set); id_set(1) = 0;
iq_set = interp1(T_KtMax,iq_KtMax,T_set); iq_set(1) = 0;

% stampa tabella
fid = fopen('tabelle.txt','w');
fprintf(fid,'//SIGLA MOTORE: %s\n',motor_name);
fprintf(fid,['//' date '\n']);
fprintf(fid,'float Tmin = 0;\n');
fprintf(fid,'float Tmax = %4.3f; //Nm\n',Tmax);
fprintf(fid,'float DT = %4.4f; //Nm\n',step);
fprintf(fid,'float inv_DT = %4.4f; //Nm^-1\n',1/step);

```

```

StampaTarga(fid,id_set,m,n+1,'ID_TAB','//MTPA - id','%6.3f')
StampaTarga(fid,iq_set,m,n+1,'IQ_TAB','//MTPA - iq','%6.3f')

fclose(fid);

% debug
figure (8)
plot(T_KtMax,id_KtMax), hold on, grid on,
plot(T_KtMax,iq_KtMax,'r'),
plot(T_set,id_set,'xk'), plot(T_set,iq_set,'xk'), hold off,
legend('id set point','iq set point','LUT','LUT');
xlabel('T\set - Nm'), ylabel('Apk')

edit tabelle.txt

```

Code inputs

-fdfq_idiq_n1600

Code outputs

-MTPA trajectory on id iq plane
-control rulez MTPA idref = f(Tref), iqref = f(Tref)
-tabelle.txt

Iterative method B

```
-----  
%%          from flux to MTPA          %%%%%%%%%%%%%%%%%%%%%%%%%%%%%%%%%%%%%%%%%  
  
%flux matrix dimension nxm  
  
n=24;  
m=24;  
  
%%p.u. value range of the current  
%%Ibase*SerieMoltD*sqrt(2)=current in d-axes. The same for the q-axes.  
Ibase=6.89775; %%Arms  
SerieMoltD= [-1.44;-1.38;-1.32;-1.26;-1.2;-1.14;-1.08;-1.02;-0.96;-0.9;-0.84;-  
0.78;-0.72;-0.66;-0.6;-0.54;-0.48;-0.42;-0.36;-0.3;-0.24;-0.18;-0.12;-0.06];  
SerieMoltQ=  
[1.44;1.38;1.32;1.26;1.2;1.14;1.08;1.02;0.96;0.9;0.84;0.78;0.72;0.66;0.6;0.54;0.  
48;0.42;0.36;0.3;0.24;0.18;0.12;0.06];  
  
%Copy and paste the FluxD [nxm] and the FluxQ [mxn] matrix and put it on the  
Workspace  
  
%depure the FluxD matrix from the magnet flux (FluxD when no current pass:  
%Id=Iq=0;  
  
FLUX_PM=0.2079;  
  
for i=1:m  
    for j=1:n  
        if (FluxD(i,j)>0)  
            FD(i,j)=FluxD(i,j)-FLUX_PM;  
        else  
            FD(i,j)=0;  
        end  
    end  
end  
  
%remove the iq=0 coloumn and id=0 row from FluxD and FluxQ --> delete it on  
%the workspace  
  
%Organization of the matrix FluxQ --> it has to become an [nxm] matrix  
%row to coloumn  
%  
for i=1:m  
    for j=1:n  
        FQ(j,i)=FluxQ(m-i+1,n-j+1);  
    end  
end  
  
% apparent inductances calculation  
LD_correct=FD./(sqrt(2)*SerieMoltD*Ibase);  
LQ_correct=abs(FluxQ./(sqrt(2)*SerieMoltQ*Ibase));  
  
Ldiff=(LD_correct-LQ_correct);  
  
% permanent flux from magnet calculation (depending on rotor temperature)  
  
Tr=40;    %%rotor temperature at continuative work condition  
Ts=80;    %%stator temp
```

```

FLUX_PM=flux_PM_spline(1,Tr*100);

%idea:
%iq(iter-1)-iq(iter)<e.

%range define for id;
id_range=-14:0.01:-0.58336; %% [1.44 to 0.6 p.u.]
sz=size(id_range);
p=sz(2);

%Considerated working point: torque [Nm]
T=[1.590000000000000 3.180000000000000 4.770000000000000 6.370000000000000
7.960000000000000 9.550000000000000 11.140000000000000 12.730000000000000];

for l=1:8 %%more ext for --> first iteration initialization and new Torque
value
    flag=0;
    iq_hold=0;

for i=1:p %% that for is used for change id value, for each value of id, we
have to iter on iq in order to have convergence on it value

    tmpd=id_range(i)/sqrt(2)/Ibase;
    %%
    %%%
    for k=2:24
        %id_pu research;
        if( tmpd>SerieMoltD(k-1) && (tmpd<SerieMoltD(k)))
            id_fix_pu=k; %%fix of p.u. Id (fix the row on the Ldiff matrix)
        else
            continue;
        end
    end
end

    %at the first iteration, we consider iq=0 (no cross saturation)
    if(flag==0)
        %interpolation beetween the two nearest point to tmpd on the
        %id_pu row
        a=abs(tmpd-k);
        b=abs(tmpd-(k-1));
        c=(Ldiff(k,24)*a+Ldiff(k-1,24)*b)/(a+b);
        flag=1; %%end of first iteration
    end

    %%%

    %%
    %%%
    if(flag==1)
        %%iq_pu research
        q_state_pu=Iq_hold(i)/sqrt(2)/Ibase;

```

```

for h=1:24
    if(q_state_pu<SerieMoltQ(h-1) && (q_state_pu>SerieMoltQ(h)))
        iq_tmp_pu=h;
        break; %column position
    else
        continue;
    end
end

%calc of Ldiff h and in h-1 with interpolation on the tmpD
intermediateD_Ldiff_h=Ldiff(id_fix_pu,h)+(tmpd-
abs(SerieMoltD(id_fix_pu)))/(abs(SerieMoltD(id_fix_pu-1))-
abs(SerieMoltD(id_fix_pu)))*(L_diff(id_fix_pu-1,h)-Ldiff(id_fix_pu,h));

intermediateD_Ldiff_hminus1=Ldiff(id_fix_pu,h-1)+(tmpd-
abs(SerieMoltD(id_fix_pu)))/(abs(SerieMoltD(id_fix_pu-1))-
abs(SerieMoltD(id_fix_pu)))*(L_diff(id_fix_pu-1,h-1)-Ldiff(id_fix_pu,h-1));

%interpolation for Q pu position
%(weighted average)
a=abs((h-1)-q_state_pu);
b=abs(h-q_state_pu);
c=(intermediateD_Ldiff_h*b+intermediateD_Ldiff_hminus1*a)/(a+b);
end
%iq calculation
iq(i,l)=T(1)/1.5*(2*(FLUX_PM+c)*Id_range(i));

%%check of the error treshold
if(abs(iq(i,l)-iq_hold(i,l))>0.1)
    iq_hold=iq;
    p=p-1; %block the id iteration
else
    continue; %%to the for with i=1:p
end

end

end

%%max kt locus research and MTPA plot
Kt=zeros;

for i=1:m
    for j=1:n
        Kt(i,j)=1.5*2*(FLUX_PM-deltaLdq(i,j)*Ibase*SerieMoltD(i)*sqrt(2));
        if (Kt(i,j)==0.623582774000000) %error for the zero value in flux matrix
to remove
            Kt(i,j)=0;
        end
    end
end

end

for l=1:8
    for i=1:m
        for j=1:n
            iq(i,l)=T(1)/Kt(i,j);
        end
    end
end

```

```

end

for l=1:8
    for i=1:m
        Is(i,l)=sqrt(iq(i,l)^2+(Ibase*SerieMoltD(i))^2);
    end
end

for l=1:8
    flag1=0;
    for i=2:m
        if(min(Is(:,l))==Is(i,l))
            I_MTPA(1,l)=(Ibase*SerieMoltD(i)*sqrt(2))/2;
            I_MTPA(2,l)=Iq(i,l)/2;
            flag1=1;
            break;
        end
    end
end
figure(1)
plot(Is)
figure(2)
plot(Iq)
figure(4)
xx=[-20:0.01:0];
MTPA_interpl=interp1(I_MTPA(1,:),I_MTPA(2,:),xx);
plot(xx,MTPA_interpl,I_MTPA(1,:),I_MTPA(2,),'o')
hold on

```

Code inputs

-fdfq_idiq_n32.mat

Code outputs

-MTPA trajectory on id iq plane

A4

Note: to use this script, the Adept program must be installed on your computer. You need also to organize the reference folder for matlab: just copy and paste a standard simulation output to the folder and add the following scripts and .bat files.

a- 60 degree elt excursion of rotor – simulations and mediated output

```
clear all %#ok<CLALL>
close all
clc

RPM      =3000;      % [rpm]
pp       =2;        % pole pairs
FN       =RPM/60*pp; % nominal freq
Irated   =7.27;     % [Arms]

%%temperature fixed
RotTemp=105;
StatTemp=65; %according to the other Adept simulations

i=1;
j=1;
k=1;

CREF=zeros;
IphiE=0;

iq=0.001*1.4142:0.03:1.4*1.4142;
pos=1;
    %%CurrentDefinition

    while i<=66 %iq=0.001*1.4142:0.03:1.4*1.4142

        Iq=iq(i);
        Id=-iq(pos);

        if ((k/66)-floor(k/66)==0&&k<4356) % è multiplo intero di 66
            flag=1;
            pos=(k/66)+1;
        end

        alpha = atan2(Iq,Id)*180/pi;
        Is(i,j) = Irated*sqrt(Id^2+Iq^2)/sqrt(2); %#ok<*SAGROW>
        CREF = Is(i,j);

        for IphiE=0:1:60
            CurrStr = num2str(CREF);
            AngleStr = num2str(IphiE);
            %%RotorAngleDefinition
            RotAngle_e = -alpha - 150 + IphiE;

            %%launch simulation program
            [data,dc_out]=launchFCSmek(RotAngle_e,CREF,RotTemp,StatTemp,0,150,pp,FN,IphiE,1)

            %%aquisition of data
            Fd(k,IphiE+1)=dc_out.data(12);
```

```

        Fq(k,IphiE+1)=dc_out.data(16);
        id_result(k,IphiE+1)=dc_out.data(21);
        iq_result(k,IphiE+1)=dc_out.data(23);
    end

    Fd_mediated(j,i)=mean(Fd(i,:)); %%mediated Flux -- filtered from
    Stator induced ripple
    Fq_mediated(j,i)=mean(Fq(i,:));
    Id_out(j,i)=id_result(k,1);
    Iq_out(j,i)=iq_result(k,1);
    k=k+1;

    if(k==200)
        break;
    end
    if(flag==1)
        i=1;
        j=j+1;
        flag=0;
    else
        i=i+1;
    end
end
end

```

Code inputs

- empty workspace

Code outputs

- Fd, Fq, id, iq mediated from stator effects (input workspace for A3 c)

b- launchFCSmek.m matlab function

```

function
[data,dc_out]=launchFCSmek(RotAngle_e,CREF,TST,TRT,source,theta0,pp,FN,IphiE,Use
_d_ax)

% [data, dc.out]=launchFCSmek(RotAngle_e,CREF,TST,TRT,source)
    ini = IniConfig();
    ini.ReadFile('FCSMEK_calc.ini');
switch source
    case 0
        % Stator source? /Current=0/Voltage=1/
        ini.SetValues(['SYDC'],'ITSTJ',source);
        % Rotational angle of the rotor
        ini.SetValues(['SYDC'],'ALFA',RotAngle_e);
        % Line current for stator
        ini.SetValues(['SYDC'],'CREF',CREF);
        % Temperature of the stator windings
        ini.SetValues(['SYDC'],'TST',TST);
        % Temperature of the rotor windings
        ini.SetValues(['SYDC'],'TRT',TRT);
        % Stator phase angle in order to fix Id and Iq value

```

```

%      only fluxes value change for ripple fact
ini.SetValues(['SYDC'], 'ANGLE', IphiE);
%      Use D_axis_angle
ini.SetValues(['SYDC'], 'USE_D_AXIS_ANGLE', Use_d_ax);
%      D_ax to theta0 150° elt
ini.SetValues(['SYDC'], 'D_AXIS_ANGLE', theta0);

ini.WriteFile('FCSMEK_calc.ini');

case 1
%      Stator source? /Current=0/Voltage=1/
ini.SetValues(['SYDC'], 'ITSTJ', source);
%      Rotational angle of the rotor
ini.SetValues(['SYDC'], 'ALFA', RotAngle_e);
%      Line current for stator
ini.SetValues(['SYDC'], 'CREF', CREF);
%      Temperature of the stator windings
ini.SetValues(['SYDC'], 'TST', TST);
%      Temperature of the rotor windings
ini.SetValues(['SYDC'], 'TRT', TRT);
%      Use D_axis_angle
ini.SetValues(['SYDC'], 'USE_D_AXIS_ANGLE', Use_d_ax);
%      D_ax to theta0 150° elt
ini.SetValues(['SYDC'], 'D_AXIS_ANGLE', theta0);
%      Stator phase angle in order to fix Id and Iq value
%      only fluxes value change for ripple fact
ini.SetValues(['SYDC'], 'ANGLE', IphiE);

ini.WriteFile('FCSMEK_calc.ini');

end

dos('launchFCSmek.bat'); %launch only magneto static with .bat

[data]=1;
dc_out = importdata('dc_out.dat',';');

fprintf( '\n\nHello, %d worlds!\n\n', 20 )

```

c- *IniConfig.m*

Download at <https://www.dropbox.com/sh/yo5fav88u1axi6o/AClapj0SvC441dfju529iGa?dl=0>

d- *launchFCSmek.bat*

```
@echo off
"C:\Program Files (x86)\Adept\FCSmek\mesh.exe"
"C:\Program Files (x86)\Adept\FCSmek\sydc.exe"
```


Thanks – Ringraziamenti

Ringrazio senza meriti o precedenze tutte le persone che mi sono state vicine in questi 5 anni di studi al Politecnico di Torino. Ringrazio l'ateneo per avermi dato la possibilità di fare questa attività di tesi in una importante azienda come l'ABB, che ringrazio a sua volta, relatori e supervisor tutti.

Un grazie particolare va a mio padre Sandro e a mia sorella Giulia.

Un grazie di cuore va alla mia ragazza.

Un grazie silenzioso ma profondo va a mia madre Elisa e a mia nonna Maria; spero che da qualche parte possiate gioire con me di questo traguardo.